Analysis of mitochondrial dynamics and oxidative phosphorylation function in neuroblast differentiation in *Drosophila melanogaster*

A thesis
submitted in partial fulfillment of the requirements of
the degree of

DOCTOR OF PHILOSOPHY

By

DNYANESH DUBAL

20122023

INDIAN INSTITUTE OF SCIENCE EDUCATION AND RESEARCH

PUNE

CERTIFICATE

It is certified that the thesis entitled **"Analysis of mitochondrial dynamics and oxidative phosphorylation in neuroblast differentiation in *Drosophila melanogaster*"** submitted by **Mr. Dnyanesh Dubal** represents his original work which was carried out by the candidate at IISER, Pune, under my guidance and supervision during the period from **August 2013 to December 2019**.

The work presented here or any part of it has not been included in any other thesis submitted previously for the award of any degree or diploma from any other University or institution. I further certify that the above statements made by him in regard to his thesis are correct to the best of my knowledge.

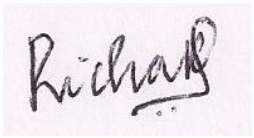

Date: 06/07/2020

Dr. Richa Rikhy

(Supervisor)

DECLARATION

I declare that this written submission represents my idea in my own words and where others ideas have been included I have adequately cited and referenced the original sources. I also declare that I have adhered to all principles of academic honesty and integrity and have not misrepresented or fabricated or falsified any idea/data/fact/source in my submission. I understand that violation of the above will be cause for disciplinary action by the Institute and can also evoke penal action from the sources which have thus not been properly cited or from whom proper permission has not been taken when needed. The work reported in this thesis is the original work done by me under the guidance of Dr. Richa Rikhy.

Date: 06/07/2020

Dnyanesh Dubal

Reg. no. 20122023

Acknowledgement

This thesis is a result of kind support and help from many individuals. I would like to take this opportunity to express my sincere gratitude towards all of these people.

First and most of all, I would like to thank my PhD advisor Dr. Richa Rikhy for allowing me to work in her lab. This endeavor would not have been possible without her constant guidance, regular suggestions, support and patience. She was always available whenever I needed help regarding the experiments. She has always encouraged me to come up with new ideas and provided all the required resources to test them. Her immense expertise in the field of genetics and microscopy helped me a lot during this project. I would also like to thank her for constantly encouraging me to participate in conferences and share my work with the scientific community.

I would like to thank my RAC members Dr. Anuradha Ratnaparaki and Dr. Nagaraj Balasubramanian for their valuable suggestions during RAC meetings. I would also like to thank Dr. Girish Ratnaparakhi for his critical comments and suggestions during our common lab meetings. I thank Dr. Kundan Sengupta for giving me opportunity to work with him during the lab rotation. During this rotation, I learned the cell culture and molecular biology techniques which helped me during my thesis work. I would like to thank Ms. Prachiti Moghe for her hard work, sincerity and valuable inputs in this project. Prachiti had worked with me on this project during her Master's thesis. She has helped me a lot in mitochondrial imaging and Notch analysis in type II neuroblasts.

I would like to thank all the past and present RR lab members for maintaining a supportive and cheerful environment in the lab. I thank my seniors Aparna, Darshika, Sayali for helping me during my initial phase in the lab. I thank Darshika for teaching me basic fly techniques and confocal imaging during my lab rotation. I would like to thank Sameer, Bipasha, Bhavin, Rohan, Radhika, Swati, Gayatri, Debasmita, Soumya, Rahul, Harsh for creating a friendly atmosphere in the lab.

I would like to thank IISER fly stock center caretaker Snehal, Yashwant and Ashwini for providing fly media and taking care of my fly stocks. I would also like to thank IISER microscopy facility member Vijay, Santosh for the microscopy training and maintaining

the facility. I also thank biology administration staff Piyush, Kalpesh, Mrinalini, Mahesh for their prompt logistic help. I would like to thank BDSC, VDRC and NCBS for fly stocks.

I would like to express my sincere gratitude towards Disha organization in IISER, Pune which gave me a unique opportunity to teach and interact with Students from an underprivileged background. This helped me to understand different social problems and added another dimension to my personality.

Padmabhushan and Shekhar have been my friends since my school days. Special thanks to them for being with me in my ups and downs. I thank Mr. Abbhijeet Nikam for his constant encouragement and support during my undergraduate studies. Coffee with Sanket and Devika has always been refreshing for me. I would like to thank Vaibhav, Swapnil B, Swapnil V, Sourabh, Abhijit, Advait, Prachiti, Nabha, Gayatri, Swanand, Yashwant, Yogesh, Mrunal, Chinmay, Akash, Yash, Vyanktesh, Manasi for the late-night tea parties and for making campus life more happening. Discussions and debates with them have always given me different perspectives about personal and social issues.

I would like to thank IISER, Pune for providing the state of the art research facilities, vibrant scientific environment and fellowship. I thank Infosys Foundation, DMM Travel Grant and Department of Biotechnology (DBT) for providing me travel support to attend international conferences.

I am very fortunate to have supportive parents. I would like to express my sincere gratitude towards my family for their unconditional support and love. Special thanks to Namrata for being my best friend and a life partner. I also would like to thank my brother for supporting me in difficult situations. And finally to my beloved Grandfather ‘Anna’ who is always been my source of inspiration. I would like to end by quoting Nelson Mandela which I think would be appropriate for the thesis completion.

“IT ALWAYS SEEMS IMPOSSIBLE UNTIL IT IS DONE”

Table of Contents

List of Figures

Chapter 1: Introduction

Chapter 2: Material and Methods

Chapter 3: Assessment of the effect of mitochondrial dynamics mutants on animal survival, mitochondrial morphology and neuroblast lineage progression.

Observation Table 1: Table showing analysis of mitochondrial morphology protein knockdown with different neuronal Gal4s.

Observation Table 2: Genetic screen of proteins relating to mitochondrial function in *Drosophila* CNS.

List of Abbreviations:

AB polarity	Apico-basal polarity
AD	Alzheimer's Disease
AICAR	5-Aminoimidazole-4-carboxamide ribonucleotide
ALS	Amyotrophic Lateral Sclerosis
AMP	Adenosine Monophosphate
AMPK	AMP kinase
AP	Anterior-posterior
APC	Anaphase Promoting Complex
ATP	Adenosine triphosphate
ATPB	ATP synthase beta subunit
Baz	Bazooka
Brat	Brain tumor
BSA	Bovine Serum Albumin
CB	Central Brain
CDK	Cyclin Dependent Kinase
CMT2A	Charcot Marie Tooth type 2A
CoVa	Cytochrome oxidase subunit Va
CRISPR	clustered regularly interspaced short palindromic repeats
DaPKC	Drosophila atypical protein kinase C
DHE	Dihydroethidium
Dlp1	Dynamin Like Protein 1
DNA	Deoxynucleic Acid
DOA	Dominant Optic Atrophy
DPBS	Dulbecco's phosphate-buffered saline
Dpn	Deadpan

Drp1	Dynamin Related Protein 1
EdU	5-ethynyl-2'-deoxyuridine
EGFR	Epidermal Growth Factor Receptor
ER	Endoplasmic Reticulum
Espl	Enhancer of Split
ETC	Electron Transfer Chain
FADH2	Flavin adenine dinucleotide
Fis1	Fission 1
GED	GTPase Effector Domain
GMC	Ganglion Mother Cell
GSC	Germline Stem Cell
hESC	Human Embryonic Stem Cell
Hnt	Hindsight
HR	Heptad Repeat
IMM	Inner Mitochondrial Membrane
INP	Intermediate Neural Precursor
Insc	Inscuteable
Lgl	Lethal Giant Larvae
LRRK2	Leucine-rich repeat kinase 2
MARCM	Mosaic Analysis with a Repressible Cell Marker
Marf	Mitochondrial Assembly Related Factor
MB neuroblasts	Mushroom Body Neuroblast
Mfn	Mitofusin
Mira	Miranda
mTOR	Mechanistic Target of Rapamycin
NADH	Nicotinamide Adenine Dinucleotide

neuroblasts	Neuroblast
NE	Neuro-Epithelium
NICD	Notch Intracellular Domain
OL	Optic Lobe
OMA1	OMA1 Zinc Metallopeptidase
OMM	Outer Mitochondrial Membrane
Opa1	Optic Atrophy 1
OxPhos	Oxidative Phosphorylation
PAN	Posterior Asense Negative
PAR3	Partitioning Defective 3
PBS	Phosphate Buffer Saline
PD	Parkinson's Disease
PFA	Paraformaldehyde
PINK1	PTEN induced putative kinase 1
Pins	Partner of Inscuteable
Pnt	Pointed
Pros	Prospero
PTEN	Phosphatase and Tensin homolog
RIP	Receptor Interacting Protein
ROS	Reactive Oxygen Species
RT	Room Temperature
SOD	Superoxide Dismutase
Stau	Staufen
Std	Stardust
STED	Stimulated Emission Depletion
Su(H)	Suppressor of Hairless
TCA	Tricarboxylic Acid Cycle

TdT	Terminal Deoxynucleotidyl Transferase
TMD	Transmembrane Domain
TPR	Tricopeptide Repeat
TUNEL	Terminal deoxynucleotidyl transferase dUTP nick end labeling
UAS	Upstream Activator Sequence
VDAC1	Voltage Dependent Anion Channel 1
VNC	Ventral Nerve Cord
WT	Wild type
YME1L	YME1 Like 1 ATPase
ZA	Zonula Adherens

Abstract

Mitochondrial structure is regulated by a dedicated machinery for fusion and fission. Recently mitochondrial architecture regulation is known to be involved in stem cell proliferation and differentiation, and the molecular mechanism underlying the process is not completely understood. In this study, we have used *Drosophila* neuroblasts as a model system to assess the role of mitochondrial morphology in stem cell development. We found that tissue specific knockdown of mitochondrial fusion proteins Opa1 and Marf showed loss of differentiated population in type II lineage. Interestingly depletion of inner membrane fusion protein Opa1 caused a reduction in both mature intermediate neural precursor (mINP) cells and ganglion mother cell (GMC) population in type II neuroblast lineages. However, depletion of outer membrane fusion protein Marf resulted in a reduction of only GMCs. Loss of differentiation was a consequence of reduced cell proliferation. We found that Notch signaling regulated this fused mitochondrial morphology in type II neuroblasts. Forced outer membrane fusion by depletion of fission protein Drp1 activity led to reversal of differentiation defects seen in *notch*, *opa1* and *marf* mutants. Similar to *opa1*, the electron transport chain complex IV and complex V mutants had decreased differentiation. Drp1 depletion reversed the defect in complex IV mutants and not complex V mutants consistent with the crucial role of complex V in cristae stabilization. Our results implicate Notch signaling in regulation of inner membrane in fused mitochondria and show that mitochondrial fusion can compensate for defects in Opa1 and complex IV mutants in neuroblast differentiation.

Synopsis

Name of the Student: **Dnyanesh Dubal**

Registration number: **20122023**

Name of Thesis advisor: **Dr. Richa Rikhy**

Date of Registration: **1st August 2014**

Place: **Indian Institute of Science Education and Research (IISER), Pune**

Title: **Analysis of mitochondrial dynamics and oxidative phosphorylation function in neuroblast differentiation in *Drosophila melanogaster*.**

1. Introduction

Mitochondria are one of the many membrane bound organelles housed by the eukaryotic cell. They were once free living prokaryotes belonging to the *Rickettsia* family of α-Proteobacter class (Lane and Martin, 2010; Wang and Wu, 2014; Wang and Wu, 2015). During the course of evolution, they got engulfed by a large eukaryotic cell that did not digest it but rather kept it for long term gain. Since then mitochondria and the eukaryotic cell have tight connections through symbiotic relationships (Lane and Martin, 2010; Wang and Wu, 2014; Wang and Wu, 2015). Mitochondria perform several major functions in the cell. They are famously recognized for their role in energy production through the process of oxidative phosphorylation (Papa et al., 2012; Vakifahmetoglu-Norberg et al., 2017). But apart from ATP synthesis they also maintain calcium homeostasis and the redox state of the cell. Mitochondria are central players in the cell execution program i.e. apoptosis (Clavier et al., 2016; Kasahara and Scorrano, 2014).

Most mitochondrial genes in the eukaryotic cell are encoded by the nuclear genome. Mitochondria are highly dynamic organelles and undergo continuous cycles of fusion and fission depending on cell type, cell cycle stage, and energy demand (Chen and

Chan, 2017; Fu et al., 2019) (Wanet et al., 2015; Zhang et al., 2018). This finetuned balance between fusion and fragmentation is regulated by large GTPase proteins belonging to the dynamin family (Garone et al., 2018). Since mitochondria are double membrane organelles, two different proteins are required for the fusion of the outer and inner membrane. Outer membrane fusion is regulated by Mitochondrial Assembly Regulatory factor (Marf, mitofusin 1 & 2 in mammals) while Optic Atrophy Protein 1 (Opa1) regulate inner membrane fusion (Bana et al., 2018) (Olichon et al., 2003; Rapaport et al., 1998). The synchronous activity of these proteins tubular and reticulated the architecture of mitochondria. Fused mitochondrial architecture produces more energy as it has higher membrane potential and numerous tight cristae (MarcLiesa and Shirihai, 2013). Mitochondrial cristae are highly curved and folded inner membrane which holds different protein complexes required for the oxidative phosphorylation process. Tight cristae architecture favors the formation of electron chain supercomplexes and ATP synthase dimerization which further speed up the process of ATP production (Cogliati et al., 2013)(Cogliati et al., 2016). Mitochondrial fragmentation is regulated by Dynamin Related Protein1 (Drp1) which is predominantly cytoplasmic protein (Smirnova et al., 2001). During the fission event, Drp1 gets recruited on mitochondria and form a multimeric ring around the mitochondrial tubule. GTP hydrolysis fueled the action of Drp1 causes contraction of a ring which ultimately results in mitochondrial fragmentation (Smirnova et al., 2001). Different Drp1 receptors such as mitochondrial fission protein 1 (Fis1), mitochondrial fission factor (Mff), and mitochondrial dynamics proteins of 49 and 51 kDa (MiD49 & MiD51) present on the mitochondrial outer membrane which regulates fission process (Losón et al., 2013; Smirnova et al., 2001). Fragmented mitochondria are associated with lower membrane potential, lower ATP synthesis, less mitochondrial DNA (mtDNA) copy number, etc (Xu et al., 2013). A cell needs small, fragmented mitochondria during cell division to distribute them equally into the daughter cells, to separate damaged and during the mitophagy process (Gomes and Scorrano, 2013; Prashant Mishra, 2014)

Recent studies have suggested that a fine balance between mitochondrial dynamics proteins is required for stem cell proliferation and differentiation (Khacho et

al., 2016; Seo et al., 2018; Zhang et al., 2018; Zhong et al., 2019). Drp1 mediated mitochondrial fragmentation is needed for Notch dependent ovarian follicle cell differentiation in *Drosophila (Mitra et al., 2012)*. Loss of Drp1 caused a lack of activation of differentiation genes such as Hindsight (Hnt) which further resulted in the loss of differentiation. Another study on mouse embryonic stem cells (ESC) highlighted the function of mitochondrial fragmentation in ESC differentiation. In ESCs, loss of Opa1 and Mfn resulted in increased mitochondrial fragmentation and ectopic expression of Notch, which in turn affects differentiation population produced by ESCs (Kasahara et al., 2013). This is contrary to the previous results where mitochondrial fragmentation led to Notch inactivation. These reports suggest that mitochondrial role during stem cell differentiation is context dependent and may vary from cell to cell. Several studies showed the effect of different signaling pathways on mitochondrial morphology and function. Epidermal Growth Factor Receptor (EGFR) is one of the key signaling pathways involved in cell differentiation (Barberán and Cebrià, 2019; Dumstrei et al., 1998; Kim et al., 2005). It is reported that downstream target of EGFR which is extracellular-signal regulated kinase (ERK) regulates high membrane potential which resulted in inhibition of Notch signaling causes loss of follicle differentiation in the *Drosophila* ovary (Tomer et al., 2018). Another report from the lung cancer cell line showed EGFR is recruited to the mitochondria where it causes mitochondrial fragmentation by interfering Mfn1 polymerization (Che et al., 2015).

Several types of pathological and disease conditions are associated with mitochondrial proteins. Mutation in mitochondrial genes is involved in a range of neurodegenerative diseases like Parkinson's disease (PD), Alzheimer's disease (AD), dominant optic atrophy (DOA), amyotrophic lateral sclerosis, Charcot Marie Tooth type II A (CMT2A), etc. (Westermann, 2010). In these diseases, either dynamics or metabolism of mitochondria is affected. PD is one of the most common neurodegenerative disorders and characterized by the loss of dopaminergic neurons in the substantia nigra (Raza et al., 2019; Westermann, 2010). Genetic studies of PD revealed that this neurogenic disorder is caused by a mutation in five genes such as

PTEN- induced kinase 1 (PINK1), Parkin, DJ-1and leucine-rich repeat kinase2 (LRRK2) (Büeler, 2010). ALS is caused by a mutation in Superoxide dismutase 1 (SOD1). SOD acts as a scavenger and reduces the ROS level of the cell. The loss of function of SOD causes the accumulation of ROS. A high concentration of ROS is toxic to neuronal survival as it damages mtDNA. mtDNA damage leads to the accumulation of toxic compounds in the neuronal cell and it eventually degenerates (Smith et al., 2019; Tafuri et al., 2015). CMT2A is a disease of the peripheral nervous system caused by a mutation in mitochondrial fusion protein Mitofusin (Mfn) (Feely et al., 2011). Loss of function of Opa1 causes dominant optic atrophy in which bilateral optic neurons degenerate and result in moderate vision loss (Alexander et al., 2000). All these studies indicate that mitochondrial function apart from energy production is also important for the normal development of animals. These reports have assessed the function of mitochondria in later development process of the neural stem cells but how mitochondrial function affects upstream stages of neural precursor cells is poorly understood.

In the present study, we have analyzed mitochondrial function in neural stem cell development in *Drosophila*. Neural stem cells in *Drosophila* are known as neuroblasts. Neuroblasts develop from stage 8 to stage 11 during embryonic development by the process of lateral inhibition (Buescher et al., 2002; Cabrera, 1990; Urbach et al., 2003). Notch Delta signaling pathway is responsible for the production of neuroblasts where Notch inhibits expression of proneural genes in the cells surrounding high Delta expressing cell (Kunisch et al., 1994). After formation, they get delaminated from neuro-epithelium and achieve apicobasal polarity in which different protein complexes localized to either apical or basal sides. Eventually, neuroblast undergoes asymmetric cell division forming ganglion mother cell (GMC) and simultaneously undergo self-renewal. Differentiated GMC further divides into pair neurons or glia depending upon the expression profile of the cell (Chia et al., 2008; Prehoda, 2009). During late embryonic stages, the major population of neuroblasts undergoes quiescence which during larval stages re-enter into the active cell division (Ding et al.,

2016; Tsuji et al., 2008). For the re-entry they require amino acid signal and mTOR activation from fat bodies which is a nutrient-sensing organ of the *Drosophila (Sousa-Nunes et al., 2011)*. The larval central brain consists of three different types of neuroblasts namely type I, type II and mushroom body neuroblasts (Boone and Doe, 2008; Homem and Knoblich, 2012). Type I and Type II neuroblasts differ from each other based on the division profile of these two neuroblasts. Type I neuroblasts progress from neuroblasts to GMC to neurons/glia whereas type II neuroblasts instead of forming GMCs first form immature neural precursor cell (ImINP). ImINP undergoes about four to six-hour long maturation process in which the sequential expression of transcription factors take place. These transcription factors are produced in a hierarchical manner with Asense expressing first followed by Deadpan and then Prospero. INPs which express all these transcription factors are called mature INP (mINP). mINP then divides to form GMC and GMC in later symmetric divisions produces a pair of neurons. In this way, type II neuroblasts produce more numbers of the differentiated cells even though they are only eight in number per brain lobe (Homem and Knoblich, 2012). Mushroom body neuroblasts are only four in number per brain hemisphere and they form memory and learning centers in the brain (Kunz et al., 2012).

In this study, we have analyzed the effects of different mitochondrial dynamics and activity proteins on the neuroblast differentiation and further assessed their role in regulating the signaling pathway required for neuroblast differentiation.

2 Results

2.1 Mitochondrial fusion and NOT fission is required for neuroblast differentiation in *Drosophila* larval brains

Multiple investigations on stem cells suggest that they harbor small and fragmented mitochondria as they are highly proliferative cells (Chen and Chan, 2017; Xu et al., 2013). To assess the mitochondrial distribution and morphology in neuroblasts we

immunostained larval brains with ATPB antibody which target ATP synthase present in the inner mitochondrial membrane followed by Stimulated Emission Depletion (STED) microscopy. We found evenly dispersed mitochondria with more fused and tubular architecture in the neuroblasts. Further, we assessed the function of fused mitochondrial architecture in neuroblast development by perturbing mitochondrial morphology. We adopted the *Drosophila* UAS-Gal4 genetic system for the assessment. We depleted mitochondrial dynamics proteins to perturb mitochondrial architecture using RNAi lines and neuroblast specific gal4. Depletion of Opa1 and Marf caused mitochondrial fragmentation while reduced Drp1 function resulted in highly clustered mitochondria indicative of hyperfusion. Then we analyzed the effect of change of mitochondrial morphology on neuroblast number polarity and differentiation. We found depletion of mitochondrial fusion proteins Opa1 and Marf and fission protein Drp1 did not affect neuroblast number and polarity. However reduction in Opa1 and Marf caused a decreased number of differentiated cells in neuroblast lineages. In type II neuroblast lineage, depletion of Opa1 and Marf resulted in the reduced number of Prospero positive GMCs, but a reduced number of Deadpan positive mINPs were observed only in Opa1 depletion which is inner membrane fusion protein and not in Marf, an outer membrane fusion protein. Surprisingly, we did not find any role of Drp1 in neuroblast differentiation. These results highlighted the interesting role of fusion and specifically inner membrane fusion in the neuroblast differentiation process.

2.2 Forced mitochondrial fusion by co-depletion of Drp1 rescues differentiation defects caused by Opa1 and Marf knockdown.

Since mitochondrial fragmentation by depletion of Opa1 and Marf caused a defect in differentiation, we asked can we reverse these defects by forced fusion. In order to fuse mitochondria, we combined a dominant negative mutant of Drp1 Drp1SD with Opa1 RNAi and Marf RNAi lines. The co-depletion of Drp1 along with Opa1 and Marf caused mitochondrial fusion. Interestingly the number of mINPs was restored in Opa1 depletion by forced mitochondrial fusion. We also found partial rescue in GMC numbers in Opa1

and Marf knockdown. These results reiterate the importance of mitochondrial fusion in neuroblast differentiation.

2.3 Reduced proliferation rate and NOT apoptosis causes loss of differentiated cells in mitochondrial mutants.

Mitochondrial fragmentation can lead to different cellular consequences such as reduced ATP levels, lowering of mitochondrial membrane potential, increased ROS, etc (Xu et al., 2013). To check whether reduced ATP was a cause of reduced differentiation, we analyzed pAMPK levels in Opa1 and Marf depleted neuroblasts. pAMPK is acted as an energy sensor and upregulates when less amount of ATP present in the cell (Garcia and Shaw, 2017; Hardie et al., 2012). We did not find elevated pAMPK levels in mutant neuroblast suggesting a lack of energy stress. Reports suggest that neuroblast metabolism depends upon glycolysis and not mitochondrial driven oxidative phosphorylation (Homem et al., 2014). This we confirmed by pharmacological inhibition of glycolysis by 2-Deoxy glucose (2-DG) (Sottnik et al., 2011) which showed increased pAMPK levels. Further, we observed increased levels of ROS and cytochrome C in the Opa1 depleted neuroblasts. Ectopic increase in ROS by hSOD1 mutant expression did not cause any defects in neuroblast numbers and differentiation and animal viability, hence increased ROS is unlikely to be a cause of loss of differentiation in Opa1 mutants. A specific increase of cytochrome C in Opa1 mutant neuroblasts indicated the possibility of apoptosis in type II neuroblast lineage. TUNEL assays and immunostaining with cleaved caspase-3 showed that apoptosis was not triggered in Opa1 depleted neuroblast lineages as lineages failed to show increased TUNEL positive cells or cleaved caspase-3 levels. Interestingly, we found a reduced number of EdU and pH3 positive cells which are markers of S-phase and mitotic phase respectively in Opa1 depleted type II neuroblast lineages. These results showed a reduced number of mINP and GMC cells in Opa1 mutant are not due to apoptosis but because of loss of proliferative potential of type II neuroblast.

2.4 Cytoplasmic retention of NICD in Opa1 depleted type II neuroblasts is reversed by co-depletion of Drp1

Notch signaling is a key pathway required for neuroblast proliferation in the type II lineage. It has been shown that ectopic expression of Notch causes overproliferation of the neuroblasts while the loss of Notch reduces the neuroblast number (Egger et al., 2010; Lee et al., 2013). It majorly affects type II neuroblasts as depletion causes a complete loss of type II lineages (Li et al., 2016). In mouse ESCs, loss of Opa1 and Mfn caused hyperactivation of Notch which in turn resulted in a reduction in cardiomyocyte number (Kasahara et al., 2013). To analyze whether the Notch pathway is affected in neuroblast lineage of mitochondrial mutants, we stained control and mutant brains with the NICD antibody followed by confocal microscopy. We then analyzed cytoplasmic to nuclear NICD ratios by quantifying NICD intensities from control and mutant brains. Interestingly, we found an increased cytoplasmic accumulation of NICD in Opa1 depletion alone and not in Control, Marf RNAi and Drp1SD. This result indicating a possible loss of Notch signaling in Opa1 depletion. This cytoplasmic accumulation of NICD not seen in Drp1, Opa1 double mutants. Together these results indicate that loss of differentiation in type II neuroblast is possibly due to defect in Notch signaling caused by Opa1 depletion.

2.5 Crosstalk between Notch signaling and mitochondrial fusion is required for type II neuroblast differentiation

Mitochondrial fragmentation mediated by loss of Opa1 caused the loss of Notch signaling in type II neuroblast. Further, we asked whether the loss of Notch signaling leads to similar defects in type II neuroblasts or not. To address this question, we used the loss of function and gain of function mutants of Notch and confirmed these mutants by quantifying neuroblast numbers. These mutants showed expected results as loss of Notch caused reduction in neuroblast number from 8 in the controls to 0-7 neuroblasts in Notch RNAi while ectopic expression of Notch receptor (NV5) caused hyperproliferation and severe increase in neuroblast number (~85). Then we analyzed

the differentiation profile of these mutant neuroblast lineages. We found a reduced number of Deadpan positive mINP and Prospero positive GMCs in Notch RNAi while these cells were unaffected in NV5 mutant. This result indicates differentiation of type II neuroblasts also depends on Notch signaling. Further, we analyzed mitochondrial morphology and its distribution in these mutants. Interestingly, we found small and fragmented mitochondria on Notch depletion and clustered mitochondria on overexpression of NV5 suggesting Notch regulates mitochondrial fusion in the neuroblast. We found that Notch regulates mitochondrial morphology via its canonical nuclear pathway because we observed similar mitochondrial fragmentation in Su(H) RNAi. Su(H) is a Notch partner and it binds to NICD in the nucleus and together they regulate gene expression program (Bailey and Posakony, 1995). Furthermore, reduced differentiation by Notch depletion was rescued by co-depletion of Drp1 suggesting fused mitochondrial morphology was necessary for type II neuroblast differentiation. We further combined NV5 overexpression transgene with Opa1 and Marf RNAi and found a decrease in the neuroblast number as compared to NV5 alone confirming the indispensability of mitochondrial fusion in Notch-mediated neuroblast proliferation and differentiation.

2.6 ATP synthase is required for Notch-mediated type II neuroblast differentiation

Differentiation defects in type II neuroblast lineage were more severe in the case of inner membrane protein Opa1 depletion as compared to outer membrane protein Marf depletion. This was further confirmed by observing increased cytochrome C levels in Opa1 which is indicative of inner membrane defect (Scorrano et al., 2002). Mitochondrial inner membrane is folded into cristae which house different electron transport chain (ETC) protein complexes essential for the process of oxidative phosphorylation. Some of these complexes such as complex I, complex III and complex IV cluster together to form respiratory chain supercomplexes (RCS) which enhances ATP production (Cogliati et al., 2016; Milenkovic et al., 2017). ATP synthase is a part of ETC and involved in the formation of ATP from ADP. ATP synthase also form a dimer and this dimerization process is important to induce curvature and bending of the inner

mitochondrial membrane to stabilize cristae (Blum et al., 2019). ATP synthase dimerization is involved in germline stem cell differentiation in the *Drosophila* ovary and unexpectedly this is an energy-independent process (Teixeira et al., 2015). Together Opa1 and OxPhos complexes are known to form and mature cristae structure in the mitochondria. (Patten et al., 2014; Quintana-Cabrera et al., 2018) We asked whether depletion of OxPhos proteins gives rise to similar defects as Opa1. To address this question, we depleted cytochrome C subunit Va (CoVa) part of complex IV and ATPB, a subunit of ATP synthase in type II neuroblasts. Surprisingly downregulation of CoVa and ATPB caused a reduction in mINP and GMC cells in type II neuroblast lineage which is similar to Opa1 depletion. Increased cytochrome C was also observed in CoVa and ATPB depletions. Further, we performed immunostaining with the pH3 antibody to check mitotically active cells in the lineage. We found decreased numbers of pH3 positive cells in CoVa and ATPB RNAi. We also found increased NICD in the cytoplasm in these depletions indicating a critical function of the inner membrane in the Notch-mediated differentiation process. Interestingly forced fusion of mitochondrial outer membrane by co-depletion of Drp1 rescued mINP cells and pH3 positive cells only in CoVa RNAi but not in ATPB RNAi. Cytoplasmic retention of NICD rescued only in CoVa and not in ATPB depletion by forced fusion. Forced fusion could not rescue defects caused by ATPB depletion suggesting a specific role of ATP synthase in neuroblast differentiation.

In a nutshell, we showed the function of mitochondrial fusion and specifically inner membrane proteins in the neuroblast differentiation process and Notch signaling. Interestingly mitochondrial fission protein Drp1 has no specific role in neuroblast development. However, forced fusion by co-depletion of Drp1 rescues defect caused by Opa1 and CoVa depletion. Our data suggest that an intact inner mitochondrial membrane is required for proper Notch activity during neuroblast differentiation. Fused mitochondria require an intact ATP synthase function for the differentiation process as forced outer membrane fusion did not rescue the defects caused by ATPB depletion. As discussed previously, ATP synthase dimerization is needed for the formation and maturation of cristae. Finally, we propose that ATP synthase dimerization is required for

Notch-mediated type II neuroblast proliferation and differentiation. Future studies will test this hypothesis by using RNAi against proteins such as subunit E and subunit G of ATP synthase which are required for the dimerization process.

References

Alexander, C., Votruba, M., Pesch, U. E. A., Thiselton, D. L., Mayer, S., Moore, A., Rodriguez, M., Kellner, U., Leo-Kottler, B., Auburger, G., et al. (2000). OPA1 , encoding a dynamin-related GTPase, is mutated in autosomal dominant optic atrophy linked to chromosome 3q28. *Nat. Genet.* **26**, 211–215.

Bailey, A. M. and Posakony, J. W. (1995). Suppressor of hairless directly activates transcription of enhancer of split complex genes in response to Notch receptor activity. *Genes Dev.* **9**, 2609–2622.

Bana, T., Kohnoa, H., Ishiharaa, T. and Ishihara, N. (2018). Relationship between OPA1 and cardiolipin in mitochondrial inner-membrane fusion. *Biochimica et Biophysica Acta (BBA) - Bioenergetics* **1859**, 951–957.

Barberán, S. and Cebrià, F. (2019). The role of the EGFR signaling pathway in stem cell differentiation during planarian regeneration and homeostasis. *Semin. Cell Dev. Biol.* **87**, 45–57.

Blum, T. B., Hahn, A., Meier, T., Davies, K. M. and Kühlbrandt, W. (2019). Dimers of mitochondrial ATP synthase induce membrane curvature and self-assemble into rows. *Proc. Natl. Acad. Sci. U. S. A.* **116**, 4250–4255.

Boone, J. Q. and Doe, C. Q. (2008). Identification of Drosophila type II neuroblast lineages containing transit amplifying ganglion mother cells. *Dev. Neurobiol.* **68**, 1185–1195.

Büeler, H. (2010). Mitochondrial dynamics, cell death and the pathogenesis of Parkinson's disease. *Apoptosis* **15**, 1336–1353.

Buescher, M., Hing, F. S. and Chia, W. (2002). Formation of neuroblasts in the embryonic central nervous system of Drosophila melanogaster is controlled by SoxNeuro. *Development* **129**, 4193–4203.

Cabrera, C. V. (1990). Lateral inhibition and cell fate during neurogenesis in Drosophila: the interactions between scute, Notch and Delta. *Development* **110**, 733–742.

Che, T.-F., Lin, C.-W., Wu, Y.-Y., Chen, Y.-J., Han, C.-L., Chang, Y.-L., Wu, C.-T., Hsiao, T.-H., Hong, T.-M. and Yang, P.-C. (2015). Mitochondrial translocation of EGFR regulates mitochondria dynamics and promotes metastasis in NSCLC. *Oncotarget* **6**, 37349–37366.

Chen, H. and Chan, D. C. (2017). Mitochondrial Dynamics in Regulating the Unique Phenotypes of Cancer and Stem Cells. *Cell Metab.* **26**, 39–48.

Chia, W., Somers, W. G. and Wang, H. (2008). Drosophila neuroblast asymmetric divisions:

cell cycle regulators, asymmetric protein localization, and tumorigenesis. *J. Cell Biol.* **180**, 267–272.

Clavier, A., Rincheval-Arnold, A., Colin, J., Mignotte, B. and Guénal, I. (2016). Apoptosis in Drosophila: which role for mitochondria? *Apoptosis* **21**, 239–251.

Cogliati, S., Frezza, C., Soriano, M. E., Varanita, T., Quintana-Cabrera, R., Corrado, M., SaraCipolat, Costa, V., Casarin, A., Gomes, L. C., et al. (2013). Mitochondrial Cristae Shape Determines Respiratory Chain Supercomplexes Assembly and Respiratory Efficiency. *Cell* **155**, 160–171.

Cogliati, S., Enriquez, J. A. and Scorrano, L. (2016). Mitochondrial Cristae: Where Beauty Meets Functionality. *Trends Biochem. Sci.* **41**, 261–273.

Ding, R., Weynans, K., Bossing, T., Barros, C. S. and Berger, C. (2016). The Hippo signalling pathway maintains quiescence in Drosophila neural stem cells. *Nat. Commun.* **7**, 1–12.

Dumstrei, K., Nassif, C., Abboud, G., Aryai, A. and Hartenstein, V. (1998). EGFR signaling is required for the differentiation and maintenance of neural progenitors along the dorsal midline of the Drosophila embryonic head. *Development* **125**, 3417–3426.

Egger, B., Gold, K. S. and Brand, A. H. (2010). Notch regulates the switch from symmetric to asymmetric neural stem cell division in the Drosophila optic lobe. *Development* **137**, 2981–2987.

Feely, S. M. E., Laura, M., Siskind, C. E., Sottile, S., Davis, M., Gibbons, V. S., Reilly, M. M. and Shy, M. E. (2011). MFN2 mutations cause severe phenotypes in most patients with CMT2A. *Neurology* **76**, 1690–1696.

Fu, W., Liu, Y. and Yin, H. (2019). Mitochondrial Dynamics: Biogenesis, Fission, Fusion, and Mitophagy in the Regulation of Stem Cell Behaviors. *Stem Cells Int.* **2019**,.

Garcia, D. and Shaw, R. J. (2017). AMPK: Mechanisms of Cellular Energy Sensing and Restoration of Metabolic Balance. *Mol. Cell* **66**, 789–800.

Garone, C., Minczuk, M., Tilokani, L., Nagashima, S., Paupe, V. and Prudent, J. (2018). Mitochondrial dynamics: overview of molecular mechanisms. *Essays Biochem.* **62**, 341–360.

Gomes, L. C. and Scorrano, L. (2013). Mitochondrial morphology in mitophagy and macroautophagy. *Biochim. Biophys. Acta* **1833**, 205–212.

Hardie, D. G., Ross, F. A. and Hawley, S. A. (2012). AMPK: a nutrient and energy sensor that maintains energy homeostasis. *Nat. Rev. Mol. Cell Biol.* **13**, 251–262.

Homem, C. C. F. and Knoblich, J. A. (2012). Drosophila neuroblasts: a model for stem cell biology. *Development* **139**, 4297–4310.

Homem, C. C. F., Steinmann, V., Burkard, T. R., Jais, A., Esterbauer, H. and Knoblich, J. A. (2014). Ecdysone and mediator change energy metabolism to terminate proliferation in Drosophila neural stem cells. *Cell* **158**, 874–888.

Kasahara, A. and Scorrano, L. (2014). Mitochondria: from cell death executioners to regulators of cell differentiation. *Trends Cell Biol.* **24**, 761–770.

Kasahara, A., Cipolat, S., Chen, Y., Dorn, G. W., 2nd and Scorrano, L. (2013). Mitochondrial fusion directs cardiomyocyte differentiation via calcineurin and Notch signaling. *Science* **342**, 734–737.

Khacho, M., Clark, A., Svoboda, D. S., Azzi, J., MacLaurin, J. G., Meghaizel, C., Sesaki, H., Lagace, D. C., Germain, M., Harper, M.-E., et al. (2016). Mitochondrial Dynamics Impacts Stem Cell Identity and Fate Decisions by Regulating a Nuclear Transcriptional Program. *Cell Stem Cell* **19**, 232–247.

Kim, S., Schein, A. J. and Nadel, J. A. (2005). E-cadherin promotes EGFR-mediated cell differentiation and MUC5AC mucin expression in cultured human airway epithelial cells. *Am. J. Physiol. Lung Cell. Mol. Physiol.* **289**, L1049–60.

Kunisch, M., Haenlin, M. and Campos-Ortega, J. A. (1994). Lateral inhibition mediated by the Drosophila neurogenic gene delta is enhanced by proneural proteins. *Proc. Natl. Acad. Sci. U. S. A.* **91**, 10139–10143.

Kunz, T., Kraft, K. F., Technau, G. M. and Urbach, R. (2012). Origin of Drosophila mushroom body neuroblasts and generation of divergent embryonic lineages. *Development* **139**, 2510–2522.

Lane, N. and Martin, W. (2010). The energetics of genome complexity. *Nature* **467**, 929–934.

Lee, K.-S., Wu, Z., Song, Y., Mitra, S. S., Feroze, A. H., Cheshier, S. H. and Lu, B. (2013). Roles of PINK1, mTORC2, and mitochondria in preserving brain tumor-forming stem cells in a noncanonical Notch signaling pathway. *Genes Dev.* **27**, 2642–2647.

Li, X., Xie, Y. and Zhu, S. (2016). Notch maintains Drosophila type II neuroblasts by suppressing expression of the Fez transcription factor Earmuff. *Development* **143**, 2511–2521.

Losón, O. C., Song, Z., Chen, H. and Chan, D. C. (2013). Fis1, Mff, MiD49, and MiD51 mediate Drp1 recruitment in mitochondrial fission. *Mol. Biol. Cell* **24**, 659.

MarcLiesa and Shirihai, O. S. (2013). Mitochondrial Dynamics in the Regulation of Nutrient Utilization and Energy Expenditure. *Cell Metab.* **17**, 491–506.

Milenkovic, D., Blaza, J. N., Larsson, N.-G. and Hirst, J. (2017). The Enigma of the Respiratory Chain Supercomplex. *Cell Metab.* **25**, 765–776.

Mitra, K., Rikhy, R., Lilly, M. and Lippincott-Schwartz, J. (2012). DRP1-dependent mitochondrial fission initiates follicle cell differentiation during Drosophila oogenesis. *J. Cell Biol.* **197**, 487–497.

Olichon, A., Baricault, L., Gas, N., Guillou, E., Valette, A., Belenguer, P. and Lenaers, G. (2003). Loss of OPA1 Perturbates the Mitochondrial Inner Membrane Structure and Integrity, Leading to Cytochrome c Release and Apoptosis. *J. Biol. Chem.* **278**, 7743–7746.

Papa, S., Martino, P. L., Capitanio, G., Gaballo, A., De Rasmo, D., Signorile, A. and Petruzzella, V. (2012). The Oxidative Phosphorylation System in Mammalian Mitochondria. In

Advances in Mitochondrial Medicine, pp. 3–37. Springer, Dordrecht.

Patten, D. A., Wong, J., Khacho, M., Soubannier, V., Mailloux, R. J., Pilon-Larose, K., MacLaurin, J. G., Park, D. S., McBride, H. M., Trinkle-Mulcahy, L., et al. (2014). OPA1-dependent cristae modulation is essential for cellular adaptation to metabolic demand. *EMBO J.* **33**, 2676–2691.

Prashant Mishra, D. C. C. (2014). Mitochondrial dynamics and inheritance during cell division, development and disease. *Nat. Rev. Mol. Cell Biol.* **15**, 634.

Prehoda, K. E. (2009). Polarization of Drosophila Neuroblasts During Asymmetric Division. *Cold Spring Harb. Perspect. Biol.* **1**, a001388.

Quintana-Cabrera, R., Mehrotra, A., Rigoni, G. and Soriano, M. E. (2018). Who and how in the regulation of mitochondrial cristae shape and function. *Biochem. Biophys. Res. Commun.* **500**, 94–101.

Rapaport, D., Brunner, M., Neupert, W. and Westermann, B. (1998). Fzo1p Is a Mitochondrial Outer Membrane Protein Essential for the Biogenesis of Functional Mitochondria in Saccharomyces cerevisiae. *J. Biol. Chem.* **273**, 20150–20155.

Raza, C., Anjum, R. and Shakeel, N. U. A. (2019). Parkinson's disease: Mechanisms, translational models and management strategies. *Life Sci.* **226**, 77–90.

Scorrano, L., Ashiya, M., Buttle, K., Weiler, S., Oakes, S. A., Mannella, C. A. and Korsmeyer, S. J. (2002). A Distinct Pathway Remodels Mitochondrial Cristae and Mobilizes Cytochrome c during Apoptosis. *Dev. Cell* **2**, 55–67.

Seo, B. J., Yoon, S. H. and Do, J. T. (2018). Mitochondrial Dynamics in Stem Cells and Differentiation. *Int. J. Mol. Sci.* **19**,.

Smirnova, E., Griparic, L., Shurland, D.-L. and van der Bliek, A. M. (2001). Dynamin-related Protein Drp1 Is Required for Mitochondrial Division in Mammalian Cells. *Mol. Biol. Cell* **12**, 2245.

Smith, E. F., Shaw, P. J. and De Vos, K. J. (2019). The role of mitochondria in amyotrophic lateral sclerosis. *Neurosci. Lett.* **710**, 132933.

Sottnik, J. L., Lori, J. C., Rose, B. J. and Thamm, D. H. (2011). Glycolysis inhibition by 2-deoxy-D-glucose reverts the metastatic phenotype in vitro and in vivo. *Clin. Exp. Metastasis* **28**, 865–875.

Sousa-Nunes, R., Yee, L. L. and Gould, A. P. (2011). Fat cells reactivate quiescent neuroblasts via TOR and glial insulin relays in Drosophila. *Nature* **471**, 508–512.

Tafuri, F., Ronchi, D., Magri, F., Comi, G. P. and Corti, S. (2015). SOD1 misplacing and mitochondrial dysfunction in amyotrophic lateral sclerosis pathogenesis. *Front. Cell. Neurosci.* **9**, 336.

Teixeira, F. K., Sanchez, C. G., Hurd, T. R., Seifert, J. R. K., Czech, B., Preall, J. B., Hannon, G. J. and Lehmann, R. (2015). ATP synthase promotes germ cell differentiation independent of oxidative phosphorylation. *Nat. Cell Biol.* **17**, 689–696.

Tomer, D., Chippalkatti, R., Mitra, K. and Rikhy, R. (2018). ERK regulates mitochondrial membrane potential in fission deficient Drosophila follicle cells during differentiation. *Dev. Biol.* **434**, 48–62.

Tsuji, T., Hasegawa, E. and Isshiki, T. (2008). Neuroblast entry into quiescence is regulated intrinsically by the combined action of spatial Hox proteins and temporal identity factors. *Development* **135**, 3859–3869.

Urbach, R., Schnabel, R. and Technau, G. M. (2003). The pattern of neuroblast formation, mitotic domains and proneural gene expression during early brain development in Drosophila. *Development* **130**, 3589–3606.

Vakifahmetoglu-Norberg, H., Ouchida, A. T. and Norberg, E. (2017). The role of mitochondria in metabolism and cell death. *Biochem. Biophys. Res. Commun.* **482**, 426–431.

Wanet, A., Arnould, T., Najimi, M. and Renard, P. (2015). Connecting Mitochondria, Metabolism, and Stem Cell Fate. *Stem Cells Dev.* **24**, 1957.

Wang, Z. and Wu, M. (2014). Phylogenomic Reconstruction Indicates Mitochondrial Ancestor Was an Energy Parasite. *PLoS One* **9**, e110685.

Wang, Z. and Wu, M. (2015). An integrated phylogenomic approach toward pinpointing the origin of mitochondria. *Sci. Rep.* **5**, 1–12.

Westermann, B. (2010). Mitochondrial fusion and fission in cell life and death. *Nat. Rev. Mol. Cell Biol.* **11**, 872–884.

Xu, X., Duan, S., Yi, F., Ocampo, A., Guang-HuiLiu, Carlos, J. and Belmonte, I. (2013). Mitochondrial Regulation in Pluripotent Stem Cells. *Cell Metab.* **18**, 325–332.

Zhang, H., Menzies, K. J. and Auwerx, J. (2018). The role of mitochondria in stem cell fate and aging. *Development* **145**,.

Zhong, X., Cui, P., Cai, Y., Wang, L., He, X., Long, P., Lu, K., Yan, R., Zhang, Y., Pan, X., et al. (2019). Mitochondrial Dynamics Is Critical for the Full Pluripotency and Embryonic Developmental Potential of Pluripotent Stem Cells. *Cell Metab.* **29**, 979–992.e4.

Chapter1: Introduction

1.1 Mitochondria

The eukaryotic cell has a plethora of membrane-bound organelles. The mitochondrion is one of such membrane-bound organelles present in the cytoplasm. They were first discovered by Altmann in 1890 (Falkenberg and Larsson, 2009; O'Rourke, 2010). However name 'mitochondrion- Greek *mitos*-thread and *chondros*-granules' originated in 1898 given by Karl Benda during the study of spermatogenesis. There is plenty of evidence that suggests that mitochondria were free living bacteria before getting incorporated into the eukaryotic cell (Archibald, 2014). Genome sequencing of mitochondria and other prokaryotic organisms revealed that it is closely related to *Rickettsia* family belonging to the α-proteobacteria class (Nunnari and Suomalainen, 2012; Wang and Wu, 2014; Wang and Wu, 2015). Approximately 2 billion years ago, one of the eukaryotic cells engulfed this free living prokaryote and instead of breaking down, it started living in a cooperative manner (Lane and Martin, 2010). Engulfed mitochondria provided energy to the cell in the form of ATP which is required for many cellular processes (Amiri et al., 2003; John and Whatley, 1975). This event is considered one of the most important events in the evolution of multicellular organisms. This phenomenon is now known as the endosymbiotic theory. Over the course of time, the nuclear genome took over the synthesis of most of the mitochondrial proteins (Roger et al., 2017). Now mitochondria have become integral parts of the eukaryotic cell and perform many functions in order to smooth the functioning of the cellular processes.

Maternal inheritance of mitochondria is predominant in sexually reproducing organisms. During the fertilization, centriole and sperm nucleus along with little cytoplasm enters into the egg. A middle piece containing mitochondria remains outside and eventually disappears after fertilization. In *C. elegans*, mitochondrial components enter into the oocyte and get degraded immediately after fertilization by the cell's autophagosomal

machinery.

In this part, I shall be discussing different aspects of mitochondrial structure, dynamics and its function in different cellular processes.

1.1.1 Mitochondria structure:

Mitochondria are double-membrane organelles and present in the cytoplasm of the cell. Each mitochondrion possesses 8-10 copies of mtDNA which encodes 13 polypeptides which are the part of respiratory proteins required for energy synthesis, 22 transfer RNAs, 2 ribosomal RNAs in humans (Sato and Sato, 2013). Mitochondrial matrix also possesses protein synthesis machinery such as ribosomes, tRNAs, rRNAs. Hence it is semi-autonomous in nature. Mitochondria are the major center of many metabolic processes hence also known as metabolic hubs of the cell (Frezza, 2017). It harbors multiple enzymes that catalyze different biochemical reactions such as the TCA cycle (Montgomery and Leyden Webb, 1956; Nunes-Nesi et al., 2013). Glucose gets oxidized into pyruvate through the series of reactions known as glycolysis (Horecker, 1976). Pyruvate via decarboxylation step gets converted into Acetyl CoA which then translocates into the mitochondrial matrix where it involved in the tricarboxylic acid (TCA) cycle (Gray et al., 2014; Horecker, 1976). Many intermediates formed during this process act as a substrate for different biochemical cycles. Mitochondrial compartmentalization provides a unique microenvironment to carry out these processes. Inner mitochondrial membrane (IMM) is folded into the structure called cristae to increase the surface area for respiration (Cogliati et al., 2016; Siegmund et al., 2018). Mitochondrial electron transfer chain (ETC) complexes embedded in oxysomes present on IMM are most densely packed in the cristae region (Cogliati et al., 2016).

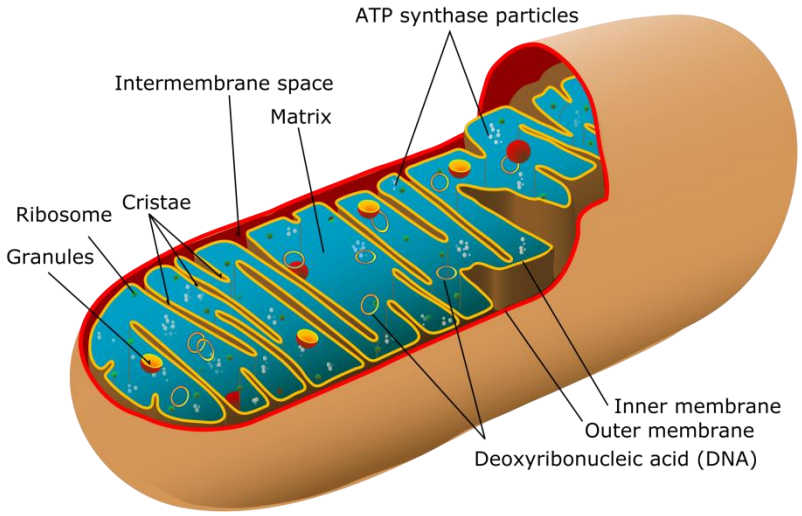

Figure 1.1: Typical organization of mitochondria

Schematic showing typical mitochondrial architecture. The outer membrane (orange) is continuous while the inner membrane (yellow) is folded into multiple cristae structures. Mitochondrial matrix (blue) contain circular DNA, ribosomes, granules. (image adapted from Biology Dictionary website)

Mitochondrial ETC comprises a series of electron carriers which include complex I (NADH dehydrogenase), complex II (fumarate reductase), complex III (cytochrome bc1 complex), complex IV(cytochrome oxidase). Two electron donors namely NADH and FADH2, generated during the process of glycolysis and Kreb's cycle, donate electrons to their respective electron carriers. Which is then transfer sequentially through different protein complexes. Finally, electrons get accepted by O2 to form metabolic water. During the process of electron transfer, H+ ions transported from the matrix to the intermembrane space through proton pumps present in complex I, III and IV to create an electrochemical gradient across the membrane. H+ ions move down to the matrix through proton channel present in the F0 unit of complex V (ATP synthase). This electromotive force is utilized to form ATP from ADP and Pi (Balaban, 1990; Brown, 1992; Ernster, 1977; Fillingame, 1997; Guo et al., 2018; Hatefi, 1985; Senior, 1988). ATP act as energy currency for several biological processes of the cell.

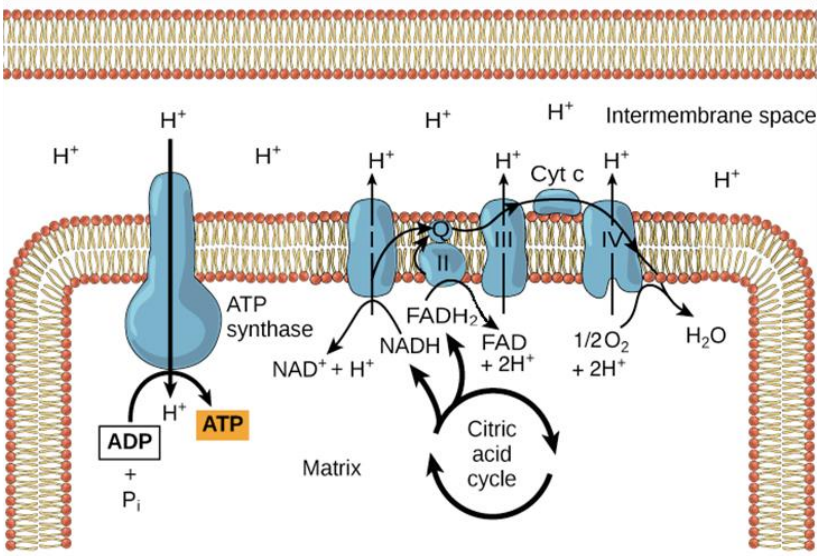

Figure 1.2: Arrangement and mechanism of mitochondrial electron transfer chain

Schematic of mitochondrial electron transport chain component. ETC complexes I, II, III, IV and ATP synthase are embedded in the inner mitochondrial membrane. Oxidizable substrates NADH and FADH2 are produced during the citric acid cycle. Oxidation of NADH and FADH2 is carried out at complex I and complex II respectively. Electrons released from NADH and FADH2 transfer through different enzyme complexes in the inner membrane of mitochondria. Asymmetric flow of protons into the intermembrane space by complex I, III and IV generate a proton gradient across the inner membrane which drives the production of ATP by ATP synthase complex. (Image adapted from Lumen Learning website)

Apart from ETC components, the mitochondrial membrane also hosts many different proteins such as voltage-dependent anion channels, transport proteins, Ca2+ uniporter, shape regulatory proteins to name a few.

1.1.2 Mitochondrial shape change

Mitochondria are highly dynamic organelles and undergo a continuous change in shape depending upon energy status of the cell, cell cycle stage and type of the cell (Chen and Chan, 2017; Fu et al., 2019; Liesa and Shirihai, 2013; Thorsness, 1992; Trotta and Chipuk, 2017; Wanet et al., 2015; Wang et al., 2018; Zhang et al., 2018). It can change shape from fused continuous reticulated network to fragmented round punctate shape. Continuous fused state of mitochondria is known to produce more ATP as cristae are

densely packed (Liesa and Shirihai, 2013). Densely packed cristae support the formation of ETC supercomplex (Cogliati et al., 2013; Cogliati et al., 2016). The fragmented state is an energy-poor state having loosely arranged cristae. Mitochondrial dynamics play a crucial role in cellular physiology. It is required to maintain calcium homeostasis, check on mitochondrial quality control, respond to change in nutrient conditions by the cell. Mitochondria take up excess calcium released by endoplasmic reticulum (ER) to maintain calcium balance in the cell (Hacker and Medler, 2008; Paupe and Prudent, 2018). Reactive oxygen species (ROS) formed during oxidative phosphorylation causes deleterious mutations in mtDNA (Wei et al., 1998) and damage other parts of mitochondria (Yoo and Jung, 2018). The damaged part of mitochondria needs to be separated from the healthy part in order to retain respiratory potential and to avoid further consequences. This is achieved by mitochondrial fission. A cell experiences environments with different nutrients, for example, low/high glucose or amino acid concentration throughout its lifespan. It responds to the changing environment by modulating mitochondrial morphology (Gomes et al., 2011; Rambold et al., 2011).

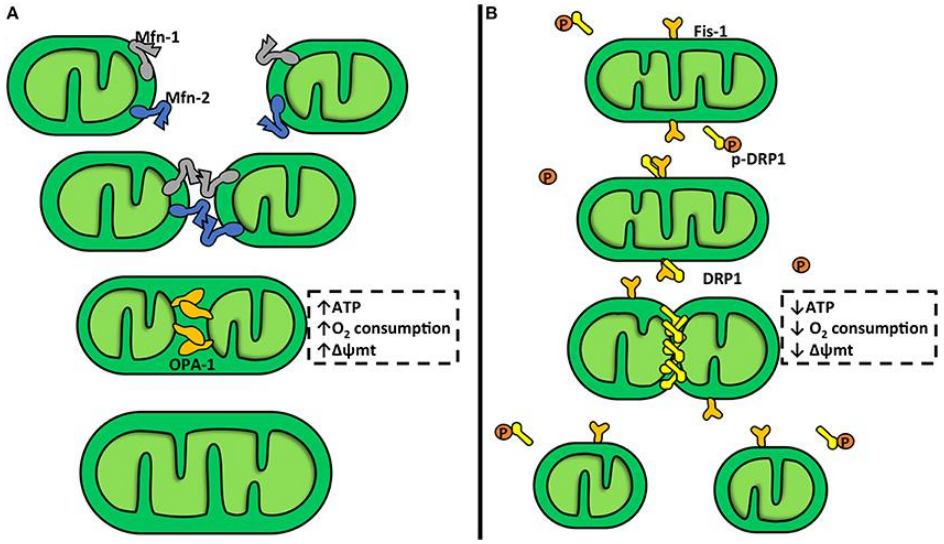

Figure 1.3: Regulation of mitochondrial fusion and fission by different dynamin family GTPases

A) Mitochondrial fusion: Mfn1 (grey) and Mfn2 (blue) present on outer mitochondrial membrane which come into the contact during OMM fusion. Opa1 (yellow) situated in the inner

mitochondrial membrane and involved in IMM fusion. Fusion causes an increase in ATP production, oxygen consumption and membrane potential

B) Mitochondrial fission: Cytosolic Drp1(yellow) gets phosphorylated which translocate Drp1 onto its receptor Fis1 (orange) present on OMM. Drp1 forms a concentric ring around mitochondrial which eventually constrict to cause mitochondrial fragmentation. Fission is associated with low ATP production, reduced oxygen consumption and low membrane potential. (Image adapted from (Chiong et al., 2014)

Change in mitochondrial shape is brought about by proteins belonging to the family of large dynamin like GTPases. Mitochondrial fusion is carried out by optic atrophy protein 1 (Opa1) and mitochondrial assembly related factor (Marf) while dynamin related protein 1(Drp1) regulates mitochondrial fragmentation (Tilokani et al., 2018). Components involved in mitochondrial shape dynamics are evolutionarily conserved from yeast to humans (Ferree and Shirihai, 2012). Opa1 regulates the fusion of the inner mitochondrial membrane (IMM) (Ban et al., 2018; Olichon et al., 2003). Yeast homolog of Opa1 is known as Mgm1 because a mutation in the gene resulted in mitochondrial genome maintenance defects in yeast (Jones and Fangman, 1992; Pelloquin et al., 1998). Later it was discovered that these defects are due to failure in IMM fusion. In humans, a mutation in Opa1 leads to a disease condition called autosomal dominant optic atrophy (DOA) (Alexander et al., 2000; Marchbank et al., 2002). DOA is characterized by the degeneration of retinal ganglion cells and optic neurons which leads to progressive vision loss (Ranieri et al., 2013). The structure of Opa1 is conserved from yeast to humans. It has a GTPase domain, middle domain, GTPase effector domain (GED) and N-terminal transmembrane domain (TMD) (Ban et al., 2017). TMD helps in the anchorage of protein into IMM. The function of the GTPase domain in the process of IMM fusion is not completely understood. Opa1 has multiple splice variants in humans and Yeast (Delettre et al., 2001; Lee et al., 2017; Song et al., 2007). Proteolytic cleavage of long or L-Opa1 produces short or S-Opa1 isoform. This process is carried out by multiple proteolytic enzymes such as Presenilin associated rhomboid like (PARL) proteases, i-AAA protease YME1L, OMA1 protease (Lee et al., 2017; Song et al., 2007). These proteases are present on the inner membrane and into the intermembrane space of mitochondria. An appropriate proportion of both L and S

isoform is required for normal IMM fusion activity. Mutation in the above-mentioned proteases leads to an increase in the proportion of L-Opa1 isoform which causes impaired IMM fusion. Similarly, the attenuated amount of S-Opa1 also results in defects in IMM fusion (Lee et al., 2017; Song et al., 2007).

The fusion of the outer mitochondrial membrane requires proteins broadly named as mitofusins. Marf is a large dynamin GTPase involved in OMM fusion in *Drosophila*. Fzo is a yeast homolog of Marf (Rapaport et al., 1998). Alteration in the *fzo* caused onion-like and fuzzy morphology of mitochondria in yeast cells (Hermann et al., 1998; Rapaport et al., 1998). Humans have two isoforms of this protein, Mitofusin 1 (Mfn1) and Mitofusin 2 (Mfn2) (Chen et al., 2003). Mfn2 and Marf have a high degree of protein sequence similarity as compared to Mfn1 (McLelland et al., 2018). Mfn has two transmembrane (TM) domains and two heptad repeats (HR). Both TD domain passes through OMM in such a way that the N and C termini of protein exposed to the cytosol (Qi et al., 2016). GTPase domain is attached to the N terminal side and exposed to the cytosol. During the fusion of OMM, HR of one molecule binds to the HR of another molecule present on different mitochondria. These interactions are homotypic (HR1-HR1 or HR2-HR2) or heterotypic (HR1-HR2). Physical intermolecular interaction of these proteins brings two mitochondria together which eventually lead to OMM fusion (Koshiba et al., 2004; Tilokani et al., 2018). Mutation in any one of the isoforms does not affect mitochondrial OMM fusion because of the redundant activity of these isoforms in mammalian cells (Chen et al., 2003). Since there is only one isoform of Marf in *Drosophila*, a mutation in this protein leads to mitochondrial fission. The fusion of mitochondria requires simultaneous action of both Opa1 and Marf. Both these proteins require GTP hydrolysis to carry out their functions. But apart from GTP, Opa1 also needs inner membrane potential for its function (Chen et al., 2003; Song et al., 2007). The role of membrane potential in inner membrane fusion is still unclear. Fused mitochondria are associated with high membrane potential and produce more energy (Yao et al., 2019). Downregulation of fusion proteins, Opa1 and Marf induces mitochondrial fragmentation which results in reduced respiratory activity. EM studies

showed that fused mitochondria have tight cristae organization which is required for the formation of ETC supercomplexes also known as respirasome (Cogliati et al., 2013). The most commonly observed respirasomes are complex I, III, IV. The formation of respirasomes enhances the ETC activity to produce more ATP. Mutation in Opa1 alters the cristae morphology resulting in disassembly of respirasomes (Olichon et al., 2003).

Mitochondrial fission primarily requires the activity of one fission protein, this is the large GTPase dynamin related protein 1 (Drp1) or Dynamin like protein 1 (Dlp1). Drp1 function in mitochondrial fission was initially studied in yeast (Bleazard et al., 1999; Sesaki and Jensen, 1999) and *C. elegans (Labrousse et al., 1999)* before extensively analyzing it in mammalian system (Smirnova et al., 2001). It has a GTPase domain which is followed by a middle domain, a variable domain, and the GTPase effector domain. The variable domain also called insert B which is required for facing protein towards the membrane. Like classical GTPase proteins, it harbors bundle signaling domain (BSE) at the C- terminus and stalk region while it lacks the pleckstrin homology (PH) domain. The exact mechanism of translocation of Drp1 onto the membrane is not clearly understood. In Yeast, Fission1 (Fis1) act as a receptor for Drp1. Other factors such as Mff, MiD49, MiD51 are also important for the translocation of Drp1 on mitochondria. Fis1 is a transmembrane protein which evenly distributed on the mitochondrial surface. It contains a tetratricopeptide repeat (TPR) which interacts with Dnm1 (the yeast homolog of Drp1) with the help of Mdv1 and Caf4. Even though Fis1 is present all over the mitochondria, how Dnm1 localizes to specific regions on mitochondria is not well understood. Recent studies in *Drosophila* suggest that the accumulation of actin to the mitochondria provides a starting point for Drp1 translocation. Binding of actin filaments triggers myosin II localization on the actin-mitochondria contact site which provides a platform for Drp1 recruitment on the mitochondria. But it is not the only mechanism by which Drp1 localizes to the mitochondria. In *vitro* study using purified Drp1 and mitochondria showed that Drp1 can translocate and initiate fission of mitochondria provided with GTP without any external stimuli. It forms an oligomeric ring around the mitochondrial tubule and then constricts

using energy derived from GTP hydrolysis. Fissioned mitochondria are thought to be energy poor mitochondria which have low membrane potential and loose cristae organization.

1.1.3 Regulation of mitochondrial dynamics

A proper balance between mitochondrial fusion and fission is necessary for the normal development of the organism. A cell can display different morphologies depending upon energy needs, cell cycle stage, and type of the cell (Kianian and Kianian, 2014). Mitochondria modulate its morphology during different cell cycle stages. In the G1-S phase mitochondria appear to be more fused and continuous while in M phase they are small, punctae and fragmented. Several cell cycle regulators such as cyclin-dependent protein kinases and their regulatory subunits cyclins involved in this process. CDK1 and cyclin B1 phosphorylates Drp1 at S565 position result in Drp1 activation which causes mitochondrial fragmentation (Taguchi et al., 2007). CDK1/Cyclin B1 dependent Drp1 activation is shown to be regulated by the anaphase-promoting complex (APC). Mitochondrial fragmentation during cell division ensures equal distribution of mitochondria in daughter cells. The G1-S transition phase is marked by the presence of hyper fused mitochondrial network and regulated by CDK2/ Cyclin E complex (Lopez-Mejia and Fajas, 2015; Wang and Kalderon, 2009). Hyperfused mitochondria have shown to be essential for the accumulation of Cyclin E during the G1-S transition (Mitra et al., 2009). Perturbation in mitochondrial morphology by downregulation of fusion proteins leads to G1-S cell cycle arrest. This way mitochondria retrospectively keep check on cell cycle progression.

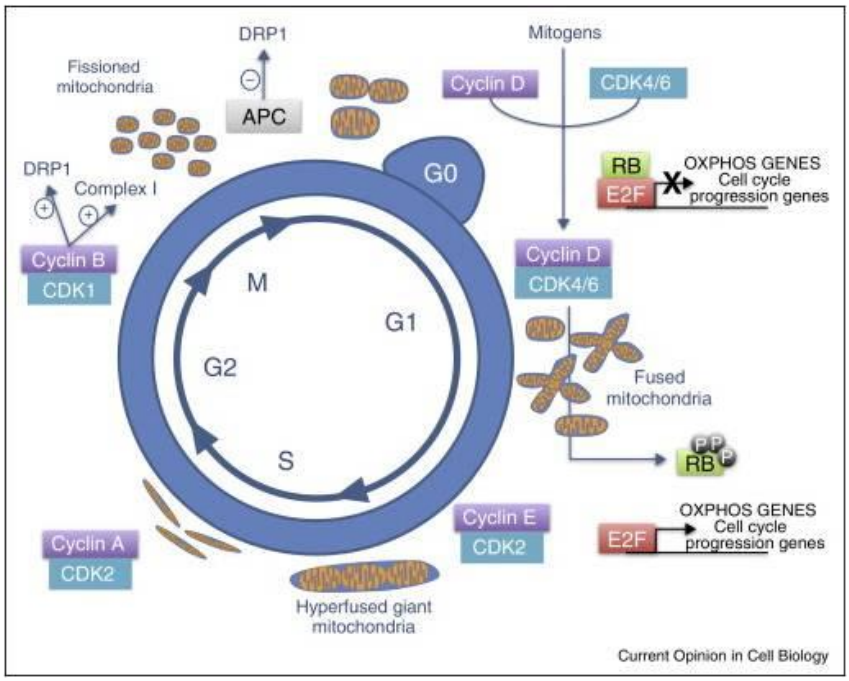

Figure 1.4: Regulation of mitochondrial morphology during the cell cycle

Schematic of cell cycle showing G1 (Growth) phase 1, S (synthesis) phase, G2 (Growth) phase 2, M (mitotic) phase. Mitochondrial shape dynamics change during different cell cycle stages and regulated by Cyclin/CDK complexes. Mitogen induced activation of cyclin D form complex with cyclin4/6 which partially inhibits RB. Inactivation of RB releases E2F to activate genes necessary for OxPhos and cell cycle progression. Mitochondria form hyper fused giant mitochondria in G1-S transition mediated by Cyclin E/ CDK2 complex. In S phase they become elongated by cyclin A/CDK2 activity. Cyclin B/ CDK1 positively regulates Drp1 to cause mitochondrial fragmentation in the M phase. Anaphase promoting complex (APC) inhibits Drp1 during anaphase which results in mitochondrial fusion. (Image adapted from (Lopez-Mejia and Fajas, 2015)

Many eukaryotic cells under starvation tend to contain a fused the mitochondrial network in order to enhance its energy producing capacity to tackle energy deprivation and to protect its mitochondria from autophagic degradation (Rambold et al., 2011). Mitochondria in fibroblasts undergo tubulation when provided with Dulbecco's PBS (DPBS) which lacks specific amino acids such as glutamine. This is a first and rapid response of mitochondria to the nutrient deprivation which is independent of autophagic machinery. Extensive tubulation occurred when additional depletion of glucose and serum takes place. This study indicates that mitochondria can respond to a specific

nutrient condition by changing its morphology (Rambold et al., 2011). Opa1 and Mfns are responsible for mitochondrial fusion under starved conditions. It is also observed that the Drp1 level also goes down to remove the counterbalancing force for unopposed fusion (Rambold et al., 2011). Prolonged starvation conditions trigger an autophagic response in which a cell eats its own components (Scott et al., 2004). It is marked by the formation of autophagosomes around cellular components such as ribosomes, proteins, cell organelles like ER and mitochondria. Selective degradation of excess and damaged mitochondria is termed as mitophagy. It is a process by which cells keep control on mitochondrial numbers and quality (Yoo and Jung, 2018). Under low ATP conditions, AMP-dependent protein kinase (AMPK) gets phosphorylated by AICAR and coenzyme Q10. Activation of AMPK brings about an autophagic response. Damaged mitochondria are sensed by voltage-sensitive kinase, Pink1. Loss of membrane potential triggers Pink1 accumulation on OMM which trigger the recruitment of Parkin to mitochondria. Parkin is an E3 ubiquitin ligase which upon recruitment ubiquitinates various mitochondrial proteins including Mitofusins and VDAC1. Ubiquitinylated proteins facilitate the translocation of autophagy machinery which eventually leads to autophagosomal degradation of damaged mitochondria (Sun et al., 2012). Inhibition of mitophagy by Parkin mutation causes severe neurodegenerative diseases like Parkinson's disease and cancer indicating the importance of the process in normal development (Chen et al., 2010; Kang et al., 2018).

1.1.4 Mitochondrial dynamics and ETC: Function in stem cell proliferation and development in association with different signaling pathways.

Invertebrates vs Vertebrates

How does an organism achieve tremendous diversity and functional coordination in different tissues is an important question in developmental biology. Maintenance of organ size and ultimately the size of the organism is a critical event during development. Tissue homeostasis is attained by a regulated balance between proliferation, determination, and differentiation. Impairments in these functions can lead to

developmental defects and cancer. Recent reports suggest that mitochondria play an important role during proliferation and cell fate determination. Clonal analysis in *Drosophila* follicle cells showed that mutation in Drp1 causes overproliferation in the expense of differentiation. Further analysis indicated that mutant cells fail to exit the cell cycle. They also showed reduced Notch activity in Drp1 mutant cells. Co-depletion of fusion protein Marf restored the mitochondrial morphology and normal Notch function (Mitra et al., 2012). Pluripotent stem cells (PSC) have fragmented mitochondria, low ETC activity and poor cristae organization which hints that mitochondria in stem cells are inactive (Xu et al., 2013). But recent studies have shown that mitochondrial function in stem cells is crucial for stem cell differentiation. Germline stem cell (GSC) differentiation in *Drosophila* oocyte requires ATP synthase activity independent of its role in energy generation (Teixeira et al., 2015). Terminal differentiation of *Drosophila* neuroblasts involves the reduction of cell size during each successive asymmetric division and finally the formation of two daughter neurons. A metabolic shift from glycolysis to oxidative phosphorylation mediated by mediator complex and mitochondrial ETC is required for this process (Homem et al., 2014). In human embryonic stem cells (hESC), mitochondrial function is required for ESC proliferation, differentiation regulation, and prevention of tumorigenesis during differentiation (Wanet et al., 2015).

1.1.5 Mitochondrial function in apoptosis

A mechanism has evolved in the multicellular organism to remove unwanted, damaged and infected cells to ensure the safety of other cells and organisms in whole called apoptosis or programmed cell death. Apoptosis is characterized by cell shrinkage, chromatin margination, and nuclear fragmentation (Cummings and Schnellmann, 2004). Mitochondria perform a central role in the apoptotic pathway. Intrinsic mechanism of apoptosis involves OMM permeabilization release of Cytochrome C from mitochondria, activation of death cascade and finally cell death (Bossy-Wetzel and Green, 1999; Cummings and Schnellmann, 2004; Ott et al., 2002). Multiple factors are responsible for the induction of apoptosis in the cell. Energy stress, oxidative stress, DNA damage act

as a death stimulus that leads cells to undergo apoptosis. The first hallmark event in apoptosis is the permeabilization of OMM to release Cytochrome C and other molecules. Cytochrome c in normal electron transfer activity shuttle electrons from complex III (Cytochrome b-c1 complex) to complex IV (Cytochrome C oxidase complex). The release of cytochrome C into the cytoplasm irrevocably activates the death program (Garrido et al., 2006). In the cytoplasm, Cytochrome C binds to Apaf-1 which causes extensive conformational changes in Apaf-1. Change in the conformation of Apaf-1 results in oligomerization to form a heptameric structure called the apoptosome. Apoptosome then activates procaspase-9 which further activates caspase-3. Activation of caspase-3 trigger series of chain reaction in which hundreds of proteins degraded in a sequential manner which eventually leads to cell death (Saleh et al., 1999; Wang and Youle, 2009).

1.1.6 Mitochondria in human diseases

Mitochondria in neurodegenerative diseases

Studies from last few decades have shown that mitochondrial mutation is involved in a range of neurodegenerative diseases like Parkinson's disease (PD), Alzheimer's disease (AD), dominant optic atrophy (DOA), amyotrophic lateral sclerosis, Charcot Marie Tooth type II A (CMT2A), etc. (Westermann, 2010). In these diseases, either dynamics or metabolism of mitochondria is affected. PD is one of the most common neurodegenerative disorders and characterized by the loss of dopaminergic neurons in the substantia nigra. Genetic studies of PD revealed that this neurogenic disorder is caused by a mutation in five genes such as PTEN- induced kinase 1 (PINK1), Parkin, DJ-1and leucine-rich repeat kinase2 (LRRK2) (Büeler, 2010). Pink1 interacts with Parkin and require for mitochondrial normal functioning. In COS-7 cells, PINK knockdown causes mitochondrial elongation and it can be reversed by overexpression of Fis1 (Su et al., 2010). Inhibition of mitochondrial complex I function by chemical inhibitor shows PD like symptoms (Schapira et al., 1990). ALS is caused by a mutation in Superoxide dismutase 1 (SOD1) (Rosen et al., 1993; Schapira et al., 1990). SOD

acts as a scavenger and reduces the ROS level of the cell. The loss of function of SOD causes the accumulation of ROS. The high concentration of ROS is toxic to neuronal survival as damage mtDNA. mtDNA damage leads to the accumulation of toxic compounds in the neuronal cell and it eventually degenerates (Flynn and Melov, 2013). CMT2A is a disease of the peripheral nervous system caused by a mutation in mitochondrial fusion protein Mfn (Feely et al., 2011). Loss of function of Opa1 causes dominant optic atrophy in which bilateral optic neurons degenerate and result in moderate vision loss (Feely et al., 2011; Pesch et al., 2004). All these studies indicate that mitochondrial function apart from energy production is also important for the normal development of the animal.

1.2 *Drosophila* neuroblasts: Formation and development

1.2.1 Formation

Neural precursor cells, also known as neuroblasts in *Drosophila* arise from the ventral neuroepithelial layer of the *Drosophila* embryo (Cabrera, 1989). The selection and formation of neuroblasts are carried out by a process known as lateral inhibition. Notch-Delta signaling pathway is a major component of this process. Proneural genes such as achaete scute are produced in a group of cells known as a proneural cluster. In lateral inhibition, the central cell of the proneural cluster expresses more Delta which acts as a ligand for Notch present on neighboring cells (Cabrera, 1989). Serrate is another transmembrane protein function a ligand for the Notch receptor. Binding of Delta and Serrate to the Notch receptor results in conformational changes in the Notch receptor which then undergo regulated intramembrane proteolysis (RIP). In RIP, the Notch receptor successively cleaved in a two-step manner, an ectodomain cleavage is followed by intramembranous cleavage. Cleavage of the intramembranous domain results in the release of the Notch intracellular domain (NICD) which then translocates into the nucleus, where it binds to suppressor of hairless [(Su(H)]. NICD and Su(H) together activate the Enhancer of split (*Espl*) gene whose product inactivates

expression of proneural genes in that cell. By this mechanism, the central cell is specified as a neural precursor cell while surrounding cells remain epithelial in nature.

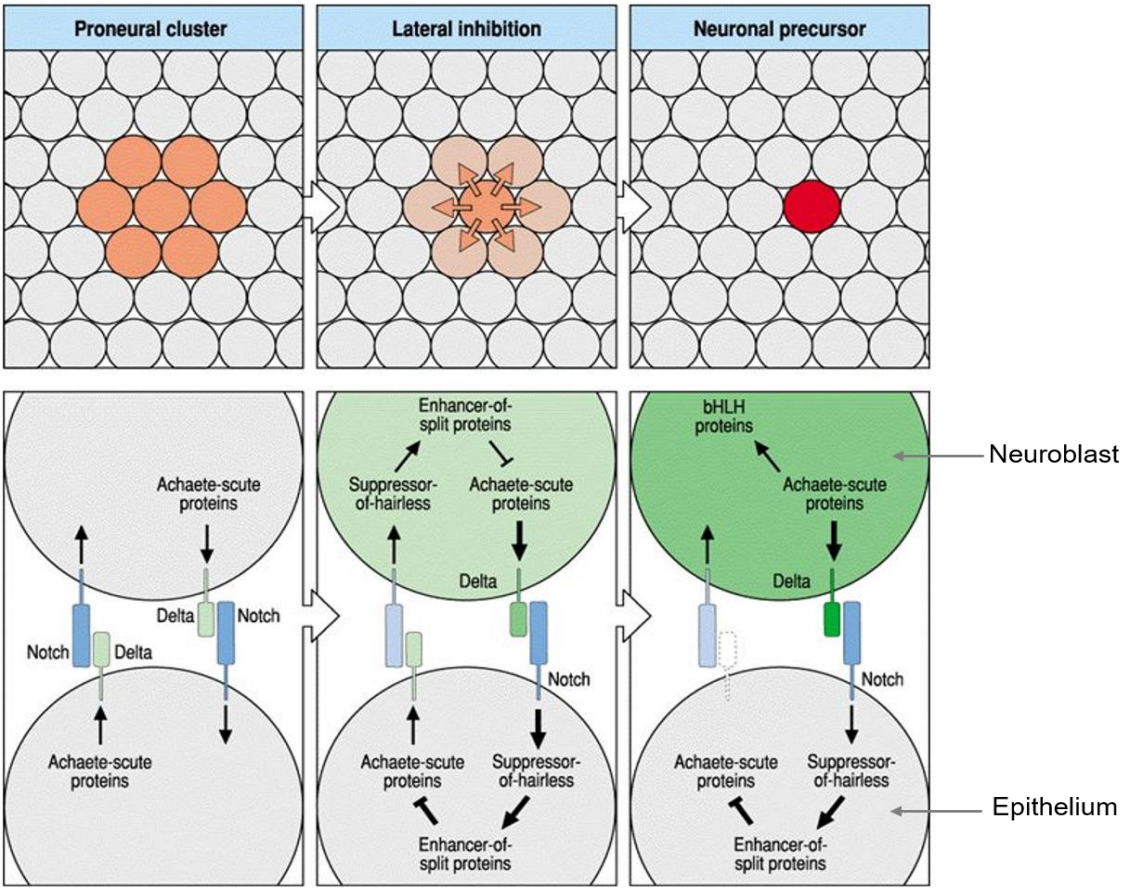

Figure 1.5: Lateral inhibition and Notch-Delta signaling pathway

Schematic showing the selection of neuroblasts from neuroepithelium by the process of lateral inhibition. Cells in the proneural cluster (orange) express proneural factors Achaete-scute proteins which in turn activate Delta, a ligand for Notch receptors. Strong expression of Delta in the central cell of the proneural cluster activates Notch signaling in surrounding cells. In surrounding cells, activation of Notch causes expression of transcription suppressor Enhancer of Split (Espl) through Suppressor of Hairless (SuH). Espl inhibit expression of Achaete scute proteins in surrounding cells result in Delta downregulation and suppression of neural fate in these cells. In the central cell, Achaete scute activates bHLH proteins which in turn activate gene expression program required for neuronal fate. (Image adapted from Khitoeducation website)

1.2.2 Delamination

The neuroblast specification event is followed by delamination from neuroepithelium (Wang & Chia, 2005). Ventral NE cells are connected to each other by zonula adherens (ZA) junction. This is a belt-like junction present at the apico-lateral side of a cell. This mainly comprises of DE-cadherin and catenin. Cells in the neuroepithelium have an equal capability to undergo asymmetric cell division which is blocked by the presence of adherens junctions (Lu, Roegiers, Jan, & Jan, 2001). During the differentiation of epithelial cells to neuroblasts, ZA junctions are removed, cells become rounded and undergo delamination. Disruption of adherens junction and acquisition of round shape by the neuroblast are characteristic features of the delamination process. The transition from columnar to round shape is thought to be an important event in neuroblasts formation. These delaminated round neuroblasts have apicobasal polarity.

1.2.3 Polarity formation

Neuroblasts of *Drosophila* have been extensively studied for localization of different protein complexes and their effect on fate determination. Neuroblast polarity is independent of the polarity determination of intact NE epithelium. Stardust (Std) and Crumbs are required for the formation of neuroepithelium polarity but mutants of these proteins do not affect neuroblast polarity (A. Wodarz & Huttner, 2003). Polarity is a prerequisite for proper spindle orientation and asymmetric cell division (A. Wodarz & Huttner, 2003). *Drosophila* atypical protein kinase C (DaPKC)/ PAR6 complex is present at the apical side of the neuroblast (A. Wodarz et al., 2003). This complex contains proteins from the PAR family including aPKC, PAR6 (fig.6M) and PDZ domain containing protein Bazooka (Baz, human PAR3 homolog) (Stein et al., 2005). Mutation in aPKC/PAR6 complex proteins can cause mislocalization of Miranda (Mira). Mira is an adaptor protein (Shen et al., 1998; Yousef et al.,2008) and has membrane binding domain as well as docking sites for Brain tumor (Brat; mammalian ortholog of Trim2, Trim3, Trim32), transcription factor Prospero (Pros; vertebrate ortholog of Prox1) and Staufen (Stau) (Shen et al., 1998). Another protein complex Inscuteable (Insc) is composed of Partner of Insc (Pins) (mammalian ortholog of Ags3 and Lgn),

protein from G protein family Gαi and Insc (A. Wodarz & Huttner, 2003). The Insc complex binds to Baz via Insc protein and holds this complex at the apical side. Current knowledge about apicobasal polarity in vertebrates shows that proteins present at the apical region of neuroblasts of *Drosophila* are also located at the same site as the neural progenitor of a vertebrate. This indicates functional conservation and impairment of these conserved proteins display the same phenotypes in fly and vertebrates.

1.2.4 Spindle rotation

After neuroblast delamination from the neuroepithelium, basally located centrioles migrate to the AP axis and form spindle fibers parallel to the plane of NE (Januschke & Gonzalez, 2010). Then these spindles rotate by 90° adjusts their plane becomes perpendicular to the NE plane (Kelsom & Lu, 2012). Spindle orientation requires the Insc protein at the apical side. Insc can bind to the spindle via the Mud complex and directs the spindle reorientation (Bowman et al., 2006). Mutation or RNAi mediated depletion of Insc or Mud mutants show a defect in spindle fiber reorientation and ultimately lead to error prone cell division. Misorientation of spindle fiber does not affect neuroblasts polarity but it can affect cleavage plane. Mud mutants show larger neuroblasts as compared to controls but it does not affect apico-basal localization of the cell fate determinants. Pins acts as a bridge between Insc and Gαi (F Yu et al., 2000). During spindle reorientation, apically located Mira is phosphorylated by aPKC and it is recruited to the basal end along with Brat, Pros, Stau (Shen et al., 1998). Brat is a tumor suppressor protein in neuroblasts and downregulation of this protein causes extensive proliferation of neuroblasts and leads to brain tumor formation (Betschingeret al., 2006). Brat is required for maintenance of the number of neuroblasts and to avoid over proliferation.

1.2.5 Neuroblast Division

During asymmetric division, neuroblasts have to maintain their own numbers as well as asymmetric protein distribution. During early anaphase, the cleavage

plane starts to migrate towards the basal cortex, from where basal cells known as ganglion mother cell (GMC) buds off. The arrangement of the spindle is itself asymmetric during anaphase. The sizes of the apical and basal pole are different from each other. The apical pole is always larger than the basal pole (reviewed in A. Wodarz & Huttner, 2003). After Telophase a neuroblast gives rise to two unequal sized daughter cells i.e. neuroblast (self-renewal) and a GMC (Differentiation). During cell division, basally located protein complexes translocate to GMCs where Mira gets degraded (Shen et al., 1998). As a result, Pros becomes free to move into the nucleus where it activates the differentiation program. GMC later divides to form differentiated neurons and/or glial cells (Urbach, 2003)**.** After the recruitment of Mira complex to the basal cortex, the apico-basal polarity of neuroblasts is completed, after which the neuroblast divides asymmetrically and produces another neuroblast and one GMC. GMCs later divide to form a pair of neurons or glia depending upon the transcription program. This division pattern is typical for type I neuroblasts that I shall discuss in more detail in the neuroblast development at the larval stages.

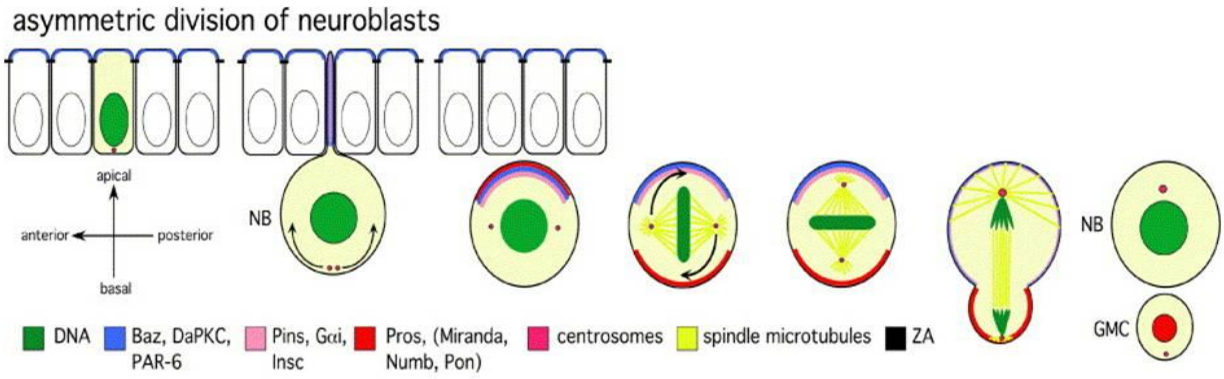

Figure 1.6: Polarity formation and asymmetric division of neuroblast

Schematic showing the formation and development of type I neuroblast in neuroepithelium (NE). Newly formed neuroblast (yellow) delaminates from the NE layer to achieve a round shape. It inherits apical complex including Baz-DaPKC-PAR6 (blue) from epithelial cells. After delamination basally located centrioles migrate to AP pole. In the mitotic phase, spindle fibers originated from these

centrioles rotate division plane by 90º with the help of the Insc-Pins complex (pink). During spindle rotation, apically located Pros-Mira-Numb-Pon (red) complex translocate to the basal pole achieving apicobasal polarity of neuroblast. Then neuroblast undergoes asymmetric cell division in which it retains its identity by self-renewal while producing one differentiated GMC. Basal complex moves into the newly formed GMC where Miranda gets degraded which results in the release of Pros (red) into the nucleus. Pros activate the differentiated program in GMC which further results in the formation of a pair of differentiated neurons or glia. (Image adapted from (Wodarz and Huttner, 2003)

1.2.6 Development of a larval central nervous system

The *Drosophila* nervous system has two phases of neurogenesis. The first wave of neurogenesis occurs during embryonic stages 8 to 11 (reviewed in Homem & Knoblich, 2012). As discussed earlier, embryonic neuroblasts are formed by the mechanism of lateral inhibition in the ventral neuroepithelium. After stage 11 most of the neuroblasts undergo apoptosis while some neuroblasts remain in a quiescent state by cell cycle arrest in the G0 stage (reviewed in Homem & Knoblich, 2012). Once larvae hatch and start to feed on nutritional medium, their nutrient-sensing organ, the fat body gets an amino acid signal which in turn activates the mTOR pathway and sends the signal to the glial cells surrounding the brain (reviewed in Homem & Knoblich, 2012). The glial cells signal the quiescent neuroblasts to activate their cell cycle and divide several times to produce more neurons and glia. This second wave of neurogenesis produces the majority of approximately 90% neurons of the entire nervous system of *Drosophila* (reviewed in Homem & Knoblich, 2012).

The *Drosophila* brain is a bilobed structure with a single ventral nerve cord (VNC). It consists of four different types of neuroblasts. The Central brain (CB) neuroblasts consist of type I neuroblasts and type II neuroblasts that develop from embryonic lineages and are located in the central brain (CB) region. Approximately 90 type I and 8 type II neuroblasts are present in a single lobe of the *Drosophila* brain (Bayraktar *et al.*, 2010). The division pattern of type I neuroblasts is discussed in the previous section. Here I shall discuss the type II neuroblasts division. Type II neuroblasts lack the expression of transcription factor Asense (Ase), hence they are also called as Posterior Asense Negative (PAN) neuroblasts. They express transcription factors like Deadpan

(Dpn), Brat and Numb. The differentiation factor Pros (Pros) which acts as a tumor suppressor is absent from these cells. Hence these lineages are more susceptible to tumor formation. The division pattern of type II neuroblasts is different from type I neuroblasts division based on types of cells and lineages it produces. Division of type II neuroblasts involves the production of transit-amplifying cells termed as intermediate neural precursor cells (INP) (Bello *et al.,* 2008) which divide several times to produce more stem cells (Bayraktar *et al.,* 2010; Boone & Doe, 2008). Production of INPs allows a single type II neuroblast lineage to generate a greater number of differentiated neurons as compared to a type I neuroblasts. Newly produced immature INPs do not divide but undergo a maturation process which takes 5-6 hours. The maturation process involves the sequential expression of different transcription factors. First, it has the expression of Ase followed by expression of Dpn and Pros. Mature INPs are more or less similar to the type I neuroblasts which divide asymmetrically to form GMCs and then a pool of differentiated neurons or glia (Boone & Doe, 2008). Collectively type II neuroblasts generate approximately 5000 neurons which contribute to the formation of the central complex in the adult brain. The central complex is involved in multiple tasks in the adult fly such as navigation, orientation, courtship, etc. It also plays a vital role in the formation and recall of short and long term visual memories.

The other types of neuroblasts are Optic lobe neuroblasts, mushroom body neuroblasts (MBneuroblasts) and ventral nerve cord (VNC) neuroblasts. The VNC neuroblasts consist of abdominal and thoracic neuroblasts and are also developed from embryonic neuroblasts lineage. MBneuroblasts are four in number in each lobe (Orihara-Ono *et al.,* 2005; Kunz *et al.,* 2012) and form olfactory learning and memory centers in the brain (Kunz *et al.,* 2012). Unlike other neuroblasts types, Optic lobe (OL) neuroblasts develop only during larval growth from optic lobe NE (Egger *et al.,* 2007; Reddy *et al.,* 2010)

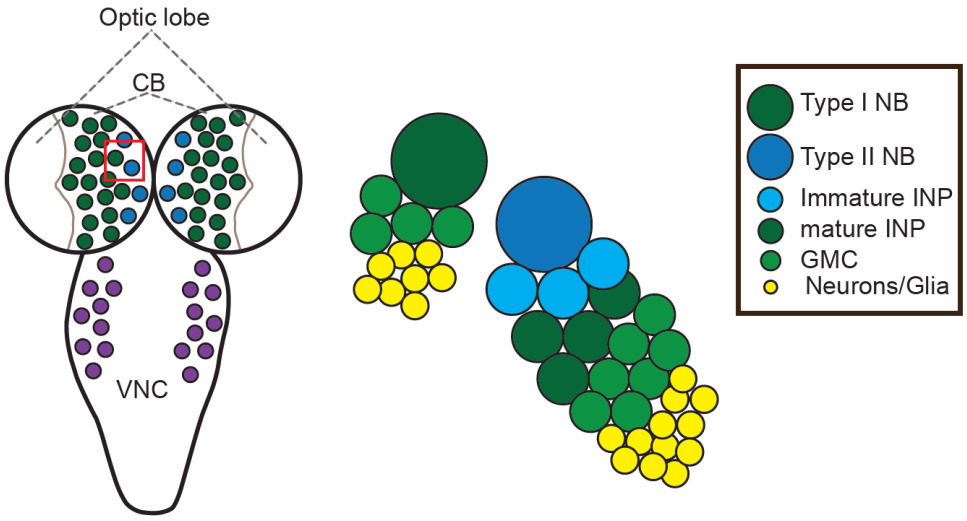

Figure 1.7: Larval central nervous system and lineage development in type I and type II neuroblasts

A) Pictorial representation larval central nervous system. It consists of two round lobes and one ventral nerve cord (VNC). VNC hosts abdominal and thoracic neuroblasts (purple). Lobe is further divided into the optic lobe and central brain (CB). CB contains type I (dark green) and type II (blue) neuroblasts.

B) Division pattern of type I and type II neuroblasts: Type I neuroblast divides asymmetrically to form GMC (pale green). GMC further divide to form neurons or glial cells (yellow).

Type II neuroblast (blue) division includes the transit amplification phase where they divide to form immature INP (pale blue). Immature INP then undergoes a maturation process in which certain transcription factors expressed in a sequential manner. Mature INPs (dark green) are like type I neuroblasts that divide asymmetrically to form GMC (pale green) and GMC divides to form neurons or glia (yellow).

1.2.7 Neuroblasts are a model system to study polarity, cell division and differentiation

Drosophila neuroblasts are a good model to study stem formation and differentiation. All the stem cell properties such as asymmetric cell division, asymmetric distribution of polarity markers, self-renewal and differentiation can be recapitulated in *Drosophila* neuroblasts (Homem and Knoblich, 2012). Various fundamental questions in cell biology, for example, how stem cells achieve unidirectional lineage progression, how

they respond to change in nutrient conditions can be answered by studying neuroblasts development. Various molecular pathways have been studied in neuroblasts such as Notch-Delta, EGFR, Fat-Hippo. Their interplay is also well established in this system. Neuroblast lineages have been well studied and their pattern of development, types of neurons they form are well established in the literature (Egger et al., 2008; Isshiki et al., 2001; Lai et al., 2008; Spana et al., 1995). This system can also be easily explored using various genetic tools and techniques such as the Gal4-UAS binary system, mosaic analysis with repressible cell marker (MARCM), gene editing technique CRISPR-Cas, etc. A lineage-specific analysis is also possible using a lineage-specific Gal4 line. For example, *pointed* (Pnt) Gal4 which expresses only in type II neuroblasts lineage. We can take advantage of this to analyze the function of different proteins in a lineage-specific manner. Recent experiments suggest that neuroblasts can also be cultured *in vitro* without affecting their stemness which enables us to perform RNA sequencing, metabolic assays, etc.

1.3 Aims and objectives of the thesis

As discussed earlier, it is clear that mitochondrial dynamics and metabolism is important for neuronal maturation and synapse function. Surprisingly little is known about mitochondrial dynamics and function in the upstream developmental stages. *Drosophila* neuroblasts provide a good platform to address questions such as is mitochondrial dynamics and its function important for stem cell formation, asymmetric cell division and polarity formation? What would happen to the numbers and lineage of neuroblasts after perturbing mitochondrial dynamics or metabolism or both? Would it affect the proliferation or differentiation pattern of neuroblasts? How do stem cells like neuroblasts respond to change in the metabolic environment of the cell? The major hypothesis that my work derives on is that **mitochondrial morphology and metabolism is crucial for the formation and differentiation of *Drosophila* neural stem cells.**

In order to examine this hypothesis, I have designed the following aims:

1. **Assessment of the effect of mitochondrial morphology protein downregulation in CNS on animal survival, mitochondrial morphology and neuroblast lineage progression.**

2. **Assessment of cell survival and cell cycle defects in mitochondrial dynamics mutants**

3. **Analysis of alteration of mitochondrial activity such as energy stress, ROS, cytochrome C in mitochondrial dynamics in neuroblasts**

4. **Assessment of signaling pathway regulating neuroblast proliferation through mitochondrial morphology and dynamics**

Chapter 2: Materials and Methods

2.1 Materials

2.1.1 Fly stocks

2.1.1.1 Gal4 Lines

Gal4	Specific for	Stock Information
Worniu-Gal4-CD8-GFP	All neuroblasts in the central nervous system	Gift from Jurgen Knoblich, Vienna, Austria
Pointed-Gal4-CD8-GFP	Type II neuroblasts	Gift from Jurgen Knoblich, Vienna, Austria

2.1.1.2 RNAi Lines

RNAi	Function	Stock number
opa1 RNAi	Mitochondrial Inner membrane fusion protein downregulation	BL32358 (BL: Bloomington Stock Number)
opa1 RNAi	Mitochondrial Inner membrane fusion protein downregulation	BL67159
marf RNAi	Mitochondrial outer membrane fusion protein downregulation	A gift from Ming Guo Lab, UCLA
cova RNAi	ETC complex IV downregulation	BL27548

atpb RNAi	ETC complex V downregulation	BL28056
*drp*1 RNAi	Mitochondrial fission protein downregulation	BL27712
drp1^{S193D}	Mitochondrial fission protein mutant	Generated by Darshika Tomer in the Richa Rikhy lab
notch RNAi	Notch signaling downregulation	BL31383
Su(h) RNAi	Notch signaling downregulation	BL67928
drp1^{S193D}; *opa1* RNAi		Generated by standard genetic crosses
drp1^{S193D}; *marf* RNAi		Generated by standard genetic crosses
drp1^{S193D}; *coVa* RNAi		Generated by standard genetic crosses
drp1^{S193D}; *atpb* RNAi		Generated by standard genetic crosses
NV5	Notch full length protein overexpression	Gift from LS Shashidhara lab, IISER, Pune
NV5 /CyOGFP; *opa1* RNAi /TM3SerGFP		Generated by standard genetic crosses

NV5 /CyOGFP; *marf* RNAi /TM3SerGFP		Generated by standard genetic crosses
UAS-Nintra	Notch ICD overexpression	Gift from LS Shashidhara lab, IISER, Pune
Nintra /CyOGFP; *opa1* RNAi /TM3SerGFP		Generated by standard genetic crosses
Nintra /CyOGFP; *marf* RNAi /TM3SerGFP		Generated by standard genetic crosses
UAS-*hid reaper*	Apoptosis inducer	Gift from Krishanu Ray, TIFR, Mumbai
UAS-hSOD1	Human Superoxide Dismutase mutant	BL33607

2.1.2 Antibodies: Table

2.1.2.1 Primary antibody Table

Primary Antibody	**dilution**	**Animal**	**Used for**	**Source**
anti-GFP	1:1000	Chicken	GFP protein	Invitrogen
anti-ATPB	1:200	Mouse	ETC ComplexV	Abcam
anti-Dpn	1:150	Rat	Neuroblasts and Mature INPs	Abcam
Anti-Pros	1:25	Mouse	GMCs	DSHB
Anti-Miranda	1:600	Rat	Neuroblasts	Abcam

Anti-Elav	1:10	Mouse	Differentiated neurons	DSHB
Anti-Broad-core	1:100	Mouse	Neuroblast late temporal marker	DSHB
Anti-CytochromeC	1:200	Rabbit	CytochromeC protein	Cell Signaling
Anti-NICD	1:10	Mouse	Notch	DSHB
Anti-Cleaved Caspase3	1:100	Rabbit	Apoptotic marker	Cell Signaling
Anti-Phosphohistone3	1:1000	Rabbit	Mitotic cells	Invitrogen
Anti-PhosphoAMPK	1:200	Rabbit	Energy sensor	Invitrogen
Anti-LAMP	1:500	Mouse	Lysosomal marker	Abcam
Anti-Cathepsin	1:200	Mouse	Lysosomal marker	Abcam

2.1.2.2 Secondary antibody table

Secondary Antibody	**Dilution**	**Source**
Anti-Mouse 568,633	1:1000	Molecular probes
Anti-Rabbit 568	1:1000	Molecular probes
Anti-Rat 568,633,647	1:1000	Molecular probes
Anti-Chicken 488	1:1000	Molecular probes

2.1.3 Dyes and Drugs

Dyes/Drugs	Used for	Source
Hoechst	DNA marker	Molecular Probes
Dihydroethidium	ROS indicator	Invitrogen
2-Deoxy-glucose	Block glycolysis	Sigma
SlowFade Gold	Anti fading agent	Molecular Probes

2.1.4 *In vitro* Assay Kits: Table

Kit Name	Used for	Source
TUNEL Assay Kit	marking apoptotic cells	Invitrogen C10246
Click-iT EdU Assay Kit	tracing proliferating cells	Invitrogen C10340

2.2 Methods

2.2.1 Fly genetics and crosses

Genetic crosses were performed in standard cornmeal agar medium at 25°C, RNAi experiments were performed at 29°C.

2.2.2 UAS-Gal4 Binary system

We have acquired a yeast UAS-Gal4 binary system in order to achieve tissue-specific downregulation or overexpression of mitochondrial genes in the neuroblasts. Gal4 is a yeast transcriptional factor and has an affinity for the upstream activator sequence (UAS) (Duffy, 2002). Flies containing Gal4 transgenes expressed in a tissue specific manner are crossed to flies having UAS element controlling either an RNAi or

overexpression construct. Binding of Gal4 to UAS leads to activation of gene or RNAi present downstream to the UAS site. Here we have used flies in which the Gal4 gene is expressing under the neuroblast specific promoter such as *worniu*, *pointed*, *inscuteable* and mitochondrial RNAi or overexpression lines under the UAS site.

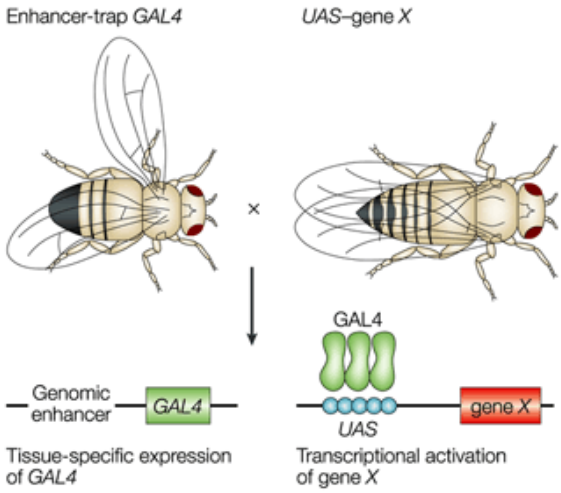

Figure 2.1: UAS- Gal4 binary system

The artificial gene activation/repression system consists of two elements viz Gal4 and UAS i.e. upstream activator sequence acquired from yeast. GAL4 is a yeast transcriptional factor expressed under genomic enhancer which can be cell/tissue/organ-specific. Genetic cross showing the mating of GAL4 containing male with UAS containing female. Progeny possesses both GAL4 and UAS elements. Since GAL4 expression is under tissue-specific genomic enhancer, it will bind and activate UAS only in designated tissue causing expression of gene X present downstream to the UAS site. This system allows tissue-specific upregulation and downregulation of specific genes. (Image adapted from (Muqit and Feany, 2002)

2.2.3 Immunohistochemistry

Third instar wandering larvae were dissected in Schneider's medium and immediately fixed in 4% PFA solution for 25 minutes at room temperature (RT). The brains were washed subsequently with 1X PBS with 0.1% Triton X-100 (PBST) for 30 minutes at

RT. The tissue was then blocked with 1% BSA for 1hr at RT. The brains were stained with the appropriate primary antibody overnight at 4°C. The brains were then washed 3 times with 0.1% PBST (first wash for 20 minutes and remaining for 10 minutes each). An appropriate fluorescently coupled secondary antibody was added for 1hr at RT followed by three washes with 0.1% PBST (first wash for 20min and remaining for 10min each) and mounted in Slow-Fade Gold (Molecular Probes).

2.2.4 Staining and live imaging of ROS

Dissected third instar larval brains were treated with Dihydroethidium (DHE) (1:1000, Molecular Probes) in Schneider's medium for 15 minutes at RT and then washed with Schneider's medium for 10 min. Brains were mounted in LabTek chamber containing Schneider's medium and imaged immediately using Zeiss LSM 710 with a 63x/1.4NA oil objective under the dihydroethidium-1 channel settings in the Zeiss 2010 software. The control and mutant brains were imaged at the same time with the same laser power. The laser power and gain were adjusted to keep the range of acquisition between 0-255 on an 8-BIT scale. The laser power, acquisition speed, frame size and gain were kept the same for both control and mutant.

2.2.5 TUNEL assay

Third instar wandering larvae were dissected in Schneider's medium and fixed in 4% PFA for 25 mins followed by washing with 0.1% PBST for 30 min at RT. Brains then washed twice with 1X PBS for 2 min. Then terminal transferase (TdT) reaction was performed as follows. First brains were treated with TdT reaction buffer and incubated for 10 min followed by treatment of freshly made TdT reaction buffer cocktail (TdT reaction buffer, 5-Ethynyl-dUTP, TdT) for 60 min at 37^{o}C and at 500 rpm. After TdT reaction brains were washed twice with 3% BSA at RT for 5 min. Then Click-iT reaction performed by adding click iT reaction cocktail (Click-iT reaction buffer, Click-iT reaction buffer additive) for 30 min at RT. At this step, samples were protected from light. Brains

were washed with 3% BSA twice for 5 min after removing the Click-iT reaction buffer cocktail and then incubated with Hoechst (1:1000) for DNA staining followed by washing with 1X PBS for 10 min. Samples mounted in Slow-Fade Gold (Molecular probes) and subsequently imaged using Zeiss LSM 710 with a 40x/1.4NA oil objective. UAS-Hid/Reaper line driven by *pointed*-Gal4 was used as a positive control. TUNEL positive nuclei were counted and plotted using GraphPad Prism 5 software.

2.2.6 Cell proliferation analysis by EdU assay

Third instar wandering larvae of selected genotypes were dissected in Schneider's medium and incubated for 1hr in 10µM EdU (5-ethynyl-2´-deoxyuridine) solution at RT followed by fixation in 4%PFA for 25min. Next brains were washed twice,5 min each, with 3% BSA in PBS and then permeabilized in 0.3% PBST for 20min at RT. Brains were then incubated with anti-GFP antibody in 0.3% BSA for 3hrs. After primary antibody incubation, brains were washed twice 5 min each) with PBS and then treated with 0.3% PBST for 20 min. Click-iT reaction cocktail was made according to the manufacturer's instruction. Alexa fluor 488 coupled anti-chicken antibody (1:1000, Molecular Probes) was added in reaction cocktail to detect GFP antibody added in the previous step. Brains were then treated with reaction cocktail for 30 min at RT followed by 3% BSA and 1X PBS wash for 5 min each. For DNA staining, brains were treated with Hoechst (1:1000) in 1X PBS for 10 min and then 5 min wash with 1XPBS and mounted in Slow-Fade Gold (Molecular probes) and subsequently imaged using Zeiss LSM710 with a 40x/1.4NA oil objective.

2.2.7 2-Deoxy Glucose (2-DG) treatment

Third instar larval brains were treated with 500µM 2-DG in Schneider’s medium for 1hr. Control and treated brains were processed for pAMPK immunostaining as mentioned above.

2.2.8 Microscopy and Image acquisition

Imaging of fixed samples using a confocal microscope

Confocal microscopy of fixed samples was done at room temperature using LSM710 or LSM780 inverted microscope (Carl Zeiss, Inc. and IISER Pune microscopy facility) with a Plan apochromat 40x 1.4NA and 63x 1.4NA oil objective. Images were acquired using the Zen2010 software at 1024x1024 pixels with an averaging of 4 and acquisition speed 7. Fluorescence intensity was kept within 255 on an 8-bit scale. The representative image for each type II lineage in the figures is shown from the center of the lineage and comprises the maximum number of cells in the lineage.

Stimulated Emission-Depletion (STED) microscopy for imaging mitochondrial morphology

Super-resolution microscopy was done for visualizing mitochondrial morphology within type II neuroblasts using the Leica TCS SP8 STED 3X Nanoscope with a 100x/1.4NA oil objective. Images were acquired using the LasX software at 1024x1024 pixels to keep pixel size 20-25nm, an averaging of 4, an acquisition speed of 200 and a zoom of 4.5. The Alexa Fluor 488 and 568 were excited with 488nm and 561nm lasers respectively and emission was collected with hybrid detectors for GFP and mitochondria labeled with ATPβ antibody. The 561nm excitation laser with the 775nm depletion laser was used for stimulated emission-depletion for visualizing mitochondria. Fluorescence intensity was kept within 255 on an 8-bit scale using the LUT mode to avoid over-saturated pixels.

2.2.9 Statistical analysis:

Neuroblasts number analysis

Neuroblasts were counted by using Miranda as a neuroblast marker in a single lobe hemisphere across different mitochondrial dynamics mutants and compared with WT. Non-parametric Student t-test was performed for statistical analysis.

The mitochondrial number and area analysis

Control and mutant brains were immunostained with the ATPβ antibody. Qualitative observation of mitochondrial distribution as tubular, clustered and dispersed was made by observing neuroblasts in various genotypes. Quantitative measurements for size and number of mitochondria were also done by using thresholding tool in ImageJ software. A single optical plane was selected approximately in the middle of the type II neuroblasts (section with the highest diameter) where the nucleus was prominently visible and the density of the mitochondria was high. All mitochondrial particles which were above size cut off of 0.12 μm^2 were analyzed for size. To clearly resolve mitochondrial particles in different genotypes we used a water shading tool from ImageJ.

TUNEL analysis

TUNEL positive nuclei per central brain region or type II neuroblasts lineage was counted in lobes of control and *opa1* RNAi and plotted using GraphPad Prism software. We induced apoptosis by expressing UAS-Hid with *pnt* Gal4 as a positive control for TUNEL assay.

ROS intensity analysis

Intensities of DHE in neuroblast and differentiated cells were measured in WT and mutant brains using ImageJ and plotted as ratios using GraphPad Prism software. Non-parametric Student t-test was performed for statistical analysis

EdU Analysis

All EdU positive cells were counted in single type II lineage for WT and mutant brains and plotted using GraphPad Prism software. Non-parametric Student t-test was performed for statistical analysis.

pH3 Analysis

pH3 positive cells were counted in type II lineage for WT and mutant brains and plotted using GraphPad Prism software. Non-parametric Student t-test was performed for statistical analysis.

Dpn and Pros quantification

Dpn positive mature INPs were counted in each type II lineage in WT and mutant brains. The number of mature INPs were then plotted using GraphPad Prism software and non- parametric Student’s t-test was performed for statistical analysis. Nuclear Pros containing GMCs were quantified in the same way

Chapter 3: Assessment of the effect of mitochondrial dynamics mutants on animal survival, mitochondrial morphology and neuroblast lineage progression

3.1 Introduction

Mitochondrial function is essential for the development and survival of an organism. Several studies on mitochondrial dynamics and function emphasized the role of mitochondria in cellular survival and organism as a whole. Mutation in mitochondrial fusion protein Opa1 causes mitochondrial fragmentation which has a deleterious effect on embryogenesis of the mouse (Davies et al., 2007; Kushnareva et al., 2016). Opa1 mutant embryos show severe developmental defects including growth retardation, exencephaly and abnormal anteroposterior patterning and death at E11.5 (Moore et al., 2010). As discussed in the introduction section, a mutation in mitochondrial proteins causes severe neurodegenerative diseases showing the importance of mitochondria in normal development.

Drosophila provides a good model system to study the effect of mitochondrial mutations on animal development. In addition, about 60% of human genes associated with cancer and other genetic diseases are found in *Drosophila* (Mirzoyan et al., 2019). The life cycle of a *Drosophila* takes 10 days at room temperature which allows us to analyze multiple generations in a very short period. A single female adult fly lays around 750-1500 eggs in her lifetime and this allows us to screen for multiple progenies in a single experiment. Fly development starts with the egg, which then hatches into a larva. After undergoing three instar stages namely first instar, second instar, third instar, larva form the pupa in which it undergoes a metamorphosis. Metamorphosis is a process in which functional organs develop from structures called imaginal discs present in the larval body. Adult flies then eclose from pupae within 8 days of larval hatching (Fernández-Moreno et al., 2007). Different stages of *Drosophila* allow studying the effect of mutations in a stage-wise manner during development. In this chapter, we have

analyzed the effect of mitochondrial fusion and fission proteins in *Drosophila* CNS and on animal development in general by downregulating proteins involved in mitochondrial dynamics using different RNAi and CNS specific Gal4 lines. Further, we checked the effect of these downregulations on animal survival and neural stem cell development.

3.2 Material and methods

3.2.1 Fly stocks

3.2.1.1 Gal4 fly stocks: *pnt*-Gal4*,* UAS-mCD8-GFP, *wor*-Gal4*,* UAS-mCD8-GFP, *prospero*-Gal4, *elav*-Gal4, *scabrous*-Gal4*,* UAS-mCD8-GFP.

3.2.1.2 RNAi fly stocks: *opa1* RNAi (Ming Guo, UCLA), *opa1* RNAi (BL32358), *marf* RNAi (Ming Guo, UCLA), *marf* RNAi (BL31157), $Drp1^{S193D}$ (GTPase domain mutant), *drp1* RNAi (BL51483), $Drp1^{S193D}$; *opa1* RNAi *,* $Drp1^{S193D}$; *marf* RNAi.

3.2.2 Antibodies:

Primary antibodies: anti-GFP (1:1000, Invitrogen), anti-ATPB (1:200, Abcam), anti-Bazooka (1:1000), anti-Numb (1:500), anti-Pros (1:25, DSHB), anti-Dpn (1:150, Abcam), anti-Miranda (1:600, Abcam), anti-Elav (1:10, DSHB)

Secondary antibodies: anti-Mouse 568,633 (1:1000, Molecular Probes), anti-Rabbit (1:1000, Molecular Probes), anti-Chicken (1:1000, Molecular Probes), anti-Rat (1:1000, Molecular Probes)

Please refer to section 2.1.2 for detailed information about antibodies and their respective dilutions

3.2.3 Immunohistochemistry: The control and mitochondrial mutant brains of third instar larvae were dissected and processed for immunostaining. Please refer to section 2.2.3 for a detailed immunostaining procedure.

3.2.4 Image acquisition and analysis: Confocal microscopy of fixed samples was done at room temperature using LSM710 or LSM780 inverted microscope (Carl Zeiss, Inc. and IISER Pune microscopy facility) with a Plan apochromat 40x 1.4NA and 63x 1.4NA oil objective. We used a STED microscope to acquire high-resolution images of mitochondria in the neuroblasts. Please refer to section 2.2.8 and 2.2.9 for detailed information about image acquisition and analysis

3.3 Results

3.3.1 Alteration of mitochondrial morphology in CNS causes developmental arrest in *Drosophila.*

In order to check the effect of mitochondrial dynamics protein downregulation on central nervous system development, we performed RNAi screening in which we used different RNAi lines specific for mitochondrial dynamics proteins Opa1, Marf and Drp1 were reduced in CNS development. For knockdown of each protein, we used at least two RNAi lines. These RNAi lines were crossed with multiple Gal4 lines which specifically expresses in different parts of the nervous system. The *inscuteable*-Gal4, *prospero*-Gal4 and *worniu*-Gal4 express in all types of neuroblasts in CNS. The *pointed*-Gal4 expression is limited to only type II neuroblasts in the brain. The *scabrous*-Gal4 expresses in sensory organ precursor cells in the larval wing disc. Gal4 virgin females were crossed with UAS-RNAi males along with control (Gal4/+ alone) on standard cornmeal agar medium and kept at two different temperatures, 25°C, and 29°C. Then we analyzed different developmental stages of control and mutant animals. More than 50 animals were scored for each cross and observations were recorded in tabular format given below (observation table 1).

We found pupal lethality in Opa1 RNAi (BL32358) and Marf RNAi (Ming Guo lab) when expressed using *worniu*-Gal4 (29°C), *inscuteable*-Gal4 (25°C), *prospero*-Gal4 (25°C). Expression of the same RNAi lines resulted in a strong sluggish phenotype when crossed with *pointed*-Gal4 (29°C) and *worniu*-Gal4 (25°C). The Opa1 RNAi (BL32358) gave stronger phenotypes as compared to Opa1 RNAi (Ming Guo Lab). The Marf RNAi (Ming Guo Lab) gave stronger phenotypes as compared to Marf RNAi (BL31157) with *inscuteable*-Gal4, *prospero*-Gal4 and *elav*-Gal4. Hence we chose these RNAi for further study. Drp1 RNAi (BL51483) showed pupal lethality with *inscuteable*-Gal4, *prospero*-Gal4 and *elav*-Gal4 at 25°C. Drp1 RNAi (VDRC 44155) did not show any defect in adult eclosion and behaviour when expressed by using *inscuteable*-Gal4 and *prospero*- Gal4. Expression of both Drp1 RNAi (BL51483) and Drp1 RNAi (VDRC 44155) by using *scabrous*-Gal4 resulted in sluggish behaviour. Interestingly, expression of Drp1 dominant negative allele, Drp1SD, did not show any behavioral phenotype or lethality with *worniu*-Gal4 (25°C and 29°C) and *pointed*-Gal4 (25°C and 29°C). From the above observations, it is clear that mitochondrial dynamics proteins Opa1, Marf and Drp1are important for animal development and downregulation of these proteins in CNS causes developmental arrest at the pupal stage. However, the effect of each depletion is variable depending on the type of Gal4 and effectiveness of RNAi lines. We observed that different RNAi used target the same protein show varied phenotype. There are multiple explanations for observation. One of the reasons could be knockdown efficiency of RNAi lines used to deplete target protein and the other reason is due to a variable lifetime of the protein in cells. Sometimes RNAi designed against a short specific region in target RNA leads to the formation of truncated proteins, which further alter the expression levels of the targeted protein. RNAi efficiency also depends upon the type of vector used to deliver this RNAi. Due to these reasons we can get phenotypic variation even if we target the same protein using multiple RNAi. Results with *pointed*-Gal4 did not show any lethality because of their limited expression only in type II neuroblasts. Studies have shown that type II neuroblasts are not required for animal viability and complete loss of type II neuroblasts does not cause lethality. However mitochondrial protein downregulation in type II neuroblasts does show sluggishness as these flies did not climb or fly properly.

Observation table 1

Gal4	RNAi	Source	Embryo	Larva	Pupae	Adults
worniu-Gal4	*marf* RNAi	Ming Guo Lab	+	+	+	Sluggish adults emerged from pupa
25ºC	*opa1* RNAi	BL32358	+	+	+	Sluggish adults emerged from pupa
	$Drp1^{SD}$	Made in Lab	+	+	+	Normal
worniu-Gal4	*marf* RNAi	Ming Guo Lab	+	+	+	No adult emerged from pupa
29ºC	*opa1* RNAi	BL32358	+	+	+	No adult emerged from pupa
	$Drp1^{SD}$	Made in Lab	+	+	+	Normal
pointed-Gal4	*marf* RNAi	Ming Guo Lab	+	+	+	Normal
25ºC	*opa1* RNAi	BL32358	+	+	+	Normal
	$Drp1^{SD}$	Made in Lab	+	+	+	Normal
pointed-Gal4	*marf* RNAi	Ming Guo Lab	+	+	+	Sluggish adults emerged from pupa
29ºC	*opa1* RNAi	BL32358	+	+	+	Sluggish adults emerged from pupa
	$Drp1^{SD}$	Made in Lab	+	+	+	Normal
inscuteable-Gal4	*marf* RNAi	BL31157	+	+	+	Normal
25ºC	*marf* RNAi	Ming Guo Lab	+	+	+	No adult emerged from pupa
	opa1 RNAi	Ming Guo Lab	+	+	+	Normal
	opa1 RNAi	BL32358	+	+	+	No adult emerged from pupa
	drp1 RNAi	VDRC 44155	+	+	+	Normal
	drp1 RNAi	BL51483	+	+	+	No adult emerged from pupa
prospero-Gal4	*marf* RNAi	BL31157	+	+	+	Normal
25ºC	*marf* RNAi	Ming Guo Lab	+	+	+	No adult emerged from pupa
	opa1 RNAi	Ming Guo Lab	+	+	+	Normal
	opa1 RNAi	BL32358	+	+	+	No adult emerged from pupa
	drp1 RNAi	VDRC 44155	+	+	+	Normal
	drp1 RNAi	BL51483	+	+	+	No adult emerged from pupa
elav-Gal4	*marf* RNAi	Ming Guo Lab	+	+	+	Few escaper adults emerged from pupa
25ºC	*opa1* RNAi	Ming Guo Lab	+	+	+	Few escaper adults emerged from pupa
	opa1 RNAi	BL32358	+	+	+	No adult emerged from pupa
	drp1 RNAi	BL51483	+	+	+	No adult emerged from pupa
scabrous-Gal4	*marf* RNAi	BL31157	+	+	+	Normal
25ºC	*marf* RNAi	Ming Guo Lab	+	+	+	Highly sluggish adults emerged from pupa
	opa1 RNAi	Ming Guo Lab	+	+	+	Normal
	opa1 RNAi	BL32358	+	+	+	No adult emerged from pupa
	drp1 RNAi	VDRC 44155	+	+	+	Sluggish adults emerged from pupa
	drp1 RNAi	BL51483	+	+	+	Highly sluggish adults emerged from pupa

* Deng et al., 2008

Observation Table 1:

Various Gal4 drivers were crossed with mutants of mitochondrial morphology genes at 25 or 29 ^{o}C and lethality or behavioral phenotype was recorded in the adult. *worniu*-Gal4 (*wor*-Gal4), *inscuteable*-Gal4, *prospero*-Gal4 and *scabrous*-Gal4 express the Gal4 in all neuroblasts, *pointed*-Gal4 (*pnt*-Gal4) express in type II neuroblasts and *elav*-Gal4 express in neurons. Adult flies from crosses with *wor*-Gal4 (25 ^{o}C) and *pnt*-Gal4 (29 ^{o}C) with *opa1* RNAi and *marf* RNAi were sluggish and the numbers obtained were at the expected frequency, no lethality was seen at the pupal stage. *elav*-Gal4 crosses gave lethality and few adults emerged. The *opa1* RNAi BL32358 gave stronger phenotypes as compared to *opa1* RNAi Ming Guo lab with *inscuteable*-Gal4, *prospero*-Gal4, *elav*-Gal4 and *scabrous*-Gal4. The *marf* RNAi Ming Guo lab gave stronger phenotypes as compared to marf RNAi BL31157 with *inscuteable*-Gal4, *prospero*-Gal4, and *elav*-Gal4. Hence we chose *opa1* RNAi BL32358 and *marf* RNAi Ming Guo lab for further analysis. The Drp1 RNAi from VDRC was weak and the Drp1 (TRIP collection, Val20, BL51483) gave inconsistent results, hence we used a lab generated GTPase domain mutant Drp1^{SD} for further analysis.

3.3.2 Downregulation of mitochondrial fusion proteins caused fragmentation while Drp1SD exhibit clustered mitochondria in neuroblasts.

In order to visualize the mitochondrial structure, we stained control third instar larval brains which were expressing UAS-CD8-GFP with *worniu*-Gal4 with ATPB antibody which targets ATP synthase beta subunit embedded in the inner mitochondrial membrane. Image acquisition was done by using STED microscopy which allowed us to resolve the mitochondrial structure better than conventional confocal microscopy. Neuroblast lineages were marked by membrane bound CD8-GFP expressed under *pointed*-Gal4. We found mitochondria to be present as a fragmented and tubular structure in control neuroblasts (Figure 3.1A). Downregulation of mitochondrial fusion proteins Opa1 and Marf showed fragmented morphology while overexpression of functionally null mutant of Drp1, Drp1SD showed clustered mitochondria on one side of the neuroblasts (Figure 3.1A). Further, we quantified mitochondrial area and number in type II neuroblasts by selecting maximum intensity optical plane. All mitochondrial particles which were above size cut off of 0.12μm^2 were selected and analyzed by ImageJ software. We observed that depletion of mitochondrial Opa1 and Marf caused an increased number of mitochondrial particles while there was a reduction in per mitochondrial area indicating mitochondrial fragmentation in these cells (Figure 3.1 B-

C). Drp1, on the other hand, showed increased mitochondria area and decreased mitochondrial numbers (Figure 3.1 B-C). These results showed that RNAi and mutant lines we were using had the appropriate and expected effect on mitochondrial morphology as seen in HeLa cells (Olichon et al., 2003), mouse embryonic fibroblast (Debattisti et al., 2014; Olichon et al., 2003) and *Drosophila* neurons (Trevisan et al. 2018). Further, we tested the effect of these morphology manipulations on neuroblast development.

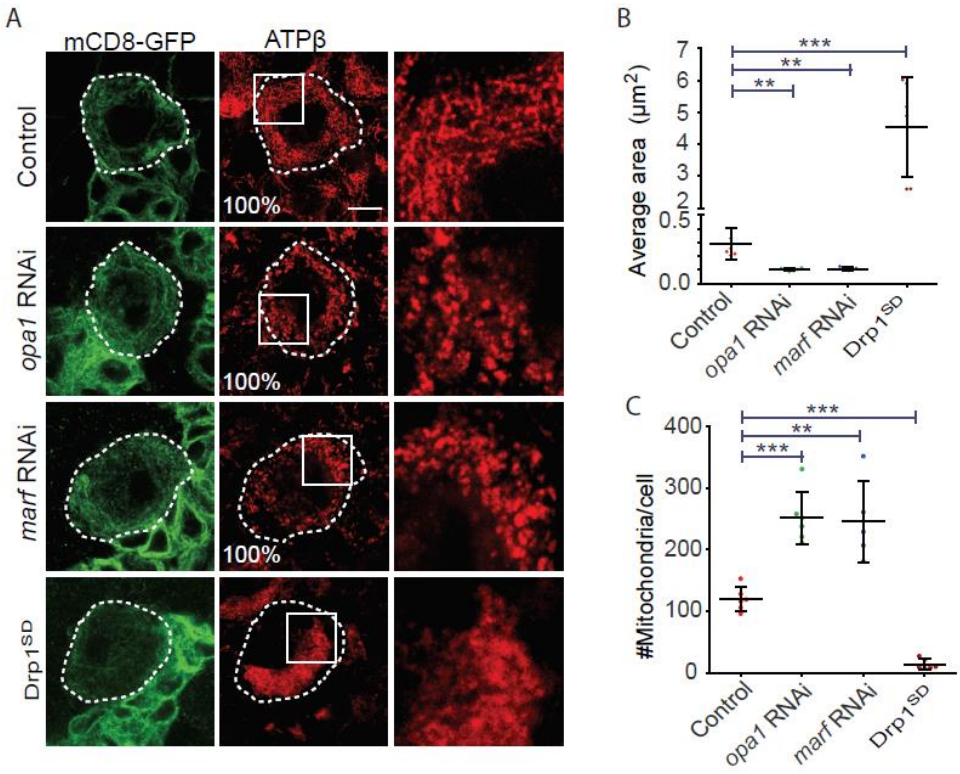

Figure 3.1: Mitochondria are fused in WT neuroblast and downregulation Opa1 and Marf cause mitochondrial fragmentation while depletion of Drp1 causes mitochondrial clustering.

A: Mitochondrial morphology characterization in morphology mutants. Super-resolution images of mitochondria stained with ATPB antibody and acquired using STED technique in Drosophila type II neuroblasts showing fused morphology in WT while appears fragmented in fusion mutants. Drp1SD expression showed mitochondrial clustering at one side of the neuroblast. *pnt*-Gal4 was used to drive the expression of RNAi and mutant.

WT (75 neuroblasts,22 Brains), opa1 RNAi (46,8), marf RNAi (45,8), drp1SD (80,10). mCD8 GFP expressed by *pnt* Gal4 to mark type II neuroblasts lineage. Cell boundary is marked by a white dotted line and a small magnified area of respective genotypes shown in the right panel. Scale bar- 5um

B: Quantification of the mitochondrial average area in control and mutant neuroblasts showed the decreased area in Opa1 and Marf knockdown while increased in Drp1 depletion. Control (6 type II neuroblasts, 3 brains), *opa1* RNAi (6,3), *marf* RNAi (5,3), $Drp1^{SD}$(6,3)

C: Analysis of mitochondrial number showed the increased mitochondrial number in Opa1 and Marf downregulation while decreased in Drp1 depletion compared to Control. Control (6 type II neuroblasts, 3 brains), opa1 RNAi (6,3), marf RNAi (5,3), Drp1SD (6,3).

Student's t-test is performed for statistical nalysis. **-p<0.01, ***- p<0.001.

3.3.3 Mitochondrial morphology perturbation does not affect neuroblast number and polarity.

The central brain of the *Drosophila* larvae has 89-100 neuroblasts per brain lobe. Type I neuroblasts are 85-90 in number while there is only 8 type II neuroblasts present in each lobe of the *Drosophila* larval CNS (Homem and Knoblich, 2012). To check the effect of mitochondrial morphology perturbation on neuroblasts number we expressed RNAi against Opa1 and Marf and mutant Drp1 in neuroblasts by using *worniu*-Gal4 and *pointed*-Gal4 drivers. *worniu*-Gal4 express in all neuroblasts irrespective of neuroblast type while *pointed*-Gal4 express only in type II neuroblasts. All crosses were set at 29ºC to achieve maximum downregulation of mitochondrial protein function. Third instar wandering larvae were dissected for each genotype and brains were stained with neuroblast marker, Miranda. We then counted the number of neuroblasts present in the central brain using Miranda as a neuroblast marker. For each genotype, we analyzed at least 10 brains and data were analyzed and compared with control (*worniu*-Gal4 CD8GFP/+) using Student t-test. We did not find a change in neuroblast numbers on down regulation of mitochondrial fusion and fission proteins (Figure 3.2 A-B). There were approximately 100 neuroblasts on downregulation of Opa1, Marf and Drp1 with *worniu*-Gal4. Similarly, downregulation of mitochondrial proteins using *pointed*-Gal4 did not affect type II neuroblast number as they were consistently 8 in number (Figure 3.2 C). This data suggests that there is no defect in neuroblast formation on downregulation of mitochondrial dynamics proteins in the *Drosophila* CNS.

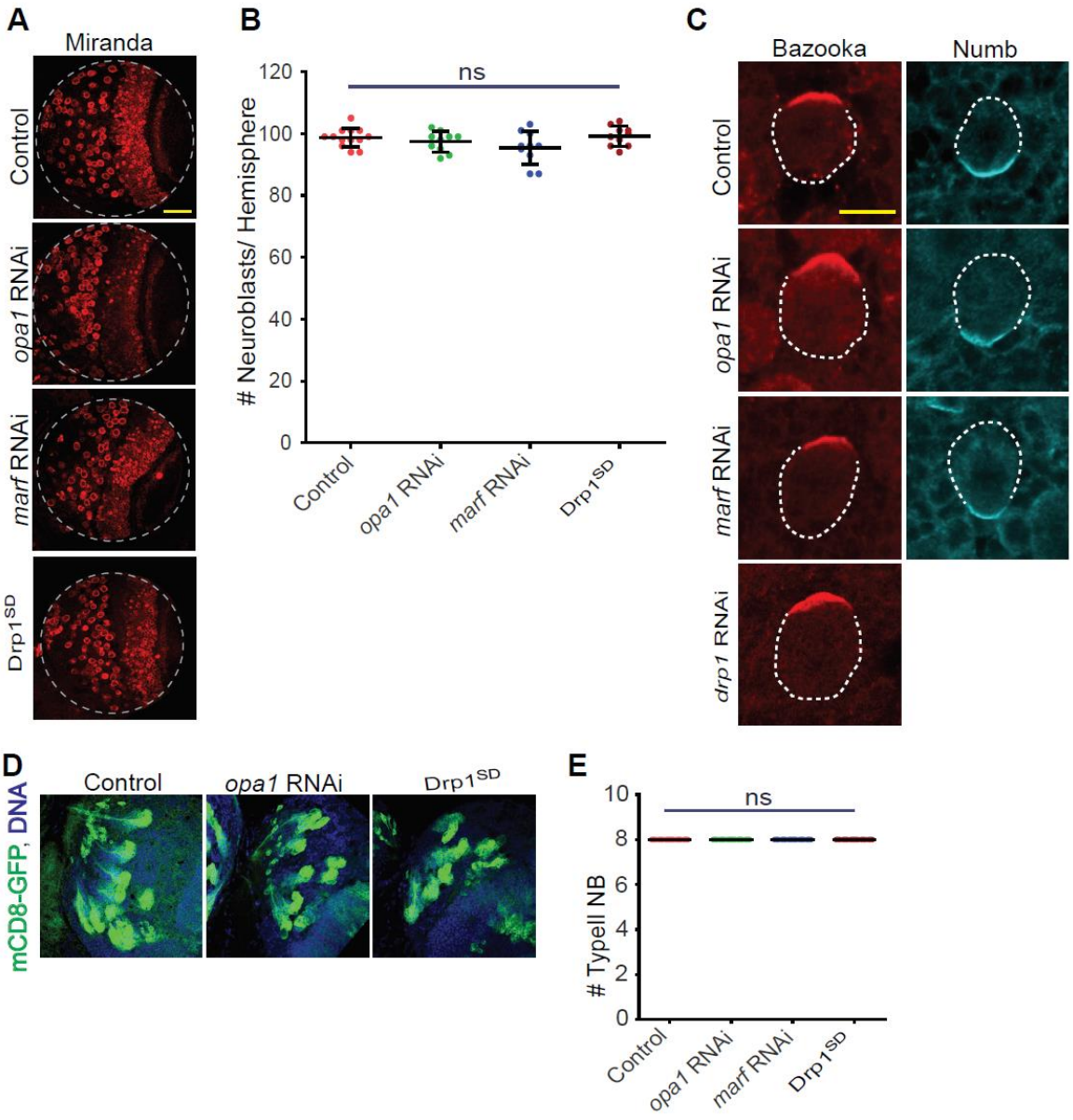

Fig. 3.2: Downregulation of mitochondrial dynamics proteins Opa1, Marf and Drp1 have no effect on neuroblast number and polarity.

A: Representative confocal images of larval brain lobes stained for Miranda (red) showing no change in neuroblasts number. Expression of *opa1* RNAi, *marf* RNAi and Drp1^{SD} mutant was done by *wor*-Gal4.

B: Quantification of neuroblasts number in larval brain lobes (D) of control (13 lobes,13 brains), *opa1* RNAi (10,10), *marf* RNAi (10,10), Drp1^{SD} (10,10). Scale bar- 50µm.

C: Representative images showing apical and basal localization of Bazooka and Numb respectively in control and mitochondrial dynamics mutants (B). Scale bar- 10µm.

D: Representative confocal images of brain lobe showing type II neuroblasts lineages (green).

E: Number of type II neuroblasts and cells per lineage in control, *opa1* RNAi, *marf* RNAi, $Drp1^{SD}$ (n= 30 neuroblasts lineages,15 brains each).

Student's t-test is performed for statistical analysis. ns – Non significant

Neuroblasts exhibit apicobasal polarity in the mitotic phase of the cell cycle. Different cell fate determinants are localized at the apical and basal poles of neuroblasts (Januschke and Gonzalez, 2008). Since mitochondrial perturbation did not affect neuroblasts number, we further analyzed the effect of downregulation of mitochondrial dynamics proteins on neuroblast polarity. Larval brains were immunostained with different polarity markers such as apical marker Bazooka and basal marker, Numb. Polarised distribution of Bazooka and Numb was seen similar to controls in neuroblasts containing a downregulation of mitochondrial dynamics proteins. We did not find any defects in neuroblast polarity formation in any mitochondrial dynamics mutants (Figure 3.2 D). Together these results show that mitochondrial morphology regulation is dispensable for the formation of neuroblasts as well as the asymmetric distribution of polarity proteins in neuroblasts.

3.3.4 Analysis of neuroblast differentiation in mitochondrial morphology protein mutants.

Since perturbation of mitochondrial morphology using CNS specific gal4 affected animal development but had no effect on neuroblast number or polarity we further analyzed neuroblast differentiation. As discussed in the introduction, type I neuroblast divides asymmetrically to form a neuroblast and a differentiated GMC. The GMC population can be identified by the presence of nuclear Pros. Pros is a transcription factor which upon nuclear translocation activates the differentiation program in GMC. We probed control and mutant brains with an antibody against Pros. Analysis of immunofluorescence images of these genotypes revealed that Opa1 had a reduced GMC population (Figure 3.3 A-B). In order to confirm this result we immunostained brains with an antibody against the neuronal marker, Elav. It is known that GMC divides to form a pair of neurons or glia. So if the GMC population is reduced then we can expect to see a

reduced population of neurons also. Consistent with previous results we found reduced neuronal population marked with Elav (Figure 3.3 C) suggesting the importance of mitochondrial fusion protein Opa1 in neuroblast differentiation.

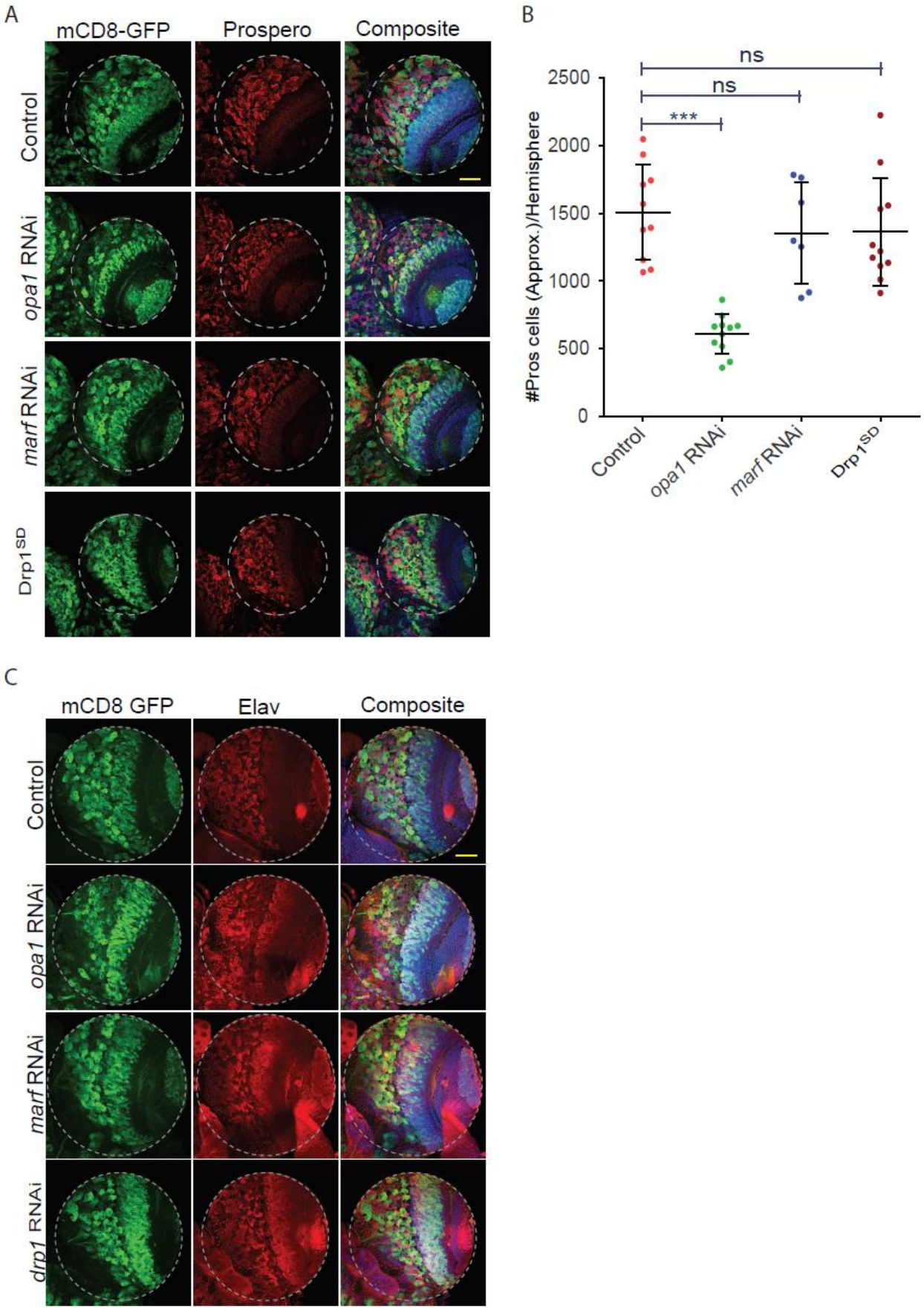
A
mCD8-GFP
Prospero
Composite
Control
opa1 RNAi
marf RNAi
Drp1SD
B
ns
ns
***
2500
2000
1500
1000
500
0
#Pros cells (Approx.)/Hemisphere
Control
opa1 RNAi
marf RNAi
Drp1SD
C
mCD8 GFP
Elav
Composite
Control
opa1 RNAi
marf RNAi
drp1 RNAi

Fig 3.3: Downregulation of Opa1 and not Marf and Drp1 in type I neuroblasts causes a reduction in Pros positive GMC and Elav positive neuronal population.

A: Representative images of brain lobes showing reduced Pros positive GMC population in *opa1* RNAi. Scale bar- 50µm
B: Analysis of Pros positive GMCs (F) in control (10 lobes,10 brains), *opa1* RNAi (11,11), *marf* RNAi (7,7), $Drp1^{SD}$ (11,11). Student's t-test is performed for statistical analysis. ns – Non-significant, ***- p<0.001.
C: Representative images of brain lobes showing reduced Elav positive GMC population in *opa1* RNAi. control (10 lobes,10 brains), *opa1* RNAi (11,11), *marf* RNAi (7,7), $Drp1^{SD}$ (11,11).Scale bar- 50µm. *wor*-Gal4 was used to drive the expression of RNAi and mutant.

Type II neuroblasts lineage comprises intermediate transit amplification step which is carried out by INP. Newly formed INPs undergo the process of maturation in which expression of transcription factors sequentially takes place. Asense expressed in the beginning which is followed by the expression of Dpn and then Pros. Mature INPs are similar to type I neuroblasts where they undergo asymmetric division to form GMC and then neurons in the later division (Homem and Knoblich, 2012). Type II neuroblasts lineage development scheme allows us to perform lineage-specific studies since most of the genetic markers are known. We further tested the effect of downregulation of mitochondrial dynamics protein in type II neuroblasts lineages using *pointed*-Gal4. Lineages are marked by expression of CD8GFP under *pointed*-Gal4 control. Mature INPs were identified by the presence of a nuclear Dpn antibody signal in lineage whereas GMCs marked by nuclear Pros. The number of mature INPs and GMCs were counted separately for each lineage in control and mitochondrial dynamics mutants. We found that the overall differentiated population including immature INP, mature INP and GMC were reduced in Opa1 while it was unchanged in Marf downregulation (Figure 3.4 A). Drp1SD showed slightly increased differentiated cells compared to control (Figure 3.4 A). Furthermore, a separate analysis of Dpn positive mature INP and Pros positive GMC showed reduced cells in Opa1 knockdown (Figure 3.4 B-D). Interestingly Marf downregulation exhibited slightly increased Mature INPs but reduced GMC cells in the type II neuroblasts lineage (Figure 3.4 B-D). Drp1SD overexpression did not show any effect on either population (Figure 3.4 B-D).

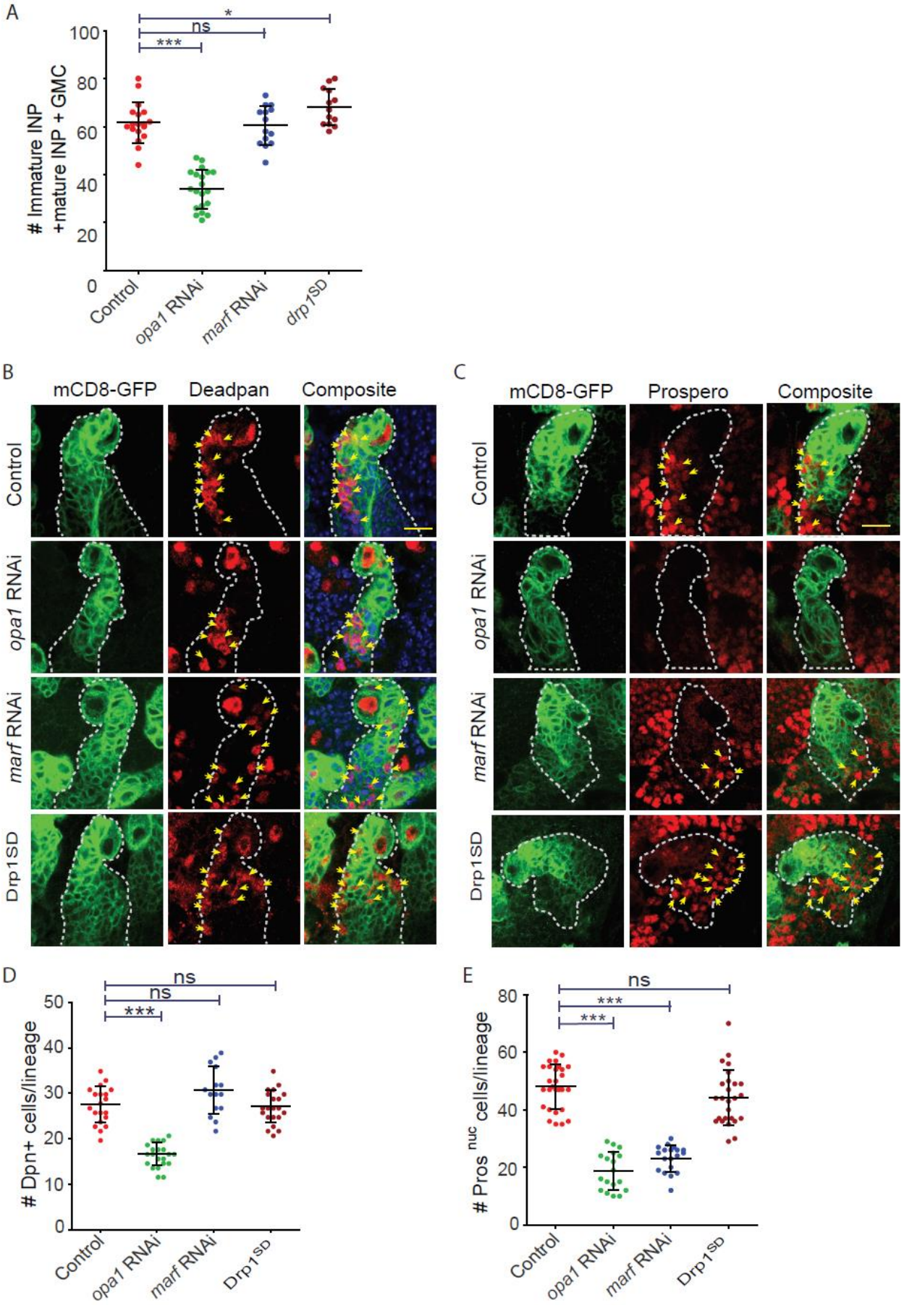
A
*
ns
***
100
80
60
40
20
0
Immature INP
+mature INP + GMC
Control
opa1 RNAi
marf RNAi
drp1SD
B
mCD8-GFP
Deadpan
Composite
Control
opa1 RNAi
marf RNAi
Drp1SD
C
mCD8-GFP
Prospero
Composite
Control
opa1 RNAi
marf RNAi
Drp1SD
D
ns
ns
***
50
40
30
20
10
0
Dpn+ cells/lineage
Control
opa1 RNAi
marf RNAi
Drp1SD
E
ns
***
***
80
60
40
20
0
Pros nuc cells/lineage
Control
opa1 RNAi
marf RNAi
Drp1SD

Fig. 3.4: Downregulation of Opa1 causes reduced differentiated population in type II neuroblasts.

A: The total number of differentiated cells per lineage is reduced in *opa1* RNAi (E). Control (18,6), *opa1* RNAi (20,6), *marf* RNAi (14,5), $Drp1^{SD}$ (13,5).

B & C: Dpn positive INPs (red, yellow arrows) are reduced in *opa1* RNAi (B &D) and Pros (red, yellow arrows) positive GMCs are lowered in *opa1* RNAi and *marf* RNAi expressing type II neuroblasts (C & E). *pnt*-Gal4 was used to drive the expression of RNAi and mutant.

D: Quantification of Dpn positive INPs in control (n=15 neuroblasts lineages, 5 Brains), *opa1* RNAi (21,6), *marf* RNAi (13,8), $Drp1^{SD}$ (28,10).

E: Quantification of Pros positive GMCs in type II lineages (E) of control (28,8), *opa1* RNAi (18,5), *marf* RNAi (19,5), $Drp1^{SD}$ (26,9). Scale bar- 10µm

A,D,E: Statistical analysis is done using an unpaired t-test. ns=non-significant, **- $p<0.01$, ***- $p<0.001$.

Together these results indicated that mitochondrial fusion proteins Opa1 and Marf are important while fission protein Drp1 is dispensable for differentiation in type II neuroblasts lineage.

3.3.5 Co-depletion of Drp1 to cause forced mitochondrial fusion in Opa1 and Marf mutants rescue type II neuroblast differentiation.

We then asked whether reduced differentiation in mitochondrial fusion protein downregulation was because of perturbation in mitochondrial morphology. To address this question we restored fused mitochondrial morphology by combining Drp1SD overexpression with Opa1 and Marf RNAi lines. Analysis of mitochondrial structure showed fused mitochondrial morphology in double mutants (Figure 3.6 A-C). Mitochondria in Opa1 and Drp1 double mutants were often present in blobs as compared to Drp1SD or Opa1 RNAi alone (Figure 3.6A). Marf and Drp1 double depletion showed a slightly resolved network as compare to Drp1SD alone (Figure 3.6 A). We also performed a control experiment to check whether a slight resolved mitochondrial network was not due to Gal4 dilution. To address this, we co-expressed UAS-RFP with Drp1SD. We found similar mitochondrial clustering as Drp1SD alone (Fig. 3.5 A-B). This result ruled out the possibility of Gal4 dilution in Drp1SD co-

depletion experiments. We did a differentiation analysis in these mutants. Dpn positive mature INP population was completely restored in Opa1 downregulation when co-depleted for Drp1 (Figure 3.6 D-E). However, we observed partial rescue in the GMC population in these double mutants (Figure 3.6 F-G).

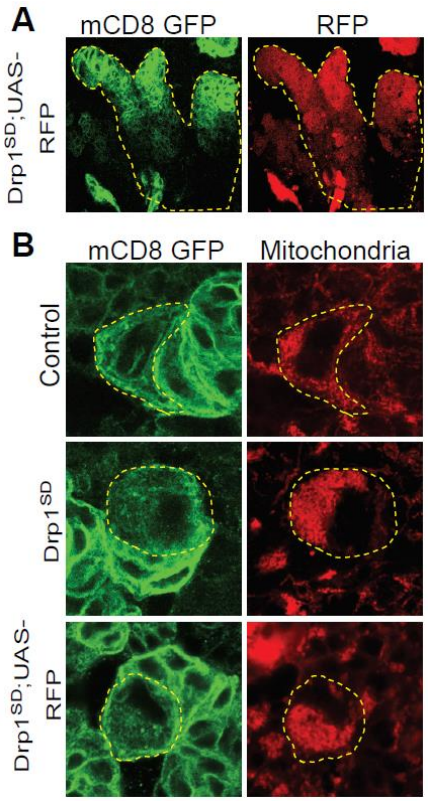

Figure 3.5: Co-expression of UAS-RFP does not dilute the effect of Drp1SD on mitochondrial clustering.

Representative confocal images of type II neuroblasts stained with RFP and ATPB showing mitochondrial clustering. Control (100%, 75 Neuroblasts, 22 Brains), Drp1SD (80%, 80 Neuroblasts, 10 Brains), Drp1SD;UAS-RFP (80%, 48 Neuroblasts, 6 Brains)

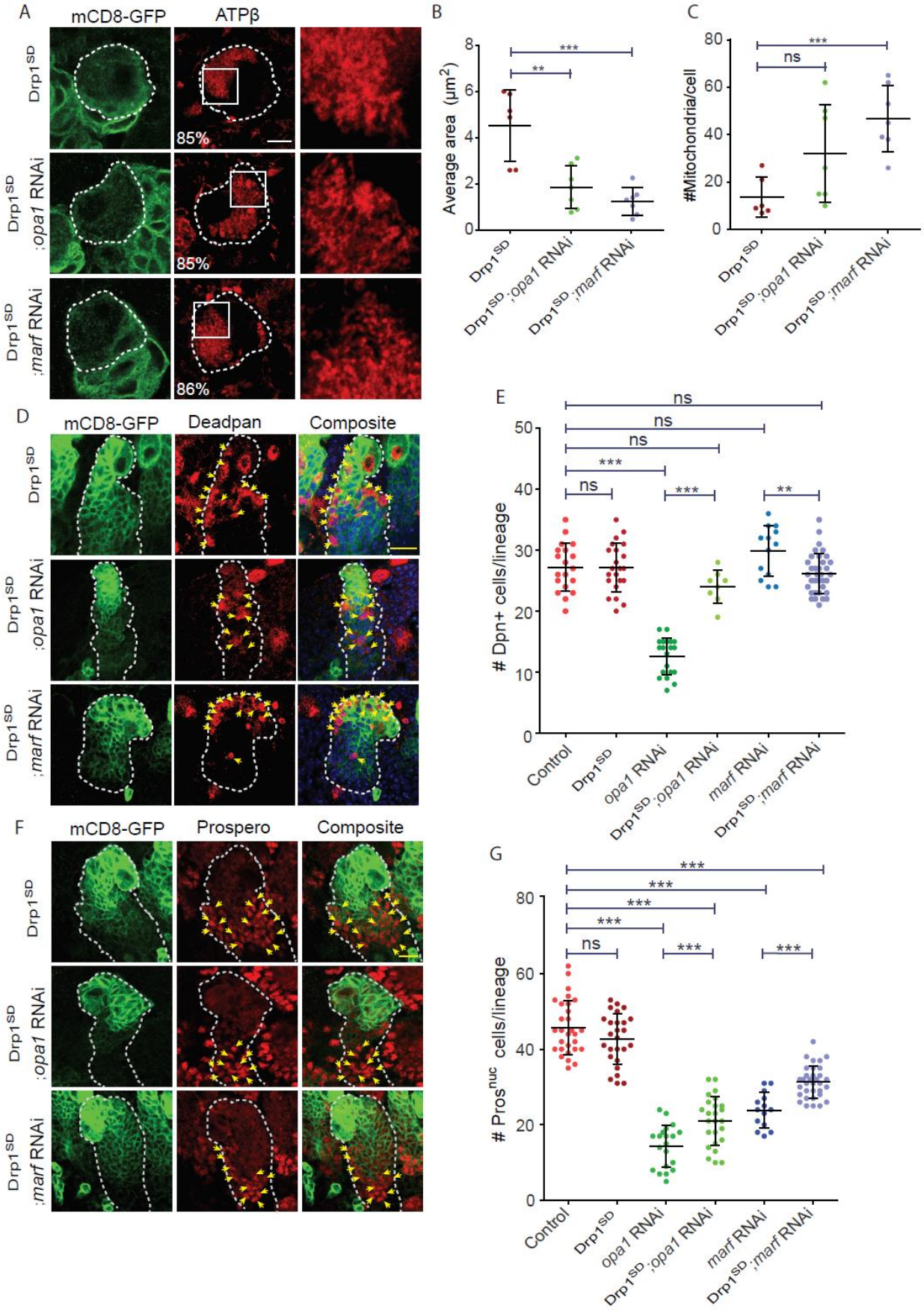
A
mCD8-GFP
ATPβ
Drp1SD
Drp1SD ;opa1 RNAi
Drp1SD ;marf RNAi
85%
85%
86%
B
Average area (μm2)
Drp1SD
Drp1SD ;opa1 RNAi
Drp1SD ;marf RNAi
C
#Mitochondria/cell
ns
D
mCD8-GFP
Deadpan
Composite
E
Dpn+ cells/lineage
Control
opa1 RNAi
marf RNAi
F
mCD8-GFP
Prospero
Composite
G
Prosnuc cells/lineage

Fig 3.6: Forced mitochondrial fusion by co-depletion of Drp1 rescues Dpn positive mature INPs and partially rescues Pros positive GMCs in Opa1 downregulation.

A-C: Type II neuroblasts (white dotted line) marked by mCD8-GFP (green) stained for mitochondrial morphology with ATPβ (red) and imaged using STED (A). $Drp1^{SD}$ (85% clustered, 80 neuroblasts,10 Brains), $Drp1^{SD}$;*opa1* RNAi (85% clustered, 96,12), $Drp1^{SD}$;*marf* RNAi (86% clustered, 96,12). Quantification of average mitochondrial area (B) in type II neuroblasts of $Drp1^{SD}$ (6,3), $Drp1^{SD}$;*opa1* RNAi (7,4), $Drp1^{SD}$;*marf* RNAi (7,4). Quantification of mitochondrial numbers (C) in type II neuroblasts of $Drp1^{SD}$ (6,3), $Drp1^{SD}$;*opa1* RNAi (7,4), $Drp1^{SD}$;*marf* RNAi (7,4). Scale bar- 10µm. *pnt*-Gal4 was used to drive the expression of RNAi and mutant.

D-E: Type II neuroblasts lineages (yellow dotted line) showing expression of mCD8-GFP (green) and Dpn (red, yellow arrows) (D). Quantification of Dpn positive mINPs (E) in control (23 neuroblasts lineages,16 brains), $Drp1^{SD}$ (28,10), *opa1* RNAi (20,8), $Drp1^{SD}$;*opa1* RNAi (8,6), *marf* RNAi (13,8), $Drp1^{SD}$;*marf* RNAi (35,8). Scale bar- 10µm.

F-G: Type II neuroblasts lineages (yellow dotted line) showing expression of mCD8-GFP (green) and Pros (red, yellow arrows) (F). Quantification of Dpn positive mINPs (G) in control (29 neuroblasts lineages,18 brains), $Drp1^{SD}$ (26,8), *opa1* RNAi (20,8), $Drp1^{SD}$;*opa1* RNAi (26,8), *marf* RNAi (14,8), $Drp1^{SD}$;*marf* RNAi (33,8). Scale bar- 10µm

B,C,E & G:Comparative analysis was done by using unpaired t-test. ns- non significant, **- $p<0.01$, ***- $p<0.001$

Taken together these data indicate that fused mitochondrial morphology is essential for neuroblast differentiation and depletion of mitochondrial fusion proteins Opa1and Marf leads to loss of differentiation. Furthermore depleted numbers of differentiated cells can be rescued by force mitochondrial fusion.

3.4 Discussion

Previous studies on mitochondrial morphology in different types of stem cells suggested that stem cells harbor small and fragmented mitochondria. These mitochondria are associated with low ATP production, low membrane potential, low mitochondrial DNA copy number. Here we have shown that mitochondrial morphology is a combination of tubular and fragmented in *Drosophila* larval neural stem cells i.e. in neuroblasts and fused architecture is also important for neuroblast differentiation. The neuroblast needs to divide its mitochondrial content into daughter cells. Our analysis showed that in Drp1

mutant despite harboring clustered probably hyper fused mitochondria, neuroblasts had no defects in terms of polarity, number and differentiation profile. This means that despite having a fused architecture, mitochondria are partitioned to the differentiated cells. On the other hand, mitochondrial fragmentation caused by depletion of mitochondrial fusion proteins Marf and Opa1 caused the loss of differentiation in neuroblast lineages. However, Opa1 and Marf did not affect neuroblast number and polarity. These results suggest that mitochondrial dynamics is not needed for neuroblast selection but for the later developmental stages. The depletion of mitochondrial dynamics proteins in CNS caused pupal lethality. This result was probably due to a lack of neurons that regulate muscle movement required for the eclosion process during late pupal stages.

Another important observation we made was that the differentiation defects caused by inner membrane fusion protein Opa1 depletion were more severe as it caused a reduction in both mature INP and GMC cells in type II neuroblast lineage compared to outer membrane fusion protein Marf depletion which resulted in the loss of GMCs only. This is one of the most interesting observations that we have made during the analysis of the role of mitochondrial fusion in neuroblast differentiation. Opa1 depletion causes a reduction in INP and GMC populations in type II neuroblast lineage while Marf depletion results in the depletion of only the GMC population. The phenotypic variation of these proteins suggests that there is a difference in the function of these proteins during neuroblast differentiation. Marf is known to be involved in the fusion of the outer membrane protein while Opa1 is involved in the fusion of the inner mitochondrial membrane. Our analysis shows that inner mitochondrial fusion regulated by Opa1 and therefore fusion of the inner mitochondrial membrane per se are more important for neuroblasts development as compared to outer membrane proteins. Interestingly depletion of other inner membrane proteins belonging to the electron transport chain also causes a similar phenotype of loss of differentiation as compared to that of Opa1. These data together suggest that inner mitochondrial membrane organization is likely to affect an organization in electron transport chain complexes and this is crucial for differentiation.

Interestingly, the reduction in the population of differentiated cells in fusion mutants was rescued by forced fusion of the outer mitochondrial membrane by co-depletion of Drp1. This result is significant because it highlights the importance of mitochondrial fusion during neuroblast differentiation. This result also emphasizes that defects in differentiation due to depletion of Opa1 and Marf were not because of the non-mitochondrial role of these proteins but specifically because of changed mitochondrial architecture. However, forced fusion did not rescue Pros positive GMCs completely in type II neuroblast lineages suggesting some defects caused by fusion protein knockdown were irreversible. Depletion in the number of differentiated cells in Opa1 and Marf knockdown lineages could be because of cell death or reduced cell proliferation. In the next chapter, we have addressed both of these possibilities. We have also seen that Opa1 depleted type II neuroblasts were expressing Broad which is a late neuronal factor while downstream lineages had very few Broad positive cells compared to control (Appendix Figure A1C). It is possible that a reduced number of differentiated populations in Opa1 mutant type II neuroblast lineage could be due to premature expression of Broad in neuroblasts. It will be interesting to see whether Broad level rescues in forced mitochondrial fusion or not. Further experiments by ectopic expression of Broad in the neuroblasts would tell whether differentiation defects are due to abnormal Broad expression or its just a consequence. Together this data showed mitochondrial fusion is indispensable for neuroblast differentiation and loss of mitochondrial fusion leads to differentiation defects in neuroblasts. Additionally forced fusion rescues differentiation to a great extent. In the following chapter, we will attempt an analysis of changes in mitochondrial activity and the cell cycle that cause defects in differentiation.

Chapter 4: Analysis of energy stress, ROS, cytochrome C in mitochondrial dynamics mutant neuroblasts

4.1 Introduction

Mitochondria are essential components of energy production through ETC which harvests more ATP from glucose as compared to anaerobic respiration (Osellame et al., 2012). Fused mitochondria tend to produce more ATP as compared to their fragmented counterparts (Westermann, 2012). Mitochondrial fusion supports densely arranged cristae and formation of ETC supercomplexes which further enhances the efficiency of the ETC process (Jiang et al., 2017). The fused mitochondrial architecture allows diffusion of energy metabolites such as ADP, NADH and FADH2 within mitochondrial tubules (Jiang et al., 2017). Under stress conditions, mitochondria tend to form a fused network in order to compensate for cellular energy demand (van der Bliek, 2009). These pieces of evidence suggest how mitochondrial metabolism is linked to its architecture. As discussed and shown earlier, fusion proteins Opa1 and Marf are crucial for mitochondrial fusion and downregulation of the same resulted in mitochondrial fragmentation. There are several consequences of fissioned mitochondria such as lowered ATP production, high ROS generation, lower membrane potential. Fragmented mitochondria have loose cristae morphology which does not favor oligomerization of respiratory complexes which in turn results in lowering of ATP production (Cogliati et al., 2016). Reduced ATP level triggers phosphorylation of AMP-dependent kinases (AMPK) in the cell. pAMPK promotes catabolic processes involved in ATP production and thus maintain ATP levels in the cell.

Generally, ROS is produced as a consequence of ETC activity. Electrons transferred within ETC complexes react spontaneously with oxygen leading to the formation of superoxide along with other ROS. ROS is essential to maintain the redox state of the cell but an increase in ROS level beyond a certain limit is detrimental to the cell (Schieber and Chandel, 2014). Damaged mitochondria produce high ROS which further leads to apoptosis. Another consequence of the change in mitochondrial

morphology is the release of cytochrome C from mitochondria to the cytoplasm where it initiates a series of reactions that finally lead to cell death (Cai et al., 1998).

In this chapter, I will analyze different cellular consequences of fragmented mitochondria caused by depletion of mitochondrial fusion proteins Opa1 and Marf in terms of energy stress, ROS increment, cytochrome C release.

4.2 Materials and methods

4.2.1 Fly stocks: *pointed*-Gal4*,* UAS-mCD8-GFP, *worniu*-Gal4*,* UAS-mCD8-GFP *opa1* RNAi (Ming Guo, UCLA), *opa1* RNAi (BL32358), *marf* RNAi (Ming Guo, UCLA), *marf* RNAi (BL31157), $Drp1^{S193D}$ (GTPase domain mutant), *drp1* RNAi (BL51483), $Drp1^{S193D}$; *opa1* RNAi*,* $Drp1^{S193D}$; *marf* RNAi, UAS-*hid reaper*, hSOD1 mutant (BL33607)

4.2.2 Antibodies: Primary antibodies: anti-phosphoAMPK (1:100, Invitrogen), anti-cytochrome C (1:200, Cell Signaling). Please refer to section 2.1.2 for detailed information about primary and secondary antibodies.

4.2.3 Immunohistochemistry: Third instar larval brains were dissected in Schneider's medium and subsequently processed for immunostaining. Please refer to section 2.2.3 for the detailed procedure.

4.2.4 DHE treatment: Control and mutant brains were dissected in Schneider's medium and further incubated with DHE (1:1000, Molecular Probes) for 15 minutes at RT. Brains were washed and mounted in Schneider's medium. Live imaging of the brain was carried out by using a Zeiss LSM 710 with a 63x/1.4NA oil objective under the dihydroethidium-1 channel settings in the Zeiss2010 software. Please refer to section 2.2.4 for the detailed procedure.

4.2.5 2-DG treatment: Third instar larval brains were treated with 500µM 2-DG in Schneider's medium for 1hr. Control and treated brains were processed for pAMPK immunostaining as mentioned in section 2.2.7.

4.2.6 TUNEL Assay: Third instar larvae were dissected in Schneider's medium and fixed in 4% PFA at RT. Further control and mutant brains were processed for TUNEL assay described in materials and methods section. For detailed information about TUNEL assay please refer to section 2.2.5.

4.2.7: EdU proliferation assay: The control and mutant brains were incubated with 10µM EdU for 1 hour. Further brains were fixed and processed for EdU staining as described in section 2.2.6 of materials and methods.

4.2.6 Image acquisition and analysis: Please refer to section 2.2.8 and 2.2.9 for detailed information about image acquisition and analysis

4.3 Results

4.3.1 Neuroblasts do not undergo energy stress upon mitochondrial fusion protein depletion.

In order to identify the mechanism by which mitochondria regulate neuroblast lineage progression, we checked different cellular consequences of fragmented mitochondria. Fissioned mitochondrial are known to produce less energy as the fragmented structure does not support the formation of ETC supercomplexes, cristae are loosely organized which reduces electron transport activity (Cogliati et al., 2016; Xu et al., 2013).

To assess whether the depletion of mitochondrial fusion proteins leads to energy stress in neuroblasts, we analyzed pAMPK levels in these mutant neuroblasts. pAMPK acts as an energy sensor. Under low ATP and high AMP conditions, AMPK gets phosphorylated by different kinases results in elevated levels of pAMPK in the cell (Hardie et al., 2012). Hence an increase in the levels of pAMPK in the cell occurs if the cell is undergoing energy stress. We probed control and mitochondrial fusion mutant brains with the pAMPK antibody. This antibody detects phosphorylation at the T172 residue in AMPK. For positive control, we treated brains with 2-deoxy glucose (2DG), an inhibitor of glycolysis. Neuroblasts rely on glycolysis for energy generation and inhibition of glycolysis is therefore likely to increase AMP and pAMPK levels. Interestingly knockdown of glucose transporter protein Glut1 in neuroblasts also caused adult lethality in our genetic screen (observation table 2). We analyzed pAMPK intensity as compared to neighboring cells in the lineage in control and mutant type II neuroblasts along with the addition of 2-DG. As expected neuroblasts from 2-DG treated brains showed an increase in pAMPK signal in neuroblasts (Figure 4.1 A-B). But we did not find increased levels of pAMPK in Opa1 and Marf mutant neuroblasts (Figure 4.1 A-B). This result suggested that mitochondrial fusion downregulation does not cause energy stress in type II neuroblasts.

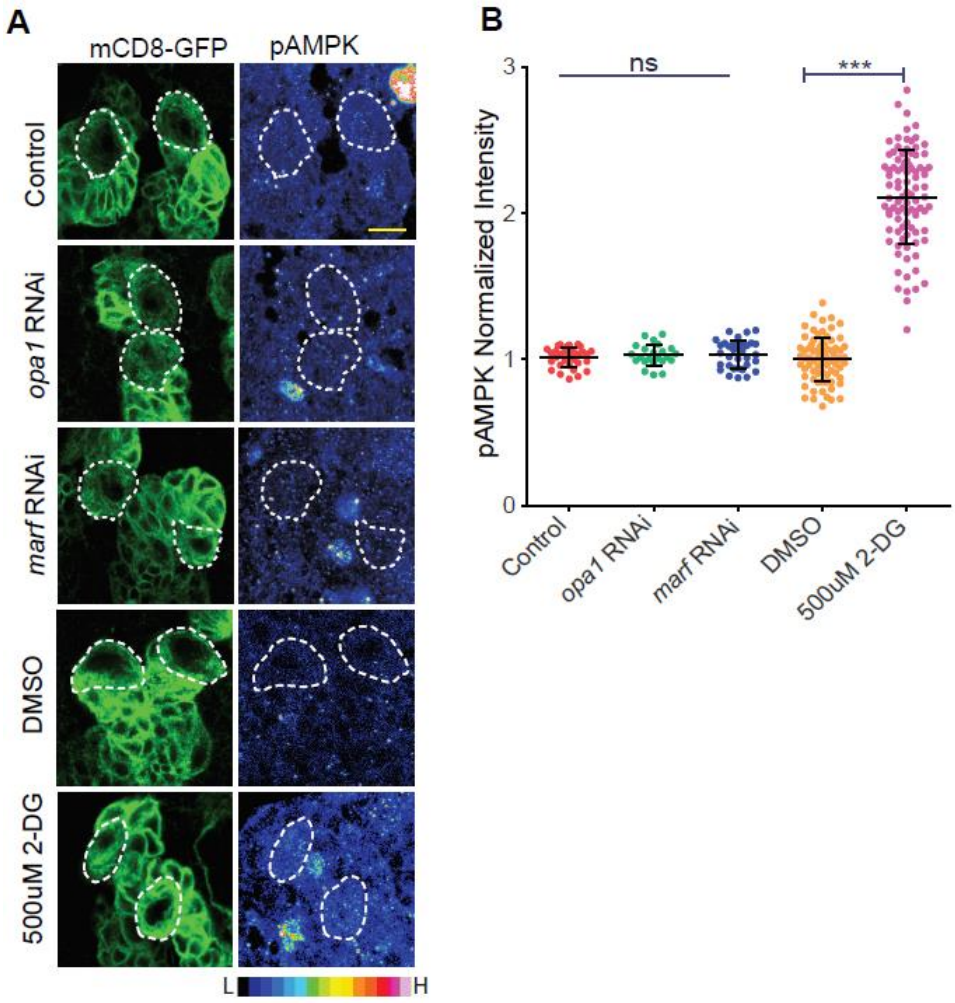

Fig 4.1: Knockdown of Opa1 and Marf does not cause energy stress in type II neuroblasts.

A: Representative images of type II neuroblasts showing unaffected levels of pAMPK represented as rainbow scale in mitochondrial dynamics mutants. Type II neuroblasts are marked by white dotted lines while lineages are marked by expression of mCD8-GFP (green). *pnt*-Gal4 was used to drive the expression of RNAi. Scale bar- 10uM

B: Analysis of pAMPK intensity normalized with neighboring control cells. Control (41 neuroblasts, 14 brains), *opa1* RNAi (33,8), *marf* RNAi (23,8), DMSO (76,8), 2-DG (91,9). Student's t-test is performed for statistical analysis. ns – Non significant, ***- p<0.001.

4.3.2. ROS is elevated in mitochondrial fusion protein Opa1 and Marf downregulation.

A change in mitochondrial architecture can cause elevated levels of ROS in cells. It has been observed that fragmented mitochondrial architecture is associated with increased ROS production (Yu et al., 2006). To check ROS levels in the mitochondrial mutants we incubated control and mutant brains with 30 nM Dihydroethidium (DHE) in Schneider's medium for 15 min. DHE is a redox sensitive dye which upon entry into the cell gets oxidized by superoxide species present in the cell. Upon oxidation, DHE converts to 2-hydroxyethidium which has emission spectra from 590-620 that can be detected by using an appropriate filter. After a single wash with fresh Schneider's medium, we immediately performed live imaging of neuroblasts with respective controls. DHE intensities for each genotype were measured in the neuroblasts as compared to background cells and plotted in the graph. We found high DHE fluorescence and therefore high cytoplasmic ROS level in Opa1 type II neuroblasts mutants whereas Marf downregulation showed increased ROS in the punctate form present in the cytoplasm (Figure 4.2 A-B). We found a similar trend in type I neuroblasts. Another interesting observation we made was, Opa1 mutants showed ROS increment in neuroblasts as well as its progenies whereas it was restricted to neuroblasts in Marf knockdown (Figure 4.2 A-B). We expressed a mutant allele of the human homolog of superoxide dismutase (SOD) as a positive control for ROS increase. SOD acts as a scavenger for ROS in the cell and mutation in SOD causes elevated ROS levels in the cell (Figure 4.2 A-B). Even though the hSOD mutant showed elevated levels of ROS in neuroblasts, it did not have any effect on neuroblasts differentiation or animal survival. We performed a small genetic screen using different RNAi lines against several ROS regulating proteins such as SOD, Catalase, Phospholipid hydroperoxide glutathione peroxidase (Phgpx) and we scored for lethality. We found no lethality in any of these protein depletions (Observation Table 2). Hence we ruled out the possibility of neuroblast differentiation being regulated by ROS.

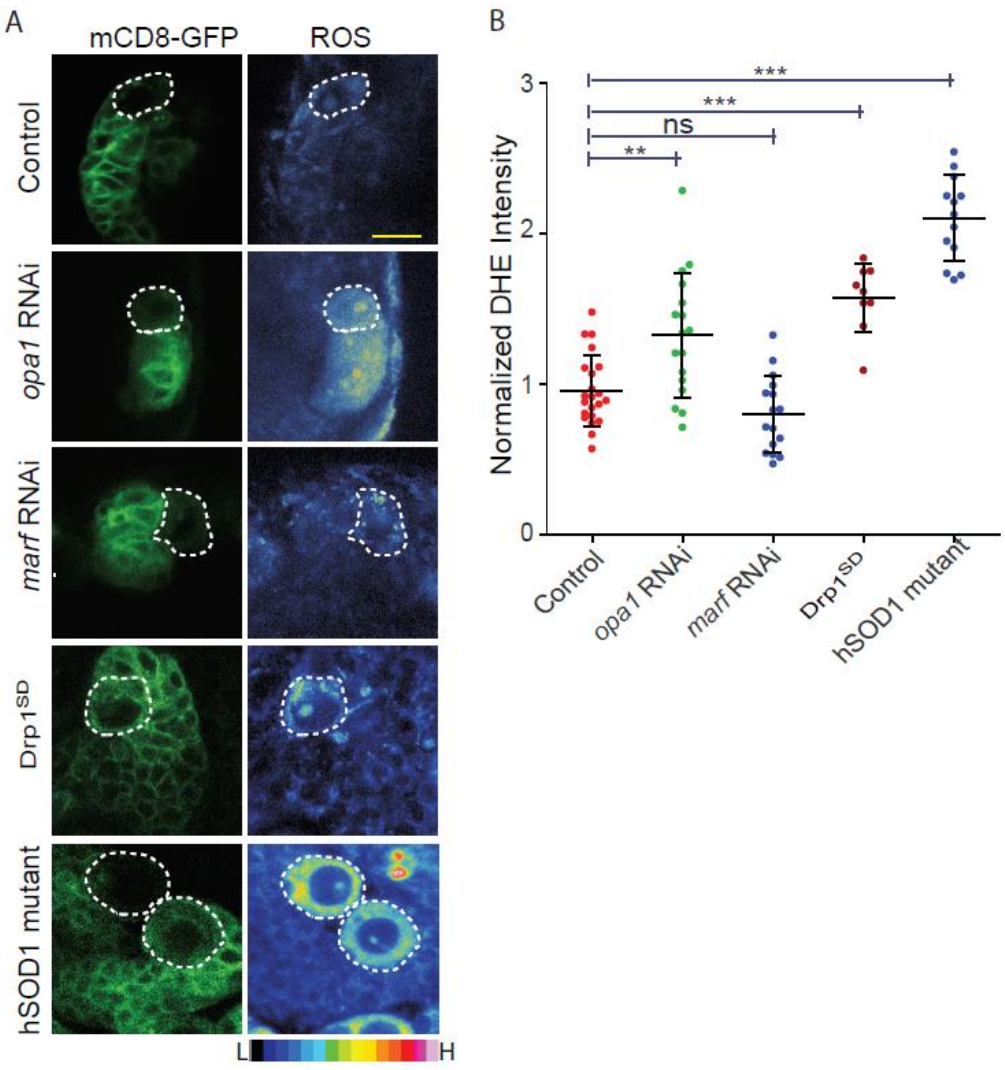

Fig 4.2: Downregulation of mitochondrial dynamics proteins Opa1, Marf and Drp1 causes increased ROS levels in neuroblasts.

A: Representative images showing increased levels of ROS (rainbow scale) in type II neuroblasts (position marked by the white dotted line) of mitochondrial dynamics mutants. *pnt*-Gal4 was used to drive the expression of RNAi and mutant.

B: Analysis of DHE intensities in type II neuroblasts as a ratio to neighboring cells of control (22 neuroblasts,6 Brains), *opa1* RNAi (17,8), *marf* RNAi (17,8), $Drp1^{SD}$ (9,5), hSOD1 mutant (13,3). Student's t-test is performed for statistical analysis. ns – Non significant, **-$p<0.01$, ***- $p<0.001$.

Observation Table 2:

RNAi Line	Function	No. of mutant flies/ Total Emerged flies	Result
Glut1 Val20	Glucose Uptake	0/98	Lethal
SOD Val20	ROS Regulation	37/135	Viable
SOD Val10	ROS Regulation	38/120	Viable
Phgpx Val22	ROS Regulation	16/91	Viable
SOD Val20	ROS Regulation	42/116	Viable
SOD val20	ROS Regulation	30/99	Viable
Catalase Val20	ROS Regulation	24/79	Viable
Catalase Val20	ROS Regulation	25/92	Viable
CamKI Val22	Mito. Calcium Regulation	017/67	Viable
Pkc 53E Val20	Mito. Calcium Regulation	024/67	Viable
Pkc 98E Val22	Mito. Calcium Regulation	50/96	Viable
Camta Val21	Mito. Calcium Regulation	31/64	Viable
Camta Val20	Mito. Calcium Regulation	0/16	Lethal

Observation Table 2: Genetic screen of proteins relating to mitochondrial function in *Drosophila* CNS.

Small genetic screen using RNAi for proteins involved in different mitochondrial functions such as calcium regulation and ROS regulation. UAS-RNAi were expressed in *Drosophila* CNS using *inscuteable*-Gal4 and crosses were maintained at 29°C. A number of mutant adults that emerged from the crosses were recorded and results represented as lethality. The depletion of ROS regulators did not show lethality and mutant animals were normal and viable. Most of the calcium protein depletions were non-harmful for animal viability except for the Camta Val20 line. Knockdown of Glut which is glucose transporter showed 100% lethality.

4.3.3 Downregulation of Opa1 showed elevated cytochrome C levels in neuroblasts.

Cristae remodeling upon loss of Opa1 has been extensively studied in the apoptotic context. During cristae remodeling, cytochrome C which is present in cristae pocket enters into the cytosol where it activates the apoptotic pathway. To check whether loss of mitochondrial fusion proteins Opa1 and Marf has elevated level of cytochrome C, we immunostained control and mutant brains with cytochrome C antibody. Images of control and fusion mutants Opa1 and Marf were taken and represented in a rainbow scale using the LUT tool in ImageJ. Miranda was used to mark neuroblasts. Interestingly, Opa1 mutant neuroblasts showed increased cytochrome C levels compared to control (Figure 4.3). Marf downregulation showed enrichment of cytochrome C similar to control neuroblasts. Opa1 downregulation showed a greater increase in cytochrome C (Figure 4.3). This result implies a differential function of Opa1 and Marf in neuroblast development.

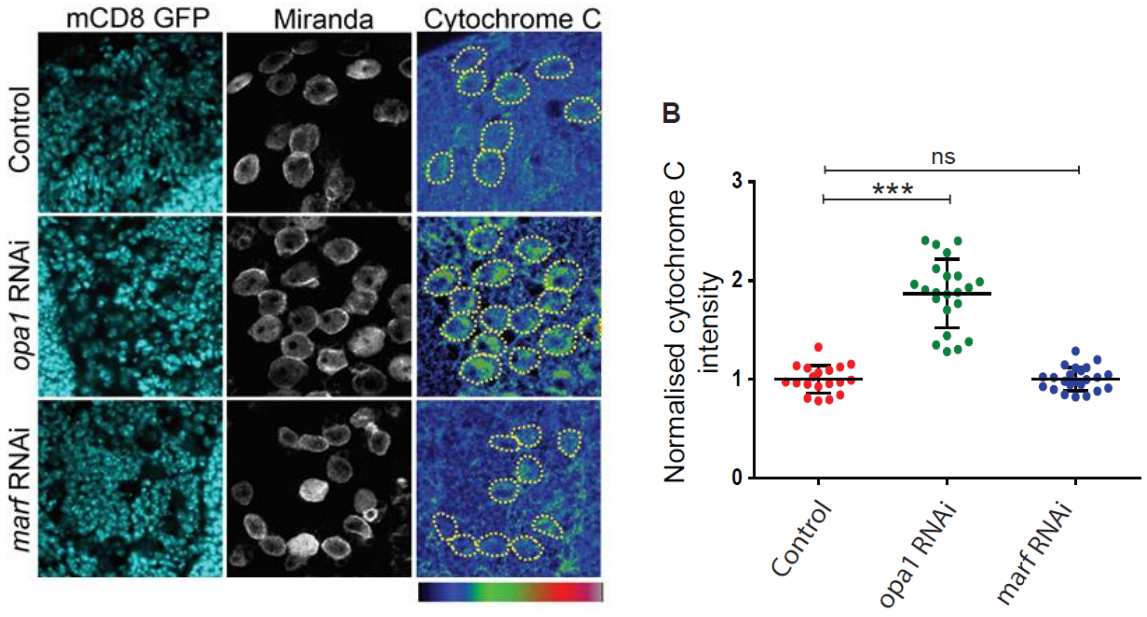

Fig 4.3: Depletion of Opa1 causes elevated levels of cytochrome C in neuroblasts

A: Fluorescence confocal images of neuroblasts showing increased cytochrome C levels in *opa1* RNAi. Control (9 Brains), *opa1* RNAi (10 Brains), *marf* RNAi (8 Brains). *wor*-Gal4 was used to drive the expression of RNAi.

B: Analysis of normalised cytochrome C intensities in control (19 Neuroblasts), Opa1 RNAi (22), Marf RNAi (23). Student's t-test is performed for statistical analysis. ns – Non significant, ***- $p<0.001$.

We further tested whether this increase in cytochrome C in Opa1 depleted neuroblasts could cause the phenotype of loss of differentiation. In order to test this hypothesis, we reduced cytochrome C in type II neuroblasts in Opa1 and Marf depleted background. Downregulation of cytochrome C using RNAi resulted in decreased levels of cytochrome C as seen by antibody staining in neuroblasts. Further we combined cytochrome C RNAi line with Opa1 and Marf RNAi. We further tested the effect of co-depletion of cytochrome C and mitochondrial dynamics proteins on neuroblast differentiation. We found that the co-depletion of cytochrome C and Opa1 partially rescued the loss of Dpn positive mature INP (Appendix Figure A3B). However, interestingly we observed reduced mature INPs in co-depletion of cytochrome C and Marf (Appendix Figure A3B). These data together imply that increased cytochrome C in Opa1 depleted neuroblasts is likely to be responsible for the differentiation defect seen in type II neuroblast lineage. Increased cytochrome C in Opa1 depletion is also an indicator of the defective inner mitochondrial membrane. So it is interesting to analyze inner membrane function in the context of neuroblast differentiation. In chapter 6, we have assessed the function of inner membrane proteins in type II neuroblast differentiation in detail.

4.3.4 Reduced differentiation caused by fusion protein downregulation is NOT due to apoptosis.

We observed the loss of neuroblast differentiation on Opa1 and Marf downregulation. Further analysis showed high levels of ROS and cytochrome C in Opa1 mutant neuroblast pointing towards the possibility of apoptosis in neuroblast lineage. The link between ROS, cytochrome C and apoptosis is well established in the literature (Akopova et al., 2012; Redza-Dutordoir and Averill-Bates, 2016; Vacca et al., 2006).

Hence we checked whether the loss of differentiation in Opa1 was due to apoptosis. To address this question we performed TUNEL assay. Extensive DNA fragmentation is the hallmark of apoptosis. TdT enzyme label 3' end of dsDNA strand with fluorescently labeled dNTP even in the absence of a template. The presence of TUNEL positive nuclei is a proxy for apoptosis. For this assay, we expressed Opa1 RNAi by *worniu*-Gal4. Hid and Reaper is apoptosis inducing factors which upon expression using *worniu*-Gal4 killed animals probably in the embryonic stages because we did not find any larval stages. We further expressed Hid and Reaper using *pointed*-Gal4 as a positive control. This did not affect the viability of the fly. We performed TUNEL assay (described in the method section) on control, Opa1 RNAi and overexpression of Hid-Reaper. We counted TUNEL positive nuclei per lobe for each genotype and compared with control. We did not see an increased number of apoptotic nuclei in Opa1 downregulation compared to control whereas expression of Hid Reaper showed a significant increase in number despite expressing only in 8 neuroblast lineages (Figure 4.4 A-B). We also confirmed this result by immunostaining with an antibody against activated caspase 3. Consistent with previous results, Opa1 downregulation had no elevated caspase 3 activity (Figure 4.4 C). These results show that the loss of differentiation in Opa1 downregulation is not due to apoptosis.

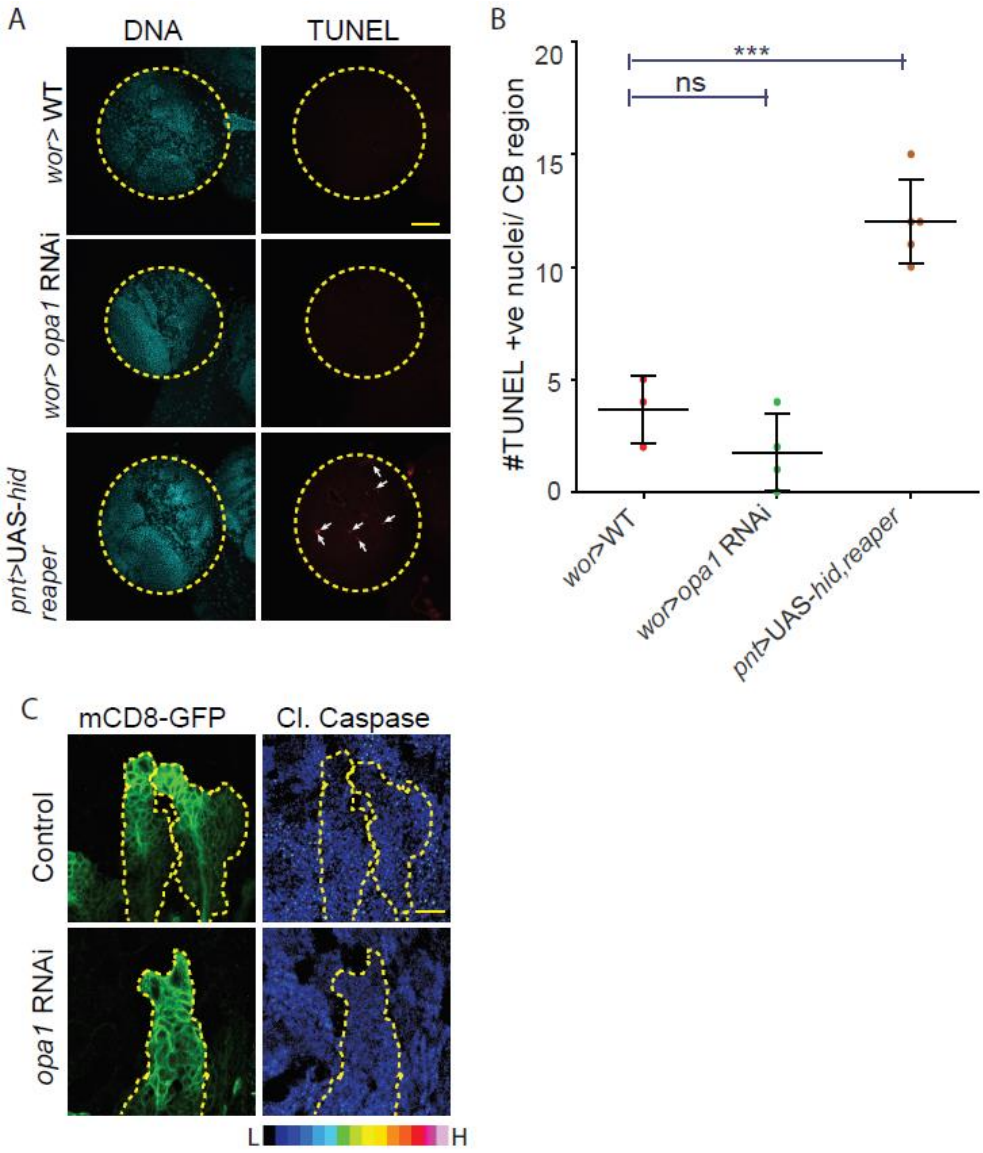

Fig 4.4: Downregulation of Opa1 does not cause apoptosis in *Drosophila* neuroblasts.

A: Fluorescence confocal images of the brain hemisphere showing no significant change in TUNEL positive nuclei (red) in *opa1* RNAi. The expression of UAS-hid shows a significant increase in TUNEL positive cells when expressed in type II neuroblasts lineage. Scale bar- 50uM

B: Quantification of TUNEL positive nuclei in *wor*>WT(3 brains), *wor*> *opa1* RNAi (4), pnt> UAS-*hid reaper* (5). Statistical analysis was performed using unpaired t-test. ns- non significant, ***- p<0.0001

C: Representative images of type II neuroblasts lineages (green) stained for cleaved caspase and represented in heatmap showing no increased level in *opa1* RNAi control (10 neuroblasts lineages,6 Brains), *opa1* RNAi (9,6). *pnt*-Gal4 was used to drive the expression of RNAi. Scale bar- 10uM

4.3.5 Reduction in Opa1 showed lowered EdU and pH3 positive cells in neuroblasts lineage.

We further explored the rate of neuroblast proliferation in mitochondrial fusion mutants. Reduced proliferation can produce a decreased number of differentiated progeny. To check this possibility, we performed the EdU uptake assay described in the method section. EdU is a thymidine analog incorporated into the DNA during the S phase of the cell cycle. We treated control and mutant brains with EdU in Schneider's medium for 1hr at room temperature. Then EdU positive cells were labeled with fluorescently tagged EdU antibody. After image acquisition, we quantified the EdU positive cells in the type II neuroblasts lineages. We found less number of EdU positive cells per lineage in Opa1 downregulation (Figure 4.5 A-B). Interestingly, Drp1 mutant showed an increase in EdU positive cells in the type II neuroblast lineage (Figure 4.5 A-B). Co-depletion of Drp1 function in Opa1 downregulation background rescued proliferation in type II neuroblasts (Figure 4.5 A-B), This result showed that loss of differentiation in neuroblasts lineage in mitochondrial fusion mutant is caused because of the reduced proliferation of neuroblasts and in the lineage.

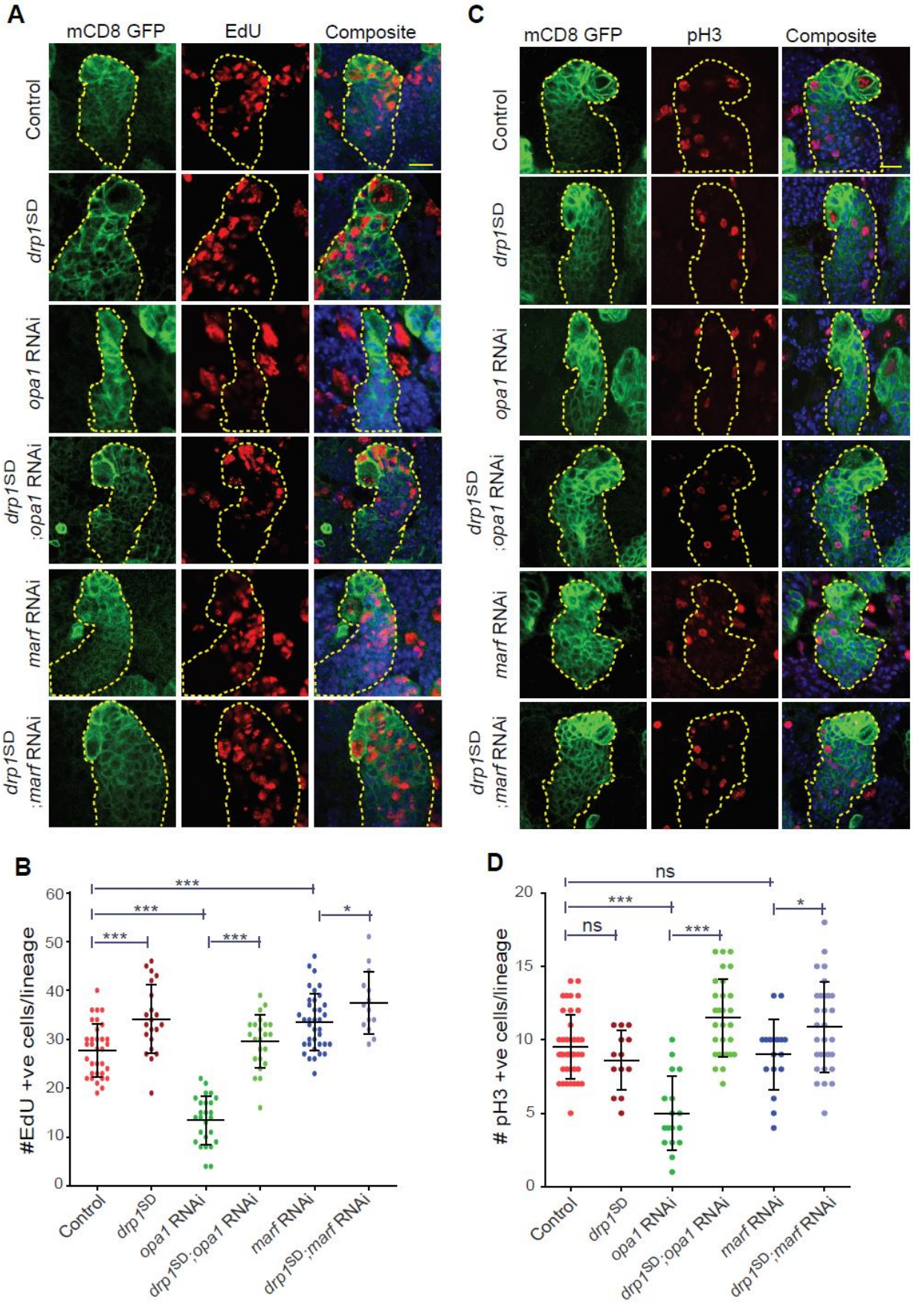
A
mCD8 GFP
EdU
Composite
Control
drp1SD
opa1 RNAi
drp1SD ;opa1 RNAi
marf RNAi
drp1SD ;marf RNAi
C
mCD8 GFP
pH3
Composite
Control
drp1SD
opa1 RNAi
drp1SD ;opa1 RNAi
marf RNAi
drp1SD ;marf RNAi
B
#EdU +ve cells/lineage
0
10
20
30
40
50
60
***
***
***
***
*
Control
drp1SD
opa1 RNAi
drp1SD;opa1 RNAi
marf RNAi
drp1SD;marf RNAi
D
pH3 +ve cells/lineage
0
5
10
15
20
ns
***
ns
***
*
Control
drp1SD
opa1 RNAi
drp1SD;opa1 RNAi
marf RNAi
drp1SD;marf RNAi

Fig 4.5: Downregulation of Opa1 causes a reduced number of EdU and pH3 positive cells in type II neuroblast lineages. The knockdown of Marf causes an increase in EdU positive cells while Drp1 has no effect.

A: Type II neuroblasts lineages (CD8-GFP, green) (yellow dotted line) show a decreased number of EdU (red) positive mitotic cells per lineage in *opa1* RNAi. *pnt*-Gal4 was used to drive the expression of RNAi and mutant.

B: Quantification of EdU positive cells in type II neuroblasts lineages (B) in control (), $Drp1^{SD}$ (), *opa1* RNAi (17,3), $Drp1^{SD}$;*opa1* RNAi (), *marf* RNAi (), $Drp1^{SD}$;*marf* RNAi ().

C: Type II neuroblasts lineages (CD8-GFP, green) (yellow dotted line) show a decreased number of pH3 (red) positive mitotic cells per lineage in *opa1* RNAi.

D: Quantification of pH3 positive cells in type II neuroblasts lineages (B) in control (40 neuroblasts lineages,6 brains), $Drp1^{SD}$ (13,3), *opa1* RNAi (17,3), $Drp1^{SD}$;*opa1* RNAi (29,4), *marf* RNAi (17,3), $Drp1^{SD}$;*marf* RNAi (30,7). Scale bar- 10µm. Statistical analysis was done by using unpaired t-test. ns- non significant, *-$p<0.05$, **-$p<0.01$, ***- $p<0.001$.

To confirm this result we further did an analysis of mitotic cells in the type II neuroblasts lineage. We used phospho histone 3 (pH3) antibody to mark mitotic cells in type II neuroblasts lineage. Quantification of pH3 positive cells in each lineage showed a reduced number of mitotic cells on Opa1 downregulation (Figure 4.5 C-D). The reduction of Drp1 and Marf did not affect a number of pH3 cells in the lineage (Figure 4.5 C-D). The forced fusion of mitochondria in Opa1 downregulation rescued pH3 positive mitotic cells in type II neuroblasts lineage (Figure 4.5 C-D).

Together these data suggested that attenuated differentiation in mitochondrial fusion proteins downregulation is caused because of impairment in cell cycle progression of type II neuroblasts lineage.

4.4 Discussion

In this chapter, we have shown that loss of differentiation population in type II neuroblast lineages was not a consequence of apoptosis but due to reduced proliferation rate in mutant lineages. Cell proliferation and differentiation are highly energetic processes in which ATP is needed for all the events happening inside the cell

ranging from DNA replication to separation of daughter cells result of force generated by actomyosin network. As discussed earlier, fragmented mitochondria produce less energy as compared to fused ones as they have loose cristae organization and poorly arranged ETC complexes. Interestingly, we did not find energy stress in neuroblasts deficient of fusion proteins as pAMPK levels were normal similar to controls. It has been reported that larval neuroblasts rely on glycolysis for their ATP requirements and not on OxPhos (Homem et al. 2014). This could be the reason why we did not find elevated pAMPK levels in fusion mutants.

We found increased cytochrome C specifically in Opa1 mutant neuroblasts indicating a defect in inner mitochondrial membrane organization. Cytochrome C acts as an activation switch for cell death program when released into the cytoplasm during mitochondrial cristae remodeling. There are very few instances where cytochrome C does not lead cells for execution rather it plays an important role in the cell fate determination. Cytochrome C is required for the terminal differentiation of spermatids in *Drosophila*. Spermatids depleted for cytochrome C failed to differentiate and lead to male sterility. This is opposite to what we found in neuroblasts. We have observed elevated levels of cytochrome C in Opa1 depleted neuroblasts where lack of differentiation was observed but not cell death. Since Opa1 is inner mitochondrial membrane protein and depletion can cause defects in the inner membrane while leaving the outer membrane unaffected. Careful analysis of cytochrome C immunostaining data in the Opa1 mutant showed that cytochrome C was not spread over the cytoplasm but it showed punctate pattern presumably trapped in the intermembrane space of mitochondria. Further lack of TUNEL positive nuclei and unchanged caspase3 levels confirmed a lack of cell death by apoptosis in Opa1 deficient neuroblast lineages. ROS is known to play a role in cell proliferation. It has been reported that increased ROS has a positive correlation with fragmented mitochondria (Yu et al., 2006). In this study, we also ruled out the possibility of differentiation defects by increased ROS as an ectopic increase in ROS level by the SOD mutant did not affect the differentiation profile of neuroblasts. Interestingly we found a lowered number of EdU and pH3 positive cells suggesting lowered

differentiation in Opa1 mutant is a consequence of reduced proliferation rate of neuroblasts. Furthermore consistent with previous results both EdU and pH3 positive cells were rescued by forced outer membrane fusion of mitochondria by co-depleting Drp1 in Opa1 knockdown. Marf is the outer mitochondrial membrane protein involved in outer membrane fusion of mitochondria. Apart from this, it is also involved in the maintenance of ER-mitochondrial contact sites (ERMCS). ERMCS are involved in calcium buffering and homeostasis in the cell. We have observed increased EdU positive cells in Marf depleted type II neuroblast lineage. EdU incorporation into the DNA takes place in the S-phase of the cell cycle and increased EdU positive cells possibly mean arrest of these cells in the S-phase. It is reported that ERMCS are involved in the proper folding of the protein in ER and defects in ERMCS result in misfolding of proteins which further trigger unfolded protein response (UPR). One of the key steps in UPR is slowing cell cycle progression. Increased EdU positive cells in Marf could be because of defects in ERMCS and subsequent activation of UPR. This can be analyzed by probing downstream targets of UPR such as eIF2α, TRAF2 etc. This analysis will provide further insight into differential phenotypes caused by Opa1 and Marf depletion in type II neuroblasts differentiation.

Together these results show that loss of type II neuroblast differentiation is caused by reduced proliferation and not by apoptosis. Further Opa1 depleted neuroblasts do not cause ATP stress or oxidation stress. It would be interesting to see whether signaling pathways involved in neuroblast proliferation are getting affected in the mitochondrial mutant. One of the signaling pathways which are known to be essential for neuroblast proliferation is the Notch signaling pathway. Loss of Notch causes a reduction in type II neuroblast numbers while type I neuroblasts are spared in this mutant indicating the special role of Notch in type II neuroblast. In the next chapter, we shall be analyzing this pathway in more detail in type II neuroblast.

Chapter 5: Assessment of requirement of the Notch signaling pathway for type II neuroblast proliferation

5.1 Introduction

Recent evidence has shown that mitochondria can regulate several key signaling pathways involved in cell proliferation and differentiation. The Notch signaling pathway is one of such pathways that is regulated by mitochondrial morphology and activity in various cell types (Chen et al., 2018; Kasahara et al., 2013; Lee et al., 2013). As discussed in section 1.2.1, Notch signaling consists of transmembrane Notch receptor and ligand Delta or Serrate present on neighboring cells. Binding of the ligand to the Notch receptor causes a cleavage of NICD which goes into the nucleus where it activates downstream transcriptional program responsible for cell proliferation and differentiation. Recent studies on *Drosophila* and mammalian system have established a link between mitochondrial morphology and the Notch pathway. Clonal analysis in *Drosophila* ovary has shown that for differentiation of ovarian follicle cells, Drp1 mediated mitochondrial fragmentation is needed for Notch activation. Mutation in Drp1 leads to fused mitochondria and the inactivation of Notch signaling which results in loss of follicle cell differentiation. Mutant Drp1 cells do not exhibit expression of differentiation factor and one of the Notch downstream targets, Hindsight (Hnt). Similarly, Opa1 and Mfn depletion leading to mitochondrial fragmentation in mouse embryonic stem cells causes hyperactivation of Notch and reduces the differentiation of ESCs into functional cardiomyocytes due to loss of calcium buffering (Kasahara et al., 2013). On the other hand, activation of Notch signaling by depletion of mitochondrial fusion and increasing reactive oxygen species (ROS) enhances differentiation in mammalian neural stem cells (Khacho et al., 2016). Another interesting study carried out in triple negative breast cancer (TNBC) cells suggests a positive feedback loop between Drp1 mediated mitochondrial fragmentation and Notch signaling. Increased Notch signaling is observed in TNBC tissue accompanied by elevated mitochondrial fragmentation compared to surrounding non-cancerous tissue. Further analysis showed

that TNBC has increased levels of Drp1 protein. Drp1 mediated mitochondrial fragmentation activates Notch which positively regulates expression of Drp1 while suppressing Mfn expression. This positive interaction between Notch and Drp1 supports survival, proliferation and thus cancer progression of TNBC (Chen et al., 2018). These studies have clearly established a link between mitochondrial morphology and specifically fragmentation and activation of the Notch signaling pathway. As seen in chapters 2 and 3, the depletion of mitochondrial fusion protein Opa1 resulted in the loss of neuroblast differentiation. It has been reported that Notch is required for the maintenance of type II neuroblasts in the *Drosophila* brain while being dispensable for type I neuroblasts (Li et al., 2016). Mutation or loss of Notch resulted in a reduction in cells in the type II neuroblast lineages while type I neuroblast remained unaffected (Li et al., 2016). In this chapter, we have analyzed the interaction between the Notch signaling pathway and mitochondrial morphology. In addition to that, we have also analyzed whether Notch signaling has any retrospective effect on mitochondrial morphology.

5.2 Materials and Methods

5.2.1 Fly stocks: *pointed*-Gal4*,* UAS-mCD8-GFP, *notch* RNAi (BL31383), *su(H)* RNAi (BL67928), UAS-NV5 (BL52309) and UAS-N^{intra} *notch* RNAi /CyOGFP; *opa1* RNAi /TM3SerGFP, *notch* RNAi /CyOGFP; *marf* RNAi /TM3SerGFP

5.2.2 Antibodies:

Primary antibodies: anti-NICD (1:10, DSHB), anti-Cathepsin (1:200, Abcam), anti-LAMP (1:500, Abcam)

Secondary antibodies: anti-Mouse 568,633 (1:1000, Molecular Probes), anti-Rabbit (1:1000, Molecular Probes), anti-Chicken (1:1000, Molecular Probes),anti-Rat (1:1000, Molecular Probes

For detailed information about primary and secondary antibodies with their respective dilutions please refer to section 2.1.2.

5.2.3 Immunohistochemistry: Third instar larval brains of control and mitochondrial mutants were dissected in Schneider's medium and further stained with antibodies mentioned above. For detailed procedure please refer to section 2.2.3.

5.2.4 Image acquisition and analysis: Image acquisition was carried out by using LSM710 or LSM780 inverted microscope (Carl Zeiss, Inc. and IISER Pune microscopy facility) with a Plan apochromat 40x 1.4NA and 63x 1.4NA oil objective. NICD intensities were quantified from cytoplasm and nucleus by drawing ROI using ImageJ software. Intensity ratios were plotted using GraphPad Prism 5 software. Please refer to section 2.2.8 and 2.2.9 for detailed information about image acquisition and analysis.

5.3 Results

5.3.1. Notch signaling is required for type II neuroblasts self-renewal and differentiation.

Notch signaling is required for type II neuroblast proliferation and self-renewal. Loss of Notch function causes a reduction in type II neuroblasts number (Li et al., 2016). Type II neuroblasts transform into type I upon knockdown of Notch. We tested whether Notch signaling interacts with mitochondrial morphology during its role in differentiation. To downregulate the Notch function in type II neuroblasts development, we used Notch RNAi and Su(H) RNAi. Su(H) binds to NICD and targets the NICD-Su(H) complex to the promoter of targeted genes. Knockdown of Notch in type II neuroblasts caused a reduction in the number of type II neuroblasts lineages (Figure 5.1 A-B) consistent with the literature. Loss of Su(H) also resulted in a loss of type II neuroblasts. We observed about 10 fold increase in neuroblast number in NV5 expressing brains (Figure 5.1 A-B). These results support previous findings where the importance of the Notch signaling pathway in type II neuroblasts self-renewal has been discussed. Downregulation of Notch function by using Notch RNAi or Su(H) RNAi did not cause complete loss of type II neuroblasts. In Notch RNAi and Su(H) RNAi the number of type II neuroblasts reduces to approximately 5 and 2 respectively (Figure 5.1 A-B). The few lineages that managed to survive, could be due to incomplete loss of Notch function. We further

analyzed Dpn positive mature INPs and Pros positive GMCs in these surviving neuroblasts. Interestingly, we found a reduction in the number of both mature INPs and GMCs in Notch RNAi, similar to the downregulation of mitochondrial fusion protein Opa1 (Figure 5.1 C-F). This data indicates that Notch regulates type II neuroblasts self-renewal as well as differentiation within the type II neuroblast lineage.

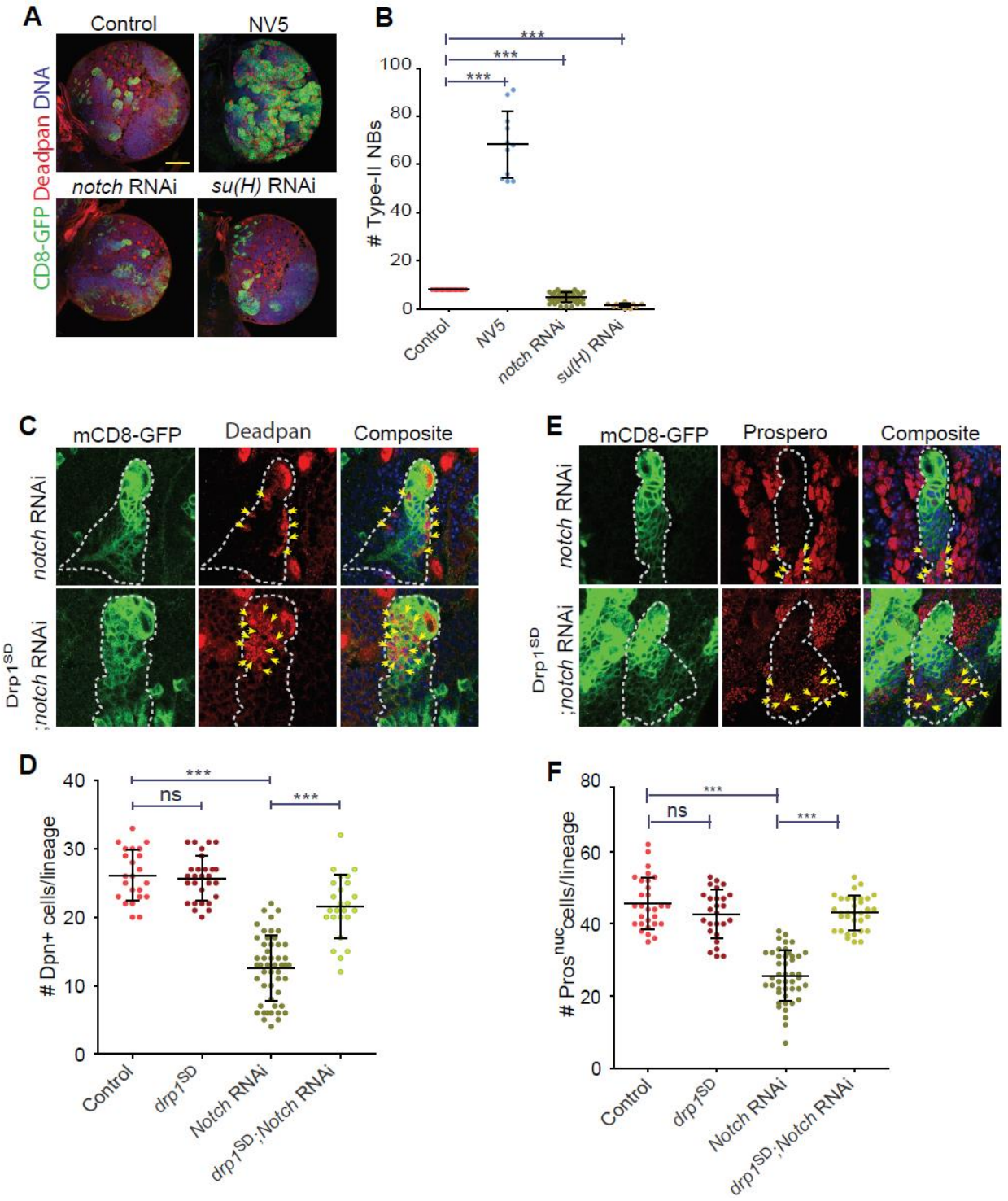

Fig 5.1: Notch signaling regulates the proliferation and differentiation of type II neuroblasts. Co-depletion of Drp1 rescues Notch-mediated differentiation defects in type II neuroblasts.

A: *pnt*-Gal4, mCD8-GFP expressing brain lobes with Notch signaling mutants show an increased number of type II neuroblasts in NV5 overexpression and a decreased number in *notch* RNAi and *su(H)* RNAi marked by GFP (green) and Dpn (red) in brain lobes.

B: Type II neuroblasts number quantification in brain lobes of Notch signaling mutant larvae (C). Control (14 brains), NV5 (11), *notch* RNAi (43), *su(H)* RNAi (12). Scale bar- 50µm.

C: Type II lineages (CD8-GFP, green) showing Dpn positive INPs (red, yellow arrows). Scale bar- 10µm

D: Quantification of Dpn positive INPs in control (23 neuroblasts lineages,16 brains), $Drp1^{SD}$ (28,10), *notch* RNAi (54,9), $Drp1^{SD}$;*notch* RNAi (25,5). Control and $Drp1^{SD}$ quantification are repeated from Figure 3E.

E: Type II lineages (CD8-GFP, green) showing Pros positive INPs (red, yellow arrows). Scale bar- 10µm

F: Quantification of Pros positive GMCs in control (29 neuroblasts lineages,18 brains), $Drp1^{SD}$ (26,8), *notch* RNAi (45,5), $Drp1^{SD}$;*notch* RNAi (33,5).

Student's t-test is performed for statistical analysis. ns – Non significant, ***- $p<0.001$.

5.3.2. Notch signaling regulates mitochondrial morphology in type II neuroblasts lineage.

Since the loss of Notch caused a similar phenotype as Opa1 knockdown, we asked whether Notch regulates mitochondrial morphology. To answer this question, we immunostained Notch RNAi and Su(H) RNAi with ATPB along with controls. Type II neuroblasts lineage was marked by expression of CD8 GFP expressed using *pointed*-Gal4. Neuroblasts in each lineage were detected by its large size and the upstream position in the lineage. Surprisingly, we found fragmented mitochondrial morphology in both Notch and Su(H) knockdown (Figure 5.2 A-C). On overexpression of the Notch receptor, NV5 and Notch Intracellular Domain, Nintra, we detected clustered mitochondrial morphology, in contrast to mitochondrial dispersal seen during the downregulation of Notch function (Figure 5.2 A-C). We quantify the size of optically resolvable spots seen in neuroblasts on Notch increase and decrease in type II neuroblasts. We found that there was an increase in mitochondrial size on Notch overexpression and a decrease in size on Notch loss of function. Together these results suggested that Notch regulates fused mitochondrial morphology in type II neuroblasts and loss of Notch causes mitochondrial fragmentation.

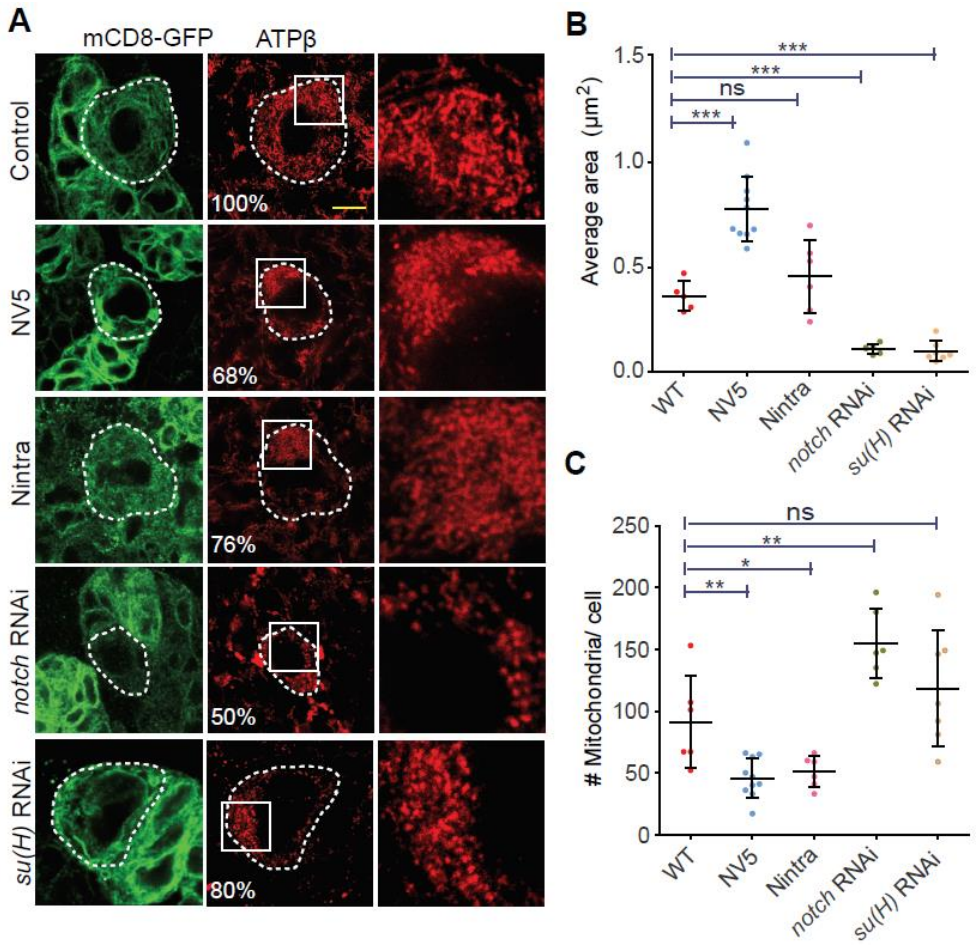

Fig 5.2: Notch regulates fused mitochondrial morphology in type II neuroblasts.

A: Type II neuroblasts (mCD8-GFP, green, yellow dotted line) showing Notch mediated regulation of mitochondrial morphology (red) stained using ATPβ antibody imaged using STED microscopy. Control (100% tubular, 75 neuroblasts, 22 Brains), NV5 (68% clustered, 103,16), Nintra (76% clustered, 58,6), *notch* RNAi (50% fragmented, 30,14), *su(H)* RNAi (80% fragmented, 23,12). *pnt*-Gal4 was used to drive the expression of RNAi and mutant.

B: Quantification of the average mitochondrial area in Control (6 neuroblasts,3 brains), NV5 (10,5), Nintra (6,4), *notch* RNAi (6,4), *su(H)* RNAi (7,4).

C: Quantification of Mitochondrial number in control (6,3), NV5 (10,5), Nintra (6,4), *notch* RNAi (6,4), *su(H)* RNAi (7,4). Scale bar- 5µm.

Student's t-test is performed for statistical analysis. ns – Non significant, *-$p<0.05$, **-$p<0.01$, ***-$p<0.001$.

5.3.3. Loss of differentiation on Notch depletion is reversed by forced mitochondrial fusion.

Loss of differentiation in type II neuroblasts mutant for Opa1 was rescued by forced fusion of mitochondria. We examined whether the same is true for Notch loss of function. We combined Notch RNAi with the Drp1SD mutant. Analysis of mature INP in the double mutant showed a rescue in mature INP and GMC number in type II neuroblast lineage (Figure 5.1 C-F) indicating the role of fused mitochondria in Notch mediated type II proliferation.

5.3.4. The depletion of Opa1 causes cytoplasmic retention of NICD in type II neuroblasts.

Notch signaling leads to the cleavage of the intracellular domain in the signal-receiving cell and subsequent translocation to the nucleus (Yamamoto et al., 2010). Cytoplasmic accumulation of the intracellular domain due to lack of acidified lysosomes results in loss of Notch signaling in *Drosophila* follicle cells (Yan et al., 2009). We examined NICD distribution in type II neuroblasts by using an antibody against the intracellular domain of the Notch receptor. We found that there was a decrease in NICD on the plasma membrane in control neuroblasts as compared to other neighboring cells in the type II neuroblasts lineage (Figure 5.3 A). We assessed the status of NICD on the plasma membrane in mitochondrial morphology mutants. We found that there was an accumulation of NICD in the cytoplasm in punctate vesicle-like compartments in Opa1 depleted brains (Figure 5.3 A-B). Fluorescence quantitation showed an increased cytoplasmic to nuclear fluorescence in Opa1 mutant neuroblasts as compared to controls (Figure 5.3 A-B). Marf and Drp1 depleted neuroblasts did not show this defective accumulation of NICD in the cytoplasm and the cytoplasm to the nuclear ratio of NICD was the same as in controls (Figure 5.3 A-B). Interestingly cytoplasmic NICD accumulation was not seen in Drp1SD; Opa1 RNAi expressing type II neuroblasts

(Figure 5.3 A-B) and this was consistent with the reversal of the phenotype of loss of mINPs in this combination (Figure 5.3 A-B).

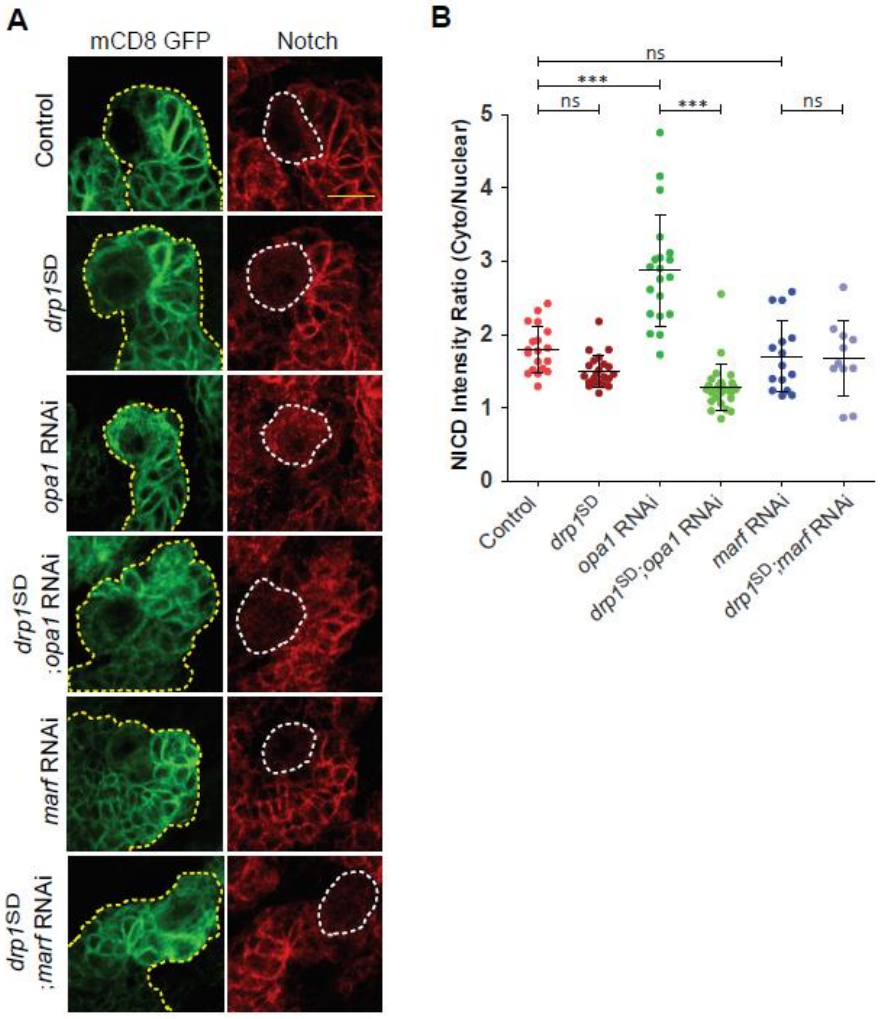

Fig 5.3: Downregulation of Opa1 causes cytoplasmic retention of NICD in type II neuroblasts.

A: Representative confocal images of type II neuroblast lineages (green) showing increased cytoplasmic levels of NICD (red) in Opa1 depletion. *pnt*-Gal4 was used to drive the expression of RNAi and mutant. Scale bar- 10uM.

B: Analysis of NICD intensity ratios in Control (19 Neuroblasts,10 Brains), Drp1SD (22,5), Opa1 RNAi (20,12), Drp1SD;Opa1 RNAi (28,6), Marf RNAi (15,12), Drp1SD;Marf RNAi (11,5). Student's t-test is performed for statistical analysis. ns – Non significant, ***- $p<0.001$.

5.3.5 Depletion of Opa1 causes an increase in cytoplasmic NECD punctae in type II neuroblasts and differentiated cells.

Previously we observed that depletion of Opa1 in type II neuroblast lineage caused cytoplasmic retention of NICD. Further, we checked the distribution of Notch Extra Cellular Domain (NECD) in Opa1 depleted type II neuroblasts lineage. We stained control and mutant brains with the NECD antibody followed by confocal imaging. Then we analyzed differential localization of NECD in control and Opa1 depleted type II neuroblasts. We found an increase in the number of NECD punctae in neuroblasts as well as downstream differentiated lineage (Figure 5.4 A-C). NECD punctae found in differentiated cells of type II lineage depleted for Opa1 were larger in size as compared to control (Figure 5.4 A). Cytoplasmic accumulation of NICD and increased NECD punctae suggests a possible defect in Notch receptor trafficking in Opa1 depleted type II neuroblast lineage. Further analysis of trafficking pathways involved in Notch processing can reveal the mechanism of Notch defect in Opa1 depleted type II neuroblasts.

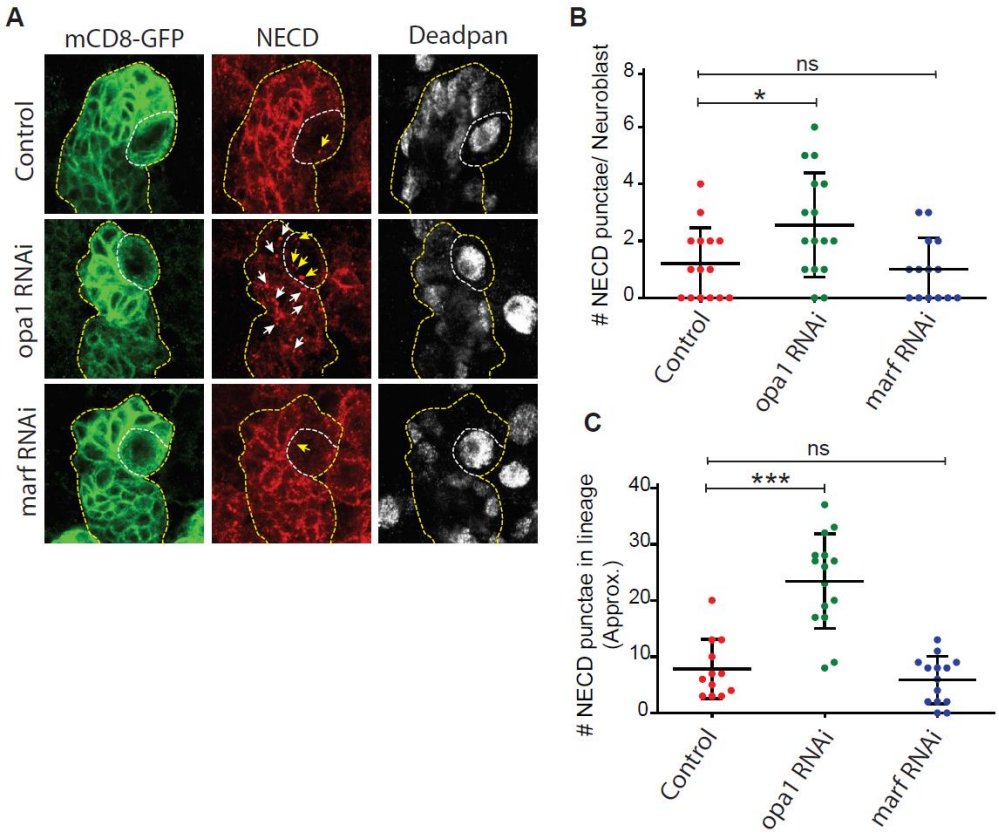

Fig 5.4: Knockdown of Opa1 in type II neuroblast lineage causes increased NECD punctae in neuroblast and differentiated cells.

A: Representative confocal images of type II lineages stained with CD8-GFP (green) showing increased NECD (red) punctae in neuroblast (grey dotted line, yellow arrows) and in differentiated cells in the lineage (yellow dotted line, white arrows) depleted for Opa1. Control (15 Neuaroblasts, 4 Brains), *opa1* RNAi (16,5), *marf* RNAi (14,5).
B: Quantification of NECD punctae in type II neuroblasts. Control (15 Neuaroblasts, 4 Brains), *opa1* RNAi (16,5), *marf* RNAi (14,5).
C: Quantification of NECD punctae (each punctae area ≥ 0.1uM^2) in the differentiated lineage. Control (13 type II neuroblast lineages, 4 Brains), *opa1* RNAi (15,5), *marf* RNAi (14,5). Statistical analysis is performed using Student's t-test. ns – Non significant, *- p<0.1, ***- p<0.001.

5.3.6. Mitochondrial fusion proteins Opa1 and Marf are required for Notch-mediated type II neuroblasts proliferation.

From previous results, it is clear that fusion is essential for Notch function. We further confirm these findings using the Notch gain of function mutants. We depleted fusion proteins Opa1 and Marf in NV5 and NICD (Nintra) overexpression background (Figure 5.4 A, C &E). The expression of Nintra in type II neuroblasts caused a massive increase in neuroblast numbers marked by Dpn (Figure 5.4 E). The elevated number of neuroblasts in both NV5 and Nintra mutant was reduced in loss of fusion proteins Opa1 and Marf (Figure 5.4 A-E), further confirming the requirement of mitochondrial fusion in Notch signaling for type II neuroblast proliferation.

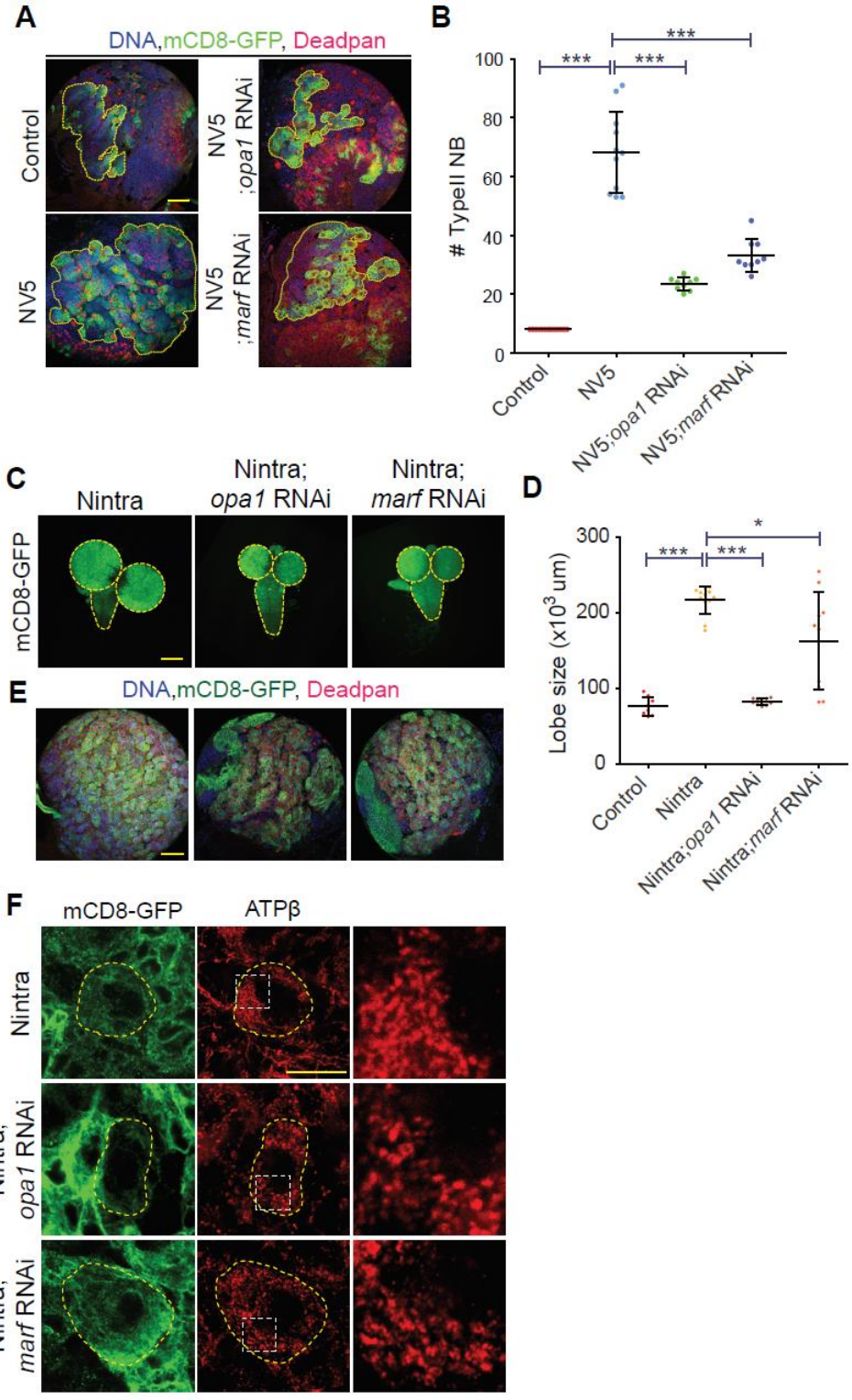

Fig 5.5: Overproliferation of type II neuroblasts caused by ectopic expression of Notch can be rescued by the co-depletion of mitochondrial fusion proteins Opa1 and Marf.

A: Larval brain lobes show rescue of Notch-mediated neuroblasts hyper-proliferation on depletion of *opa1* and *marf*. *pnt*-Gal4 was used to drive the expression of RNAi and mutant. Scale bar- 50µm

B: Quantification of neuroblasts number in control (14 lobes), NV5 (11), NV5;*opa1* RNAi (9), NV5;*marf* RNAi (9).

C: Larval brain (CD8-GFP, green) shows the big brain phenotype on Nintra overexpression which is rescued by *opa1* RNAi and *marf* RNAi expression.

D: Quantification of lobe size in control (8 brains), Nintra (12), Nintra;*opa1* RNAi (10), Nintra; *marf* RNAi (12). Statistical analysis was performed using the unpaired t-test. *-p<0.05, ***- p<0.001. Scale bar- 200µm.

E: Representative images of larval brain hemisphere showing the partial rescue of neuroblasts hyperproliferation in Nintra expression by *opa1* RNAi and *marf* RNAi. Nintra (8 lobes, 8 brains), Nintra;*opa1* RNAi (10,10), Nintra; *marf* RNAi (10,10). Scale bar- 50µm

D: Representative superresolution STED images of mitochondria showing clustered morphology in Nintra mutant and punctate appearance in *opa1* and *marf* RNAi expressing type II neuroblasts in the Nintra background. Nintra (76% tubular, 58 Neuroblasts, 6 Brains), Nintra;*opa1* RNAi (10%, 95, 20), Nintra*;marf* RNAi (10%, 98, 14). Scale bar- 10µm

Together these results showed that Notch signaling is required to maintain fused mitochondrial architecture in type II neuroblasts. Similarly, the function of Notch is dependent on mitochondrial fusion and perturbation in any of the fusion proteins leads to defects in type II neuroblast differentiation.

Lysosome mediated processing of NICD has been thought to be essential for Notch signaling in mammalian cells and *Drosophila* follicle cells (Valapala et al., 2013; Yan et al., 2009). Loss of mitochondrial membrane potential seen in Opa1 and ETC mutants could also result in loss of lysosome function and Notch signaling. To check whether depletion of lysosomal function causes cytoplasmic retention of NICD, we performed immunostaining with antibodies specific for Lysosomal Associated Membrane Protein (LAMP) and Cathepsin. LAMP is a lysosomal membrane protein while Cathepsin is a lysosomal enzyme (Rout et al., 2014; Verma et al., 2016). Co-immunostaining with mitochondrial marker showed unaffected levels of LAMP and Cathepsin in Opa1 depleted type II neuroblasts (Figure 5.5 A-B). This result showed that the lysosomal function was not compromised in this mitochondrial mutant and the loss of

differentiation seen in these lineages is not likely to occur due to loss of lysosomal function.

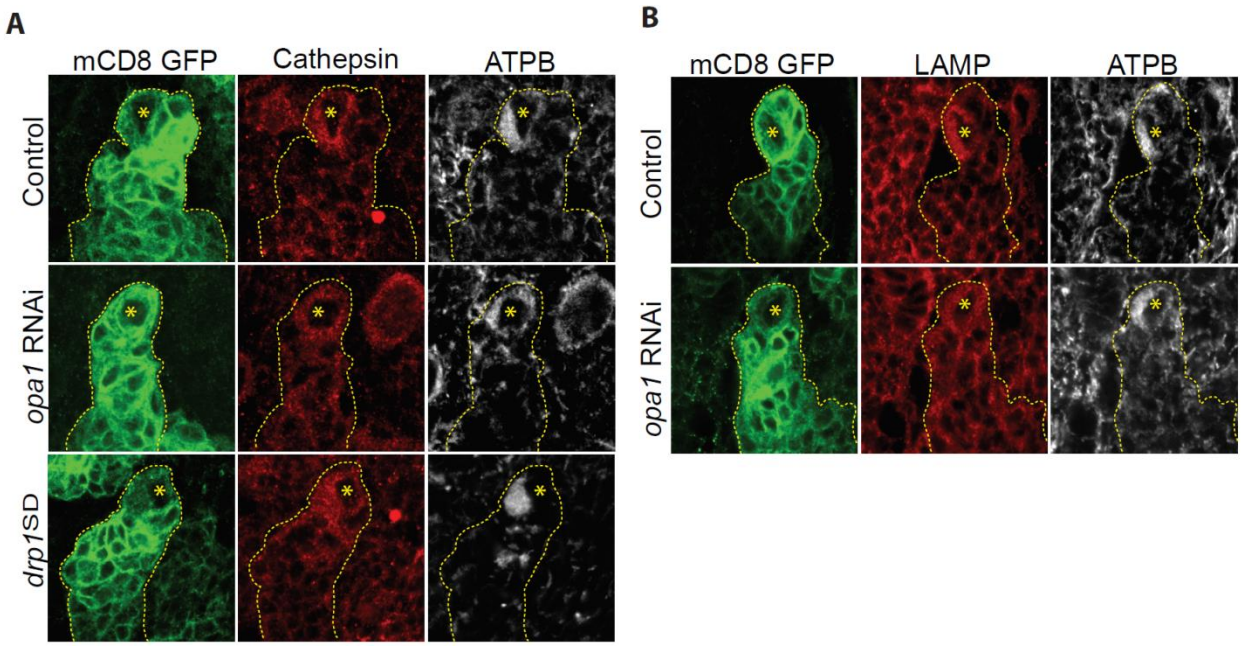

Fig 5.6: Cathepsin and LAMP levels were not affected in Opa1 RNAi.

A: Representative fluorescence images of type II neuroblasts marked with CD8-GFP (green) showed unchanged levels of Cathepsin (red) in Opa1 RNAi and Drp1SD mutant. Control (17 Neuroblasts, 6 Brains), Opa1 RNAi (17,6), Drp1SD (8,5). *pnt*-Gal4 was used to drive the expression of RNAi and mutant.

B: Confocal images of type II neuroblasts (green) showing unaffected levels of LAMP staining (red) in Control and Opa1 RNAi. Control (14 Neuroblasts, 5 Brains), Opa1 RNAi (17,4).

The Notch receptor is produced in the Endoplasmic Reticulum compartment and then trafficked to the membrane via the Golgi apparatus. Then it re-enters in the cell by endocytosis, a process by which vesicles invaginate into the cytoplasm from the plasma membrane. Invaginated vesicles fuse to early endosome and from there they can undergo different fates. Early endosomes transport back to the plasma membrane or convert into late endosomes which eventually fuse with the lysosome and undergo degradation. Different Rab-GTPases play an important role in this process. A study in *Drosophila* wing vein and bristle showed that depletion

of Rab7 and Rab8 causes mislocalization and trafficking defects of the Notch receptor. We found cytoplasmic retention of NICD and increased punctae of NECD in Opa1 depleted type II neuroblasts. To check whether these defects are due to defective Rab mediated Notch receptor trafficking, we immunostained larval brains with Rab5, Rab7 and Rab8 antibodies followed by confocal imaging. Analysis of these different Rabs in Opa1 depleted type II neuroblast lineages showed no change in distribution pattern as well as intensities compared to control (Figure 5.7 A-C). This result suggests that the Notch defect observed in Opa1 depleted type II neuroblasts is independent of Rab mediated trafficking.

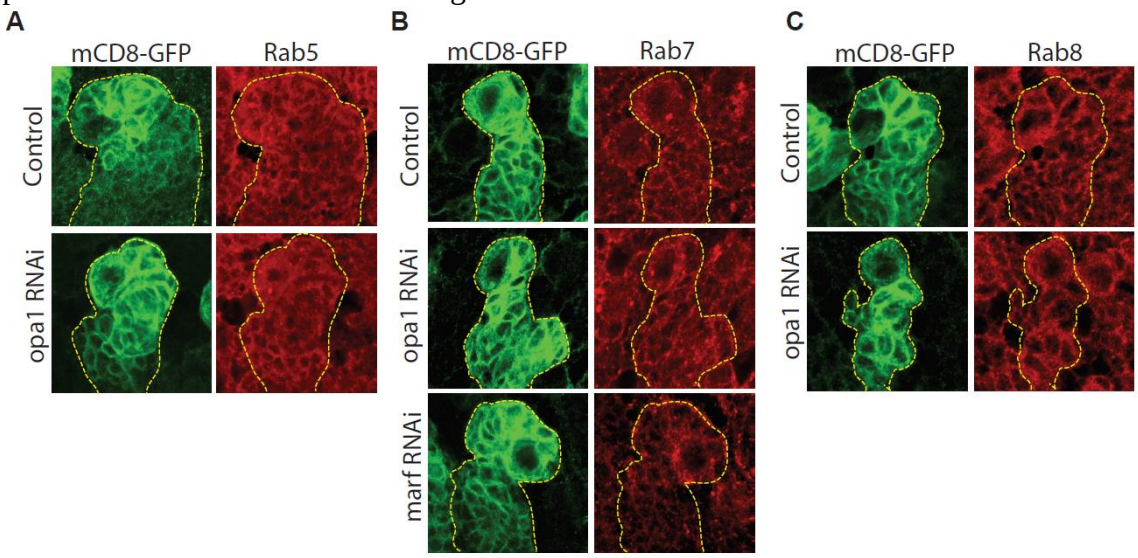

Figure 5.7: Opa1 depletion does not affect Rab5, Rab7 and Rab8 distribution and levels in type II neuroblasts.

A: Representative confocal images of type II neuroblast lineages (green) stained for Rab5. Control (8 type II neuroblasts, 3 Brains), *opa1* RNAi (10,3).

B: Representative confocal images of type II neuroblast lineages (green) stained for Rab7. Control (9 type II neuroblasts, 3 Brains), *opa1* RNAi (8,3), *marf* RNAi (9,3).

C: Representative confocal images of type II neuroblast lineages (green) stained for Rab8. Control (6 type II neuroblasts, 2 Brains), *opa1* RNAi (7,2).

5.4. Discussion

In this chapter, we show that Notch signaling in type II neuroblasts is required for the maintenance of fused mitochondrial morphology. We observed rescue of overproliferation phenotype of neuroblasts in Notch gain of function mutants by co-depletion of Opa1 and Marf. This indicates the positive feedback loop between fused mitochondrial morphology and Notch signaling during type II neuroblasts development. How do fused mitochondria cooperate with the Notch pathway for neuroblast proliferation is still under investigation. This is in striking contrast to recent literature including work in the lab wherein fused mitochondrial morphology is correlated with loss of Notch activity. Previous work in triple-negative breast cancer (TNBC) shows that Notch signaling enhances mitochondrial fission via Drp1 (Chen et al., 2018). In *Drosophila* ovarian posterior follicle cells, forced fusion induces an increase in mitochondrial membrane potential and loss of Notch signaling (Tomer et al., 2018). In cardiomyocytes loss of Opa1 leads to a decrease in differentiation due to enhanced Notch processivity (Kasahara et al., 2013).

It is interesting to speculate the reasons for observing tissue-specific differences in the requirement of mitochondrial fusion for Notch signaling in differentiation. In the previous analysis of follicle cells, we found that EGFR signaling regulates fragmented morphology required for appropriate Notch signaling (Mitra et al., 2012). It is likely that fragmented mitochondrial morphology leads to an interaction between EGFR and Notch signaling pathways in follicle cells and possibly other cell types such as cardiomyocytes and TNBCs where increased Notch signaling has been predicted upon mitochondrial fragmentation or loss of membrane potential (Chen et al., 2018; Kasahara et al., 2013; Mitra et al., 2012).

At the heart of this discussion on the interaction between Notch signaling and mitochondrial morphology, lies an analysis of how Notch signaling regulates inner mitochondrial membrane architecture or function and how alteration of inner mitochondrial membrane architecture affects Notch signaling. We found a cytoplasmic accumulation of NICD in Opa1 mutant type II neuroblasts which might be failing to enter

into the nucleus to activate the gene expression program essential for neuroblast proliferation. Loss of Su(H) also showed fragmented mitochondria and loss of differentiated cells in type II neuroblasts lineage similar to the downregulation of Notch. Since the action of both NICD and Su(H) is needed in the nucleus to activate downstream targets, it is possible that Notch regulates fused mitochondrial morphology. This could be through the canonical pathway by enhancing expression or activity of fusion genes *opa1* and *marf* in type II neuroblasts and reducing activity or expression of fission gene Drp1.

The non-canonical Notch pathway including mTOR and AKT is involved in the maintenance of type II neuroblasts self-renewal. Also, the mTOR pathway plays a role with PINK1 in promoting neuroblasts proliferation upon Notch overexpression (Lee et al., 2013). It would be interesting to ascertain the role of the mTOR pathway in regulating mitochondrial morphology in the type II neuroblasts. Fragmented mitochondria may result in alteration of trafficking pathways in the type II neuroblasts, leading to cytoplasmic retention of cleaved NICD and lack of transport to the nucleus to activate gene expression.

Chapter 6: ATP synthase is required for Notch-mediated proliferation of type II neuroblasts lineage

6.1 Introduction

The mitochondrial inner membrane houses a plethora of different proteins involved in the electron transport chain and various transport and structural processes in the mitochondria. Most of these proteins consist of different complexes required for ATP production through the process of Oxidative phosphorylation. Some of the ETC complexes like complex I, complex III and complex IV cluster together to form the respiratory chain supercomplexes (RCS). The formation of RCS enhances the efficiency of ATP production. Similarly complex V i.e. ATP synthase form dimer at high curvature area in the inner membrane. Subunit E and subunit G of the ATP synthase are involved in the process of dimerization. Studies have shown that ATP synthase dimerization induces curvature in the inner mitochondrial membrane to form cristae. Mutation or inhibition of ATP synthase dimerization leads to aberrant cristae formation. Recent evidence suggests the function of cristae morphology and ATP synthase dimerization in stem cell differentiation (Teixeira et al., 2015). ATP synthase levels are increased during germline stem cell differentiation in the *Drosophila* ovary. The knockdown of ATP synthase in germline stem cells leads to loss of differentiation. Interestingly, the function of ATP synthase in germline stem cell differentiation is OxPhos independent. Cristae maturation through ATP synthase dimerization is thought to be important for germline stem cell differentiation. *Drosophila* neuroblast undergoes progressive cell size reduction at the end of larval stages and finally terminally differentiate into neurons during pupal stages. This phenomenon is governed by a metabolic switch regulated by OxPhos and mediator complex proteins. Loss of OxPhos proteins in neuroblasts leads to failure of neuroblast size reduction and terminal differentiation and they present even in the pupal stages. The depletion of OxPhos in neuroblasts does not cause any energy stress as they are dependent on glycolysis for ATP requirements. However, another recent study suggested that OxPhos is required not only for the terminal differentiation

of neuroblasts but also for the overall development of neuroblasts (Homem et al., 2014; van den Ameele and Brand, 2019). Depletion of OxPhos proteins leads to a reduction in neuroblast proliferation as a consequence of delayed cell cycle progression and temporal patterning, in turn, result in decreased lineage size. As discussed in the previous chapters, depletion of Opa1 which is inner mitochondrial protein has a greater impact on neuroblast proliferation and differentiation as compared to depletion of outer membrane fusion protein Marf. These observations led us to hypothesize that differentiation defects caused by Opa1 knockdown are due to the perturbed architecture of the inner mitochondrial membrane. As discussed before, OxPhos proteins play an important role to form and maintain the integrity of the inner membrane. In this chapter, we have assessed function on OxPhos by depleting levels of complex IV and complex V in type II neuroblast differentiation and Notch signaling.

6.2 Material and methods

6.2.1 Fly stocks: *pnt*-Gal4, UAS-mCD8-GFP, *cova* RNAi (BL27548), *atpβ* RNAi (BL28056), $Drp1^{S193D}$ (GTPase domain mutant), $Drp1^{S193D}$;*cova* RNAi, $Drp1^{S193D}$;*atpb* RNAi

6.2.2 Antibodies:

Primary antibodies: anti-pH3 (1:1000, Invitrogen), anti-NICD (1:10, DSHB), anti-Dpn (1:150, Abcam), anti-Pros (1:25, DSHB), anti-GFP (1:1000, Invitrogen)

Secondary antibodies: anti-Mouse 568,633 (1:1000, Molecular Probes), anti-Chicken (1:1000, Molecular Probes),anti-Rat 568, 633, 647 (1:1000, Molecular Probes).

For detailed information about primary and secondary antibodies with their respective dilutions please refer to section 2.1.2.

6.2.3 Immunohistochemistry: Third instar larvae were dissected in Schneider's medium and immunostained with antibodies mentioned above. For detailed procedure please refer to section 2.2.3.

6.2.4 Image acquisition and analysis: Images were acquired by using LSM710 or LSM780 inverted microscope (Carl Zeiss, Inc. and IISER Pune microscopy facility) with a Plan apochromat 40x 1.4NA and 63x 1.4NA oil objective. Please refer to section 2.2.8 and 2.2.9 for detailed information about image acquisition and analysis.

6.3 Results

6.3.1 Mitochondrial OxPhos is required for type II neuroblasts differentiation.

The data presented in the thesis so far shows that neuroblast proliferation and differentiation are affected by mitochondrial fusion protein downregulation and loss of Notch function. An increase in cytochrome C levels in Opa1 downregulation indicates a possible role of inner mitochondrial membrane organization in neuroblast differentiation. It is known that Opa1 has a role in the maintenance of cristae organization apart from mitochondrial fusion (Frezza et al., 2006; Patten et al., 2014). In addition to the Opa1, ETC complexes also play an important role in regulating cristae morphology. The ATP synthase complex and its dimerization have been specifically known to play a role in *Drosophila* germ cell differentiation. The requirement of ATP synthase for germ cell differentiation is independent of its role in ATP production (Teixeira et al., 2015). They suspected the role of mitochondrial cristae during this process. Opa1 loss leads to a specific decrease in complex IV levels and activity in pancreatic cells (Zhang et al., 2011). Opa1 depletion also leads to loss of dimerization of complex V and Opa1 and complex V together play a profound role in stabilization of cristae in the inner mitochondrial membrane (Paumard et al., 2002; Quintana-Cabrera et al., 2018). To analyze the function of cristae morphology in neuroblast differentiation in detail, we used RNAi against cytochrome oxidase subunit Va (CoVa) and ATP synthase subunit beta (ATPB) to disrupt the ETC complexes. Further, we analyzed the differentiated populations by Dpn and Pros immunostaining. Both CoVa and ATPB mutants showed a decreased number of Dpn positive mature INPs and Pros positive GMCs in type II lineage similar to Opa1 depletion (Figure 6.1 A-D). To check whether these defects can be reversed by forced fusion, we co-depleted Drp1 along with CoVa and ATPB.

Interestingly co-depletion of Drp1 and CoVa showed rescue in mature INP number but differentiation was not rescued on co-depletion of Drp1 and ATPB (Figure 6.1 A-D). This again highlighted the importance of an intact ATP synthase complex in neuroblast differentiation. The GMC population failed to appear in forced fusion in both CoVa and ATPB downregulation background (Figure 6.1 A-D).

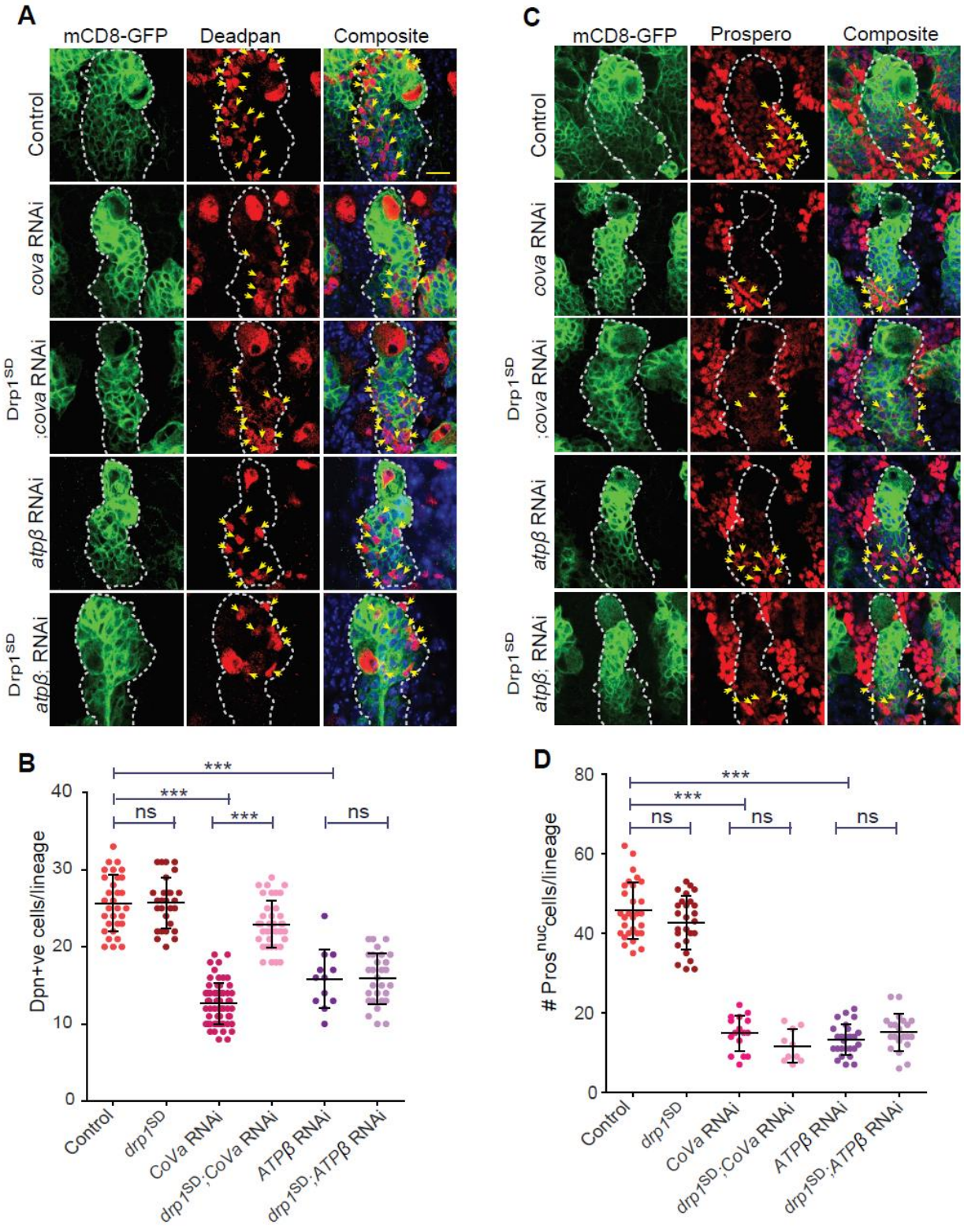

Fig 6.1: Drp1 depletion shows rescue in differentiation in *cova* but not in *atpβ* RNAi expressing type II neuroblasts lineages.

A: Type II lineages (CD8-GFP, green) showing Dpn positive INPs (red, yellow arrows). *pnt*-Gal4 was used to drive the expression of RNAi and mutant. Scale bar- 10µm

B: Quantification of Dpn positive INPs in control (23 neuroblasts lineages,16 brains), $Drp1^{SD}$ (28,10), *cova* RNAi (62,10), $Drp1^{SD}$;*cova* RNAi (39,6), *atpβ* RNAi (12,5), $Drp1^{SD}$;*atpβ* RNAi (29,5). Control and $Drp1^{SD}$ quantification is repeated from Figure 3E.

C: Type II lineages (CD8-GFP, green) showing Pros positive INPs (red, yellow arrows). Scale bar- 10µm

D: Quantification of Pros positive GMCs in control (29 neuroblasts lineages,18 brains), $Drp1^{SD}$ (26,8), *cova* RNAi (16,4), $Drp1^{SD}$;*cova* RNAi (10,4), *atpβ* RNAi (26,6), $Drp1^{SD}$;*atpβ* RNAi (21,5).

Student's t-test is performed for statistical analysis. ns – Non significant, ***- $p<0.001$.

6.3.2 Loss of differentiation in OxPhos mutants is caused due to impaired cell cycle progression.

To check the decreased differentiated population in the ETC mutant was because of impairment in the cell cycle, we quantified mitotic cells in type II neuroblasts lineages of ETC mutants labeled with pH3 antibody. Mitotic cell quantification in ETC mutant type II neuroblasts lineages showed reduced pH3 labeled cells in CoVa and ATPB downregulation (Figure 6.2 A-B). Reduced mitotic cells were rescued on co-depletion of CoVa and Drp1 but not on the co-depletion of Drp1 and ATPB (Figure 6.2 A-B). This further confirmed the requirement of an intact ATP synthase complex for normal cell cycle progression of type II neuroblasts.

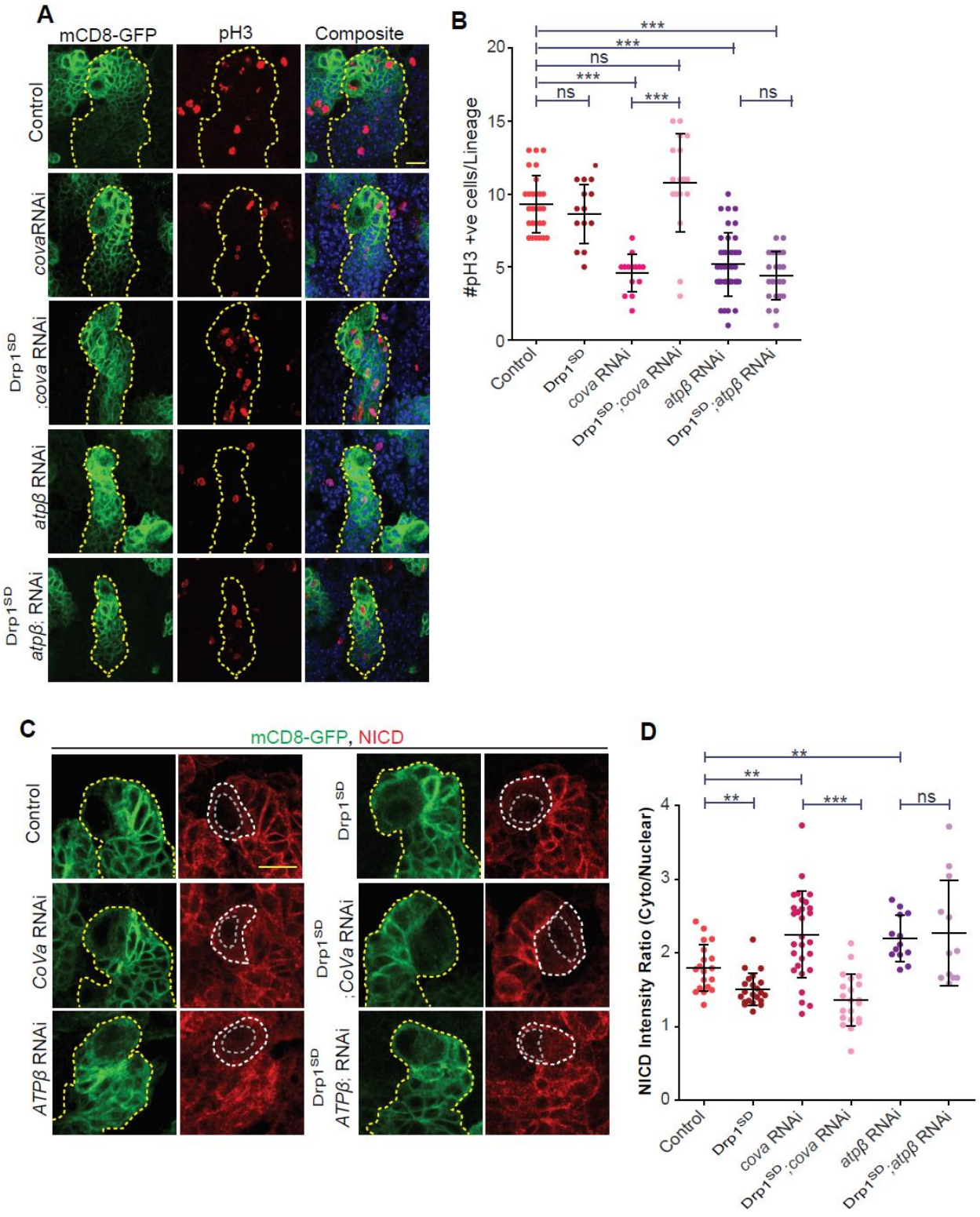
A
mCD8-GFP
pH3
Composite
Control
covaRNAi
Drp1SD ;cova RNAi
atpβ RNAi
Drp1SD atpβ; RNAi
B
#pH3 +ve cells/Lineage
***
***
ns
***
***
ns
Control
Drp1SD
cova RNAi
Drp1SD ;cova RNAi
atpβ RNAi
Drp1SD ;atpβ RNAi
C
mCD8-GFP, NICD
Control
CoVa RNAi
ATPβ RNAi
Drp1SD
Drp1SD ;CoVa RNAi
Drp1SD ATPβ; RNAi
D
NICD Intensity Ratio (Cyto/Nuclear)
**
**
**
***
ns
Control
Drp1SD
cova RNAi
Drp1SD ;cova RNAi
atpβ RNAi
Drp1SD ;atpβ RNAi

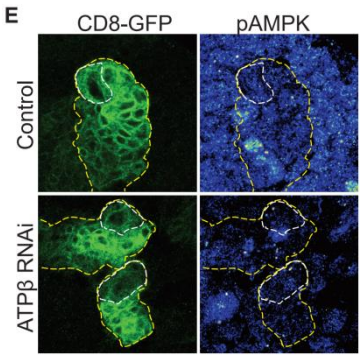

Fig 6.2: Forced fusion by co-depletion of Drp1 rescue pH3 positive cells and cytoplasmic accumulation of NICD in CoVa RNAi but not in ATPβ RNAi.

A: Type II neuroblasts lineages (CD8-GFP, green) stained show loss of pH3 positive mitotic cells (red). *pnt*-Gal4 was used to drive the expression of RNAi. Scale bar- 10uM

B: Quantification of pH3 positive cells in control (28 neuroblasts lineages,6 brains), $Drp1^{SD}$ (13,3), *cova* (14,4), $Drp1^{SD}$;*cova* RNAi (19,4), *atpβ* RNAi (38,8), $Drp1^{SD}$;*atpβ* RNAi (23,4). Scale bar- 10µm. Statistical analysis was done by using unpaired t-test. ns- non significant, ***- p<0.001

C: Type II neuroblasts (CD8-GFP, green, yellow dotted line) stained for NICD and observed for distribution in control, $Drp1^{SD}$, *cova* RNAi, $Drp1^{SD}$;*cova* RNAi, *atpβ* RNAi, $Drp1^{SD}$;*atpβ* RNAi . Scale bar- 10µm

D: Quantification of NICD (B) in control (19,10), *opa1* RNAi (20,12), *marf* RNAi (15,12), $Drp1^{SD}$ (22,5), $Drp1^{SD}$;*opa1* RNAi (28,6), $Drp1^{SD}$;*marf* RNAi (11,5), *cova* RNAi (29,5), $Drp1^{SD}$;*cova* RNAi (21,5), *atpβ* RNAi (13,5), $Drp1^{SD}$;*atpβ* RNAi (12,7).

E: Representative confocal images of type II neuroblast showing pAMPK levels in control (15 Neuroblasts, 3 Brains) and ATPB RNAi (13,3)

6.3.3 Downregulation of CoVa and ATPB causes cytoplasmic retention of NICD which is rescued by forced fusion in CoVa depletion but not ATPB depletion.

Both CoVa and ATP synthase are mitochondrial inner membrane proteins and depletion of these give similar defects as Opa1 downregulation. We have found cytoplasmic retention of NICD in Opa1 depletion in type II neuroblasts (chapter 5). To check whether depletion of CoVa and ATP synthase depletion gives a similar defect, we performed NICD immunostaining in CoVa and ATPB RNAi mutants. Consistent with previous results, we found increased cytoplasmic retention of NICD in both CoVa and ATPB downregulation highlighting the role of the inner membrane in the regulation of the

Notch signaling pathway (Figure 6.2 C-D). Forced fusion of mitochondrial outer membrane by depletion of Drp1 function caused rescue of NICD localization in CoVa downregulation but not in ATPB downregulation (Figure 6.2 C-D). These results pointing toward the specialized function of ATP synthase complex in Notch-mediated type II neuroblast differentiation.

6.4 Discussion

Our study showed that mitochondrial OxPhos proteins complex IV and V are essential for type II neuroblast proliferation and differentiation. We found similar type II neuroblast differentiation defects in complex IV and V mutants as compared to Opa1 depletion. Both complex V and Opa1 are essential for the formation and maturation of cristae architecture suggesting a role for cristae in neural stem cell differentiation. We also observed cytoplasmic retention of NICD in both CoVa and ATPB knockdown. Previous studies from the lab have shown an increased mitochondrial membrane potential upon Drp1 mutation in *Drosophila* follicle cells. This was found to be responsible for inhibition Notch signaling which resulted in the loss of follicle cell differentiation. It would be interesting to assess the function of membrane potential in the differentiation of mitochondrial mutant neuroblast differentiation. Interestingly forced fusion of mitochondrial outer membrane rescued differentiation defects caused by Opa1 and CoVa knockdown but not ATPB knockdown. This result shows an indispensable function of ATP synthase in neuroblast differentiation. We observed that depletion of ATP synthase did not cause energy stress in type II neuroblast lineage (Figure 6.2 E) suggesting energy independent function of ATP synthase in neuroblast differentiation. Previous evidence showed the function of ATP synthase in germline stem cell differentiation. ATP synthase dimerization is thought to be essential for this function independent of its role in ATP production as knockdown of ATP synthase subunits E and G gave defects similar to subunit B as these subunits do not participate in energy production function directly. These subunits are required to form dimers of ATP synthase. Future experiments by using RNAi lines against subunit E and G would highlight the function of complex V in more detail. Since co-depletion of Drp1 could

rescue defects only in Opa1 and CoVa depletion, we propose that by force fusing the outer membrane could somehow rescue neuroblast differentiation through ATP synthase dimerization. However in ATPB knockdown, since the complex is itself getting down-regulated it cannot rescue dimerization and in turn differentiation. Electron microscopy studies on control and mutant larval brains would tell us whether inner mitochondrial membrane and cristae are getting affected in mutants or not and are reversed in double mutants. The role of ATP synthase dimerization in neuroblast differentiation and Notch signaling is however still an open question.

7 Thesis Summary and future directions

The Current understanding of mitochondria has enhanced the perspective of its role in the cell. Non-nuclear eukaryotic organelles not only play a supportive role but also take part in an instructive role to decide cell function and fate. Studies from the last few decades have added enormous knowledge about different organelles function during cell formation, division, differentiation and apoptosis. Mitochondria have emerged as one of the most important organelles which take part in all functions mentioned above apart from its core function of ATP generation. Mitochondria are no longer believed to small rounded organelles as depicted in a textbook, rather they occur in various shapes and sizes and are often tubular. Several studies have shown that the dynamic nature of mitochondria is essential for cell fate determination. Loss of the ability to change mitochondrial morphology leads to a plethora of diseases including neurodegenerative diseases like Alzheimer's disease, Optic atrophy, Charcot Marie Tooth type 2A. But how does mitochondrial architecture and function interact with signaling pathways involved in the progression of these diseases is not clearly understood. Mutation in mitochondrial proteins also causes different types of cancers in humans. Identification of molecular pathways that regulate mitochondrial morphology and metabolism in the context of cancer and other diseases will enable us to come up with new intervention techniques to treat or cure these diseases. In addition to that, this will also add a new dimension to our understanding of organism development.

Mitochondrial fusion is essential for neuroblast proliferation and differentiation

Several studies on stem cells have shown that they harbor small and punctate mitochondria (Xu et al., 2013). Fragmented mitochondrial morphology is usually associated with less mitochondrial mass, ATP production, mtDNA copy number and OxPhos (Xu et al., 2013). These findings underestimate the role of mitochondria in stem cell development. We first characterized mitochondrial morphology in *Drosophila* neuroblasts. We found that mitochondria are dispersed throughout the cell and exhibit more a balance between tubular and dispersed structures in neuroblasts. Mitochondrial

fragmentation mediated by depletion of fusion proteins Opa1 and Marf had a specific effect on neuroblast differentiation. However, change in mitochondrial morphology did not cause energy stress in the cell. Previous studies have shown that neuroblasts largely depend on glycolysis for their ATP need which could explain the absence of energy stress in fusion depleted neuroblasts (Homem et al., 2014). Interestingly, the depletion of Drp1 despite causing mitochondrial clusters did not show any phenotypic effect on neuroblast differentiation suggesting that Drp1 is dispensable for neuroblast development.

In *Drosophila* follicle cells, the depletion of Drp1 causes loss of follicle cell differentiation (Mitra et al., 2012). The transition from small and punctate mitochondrial morphology to tubular morphology is essential for the differentiation of cardiomyocytes from human induced pluripotent stem cells (iPSCs). Drp1 depleted human iPSCs also fail to differentiate into cardiomyocytes (Hoque et al., 2018). This evidence and our findings in neuroblasts indicate the context-dependent role of Drp1 in stem cell differentiation. The Co-depletion of Drp1 was able to restore mature INP number in Opa1 depleted type II neuroblast lineages. We observed clustered mitochondrial morphology in Drp1 and Opa1 co-depleted neuroblasts indicating that the rescue in differentiation could be because of the restoration of mitochondrial fusion and not due to depleted Drp1. It will be interesting to see whether overexpression of mitochondrial fusion protein such as Marf will also be able to rescue Opa1 defects or not.

To understand the mechanism by which fused mitochondria regulate neuroblast differentiation, we analyzed different aspects of mitochondrial activity affected during fragmentation caused by the depletion of Opa1 and Marf. Increased cytochrome C observed in Opa1 depleted neuroblasts raised the possibility of apoptosis and thereby loss of differentiation. But we found that loss of type II neuroblast differentiation is caused due to proliferative defects and not because of apoptosis in the lineage. In the canonical apoptosis pathway, the release of cytochrome C from mitochondria activates caspases which irreversibly trigger apoptosis (Ott et al., 2002). But this does not apply to all cell types. During *Drosophila* spermatogenesis, cytochrome C and caspase

activation are required for their terminal differentiation (Arama et al., 2003). We observed that cytochrome C is not diffused but present in a punctate pattern in the cytoplasm. It is also possible that cytochrome C is trapped in the intermembrane space of the mitochondria in Opa1 depleted neuroblasts and hence cannot activate the apoptosis pathway. Further experiments are needed to check whether the cytochrome C punctae colocalizes with mitochondria. Nevertheless, increased cytochrome C in Opa1 mutant neuroblasts suggest defects in inner membrane architecture. It is still unclear how the defect in the inner mitochondrial membrane leads to loss of differentiation of neuroblasts.

Mitochondrial inner membrane stability and ATP synthase play a critical role in neuroblast differentiation

Increased levels of cytochrome C and severe differentiation defects observed in Opa1 RNAi as compared to Marf RNAi raised the possibility of the function of the inner mitochondrial membrane in neuroblast differentiation. Opa1 loss leads to a specific decrease in complex IV levels and activity in pancreatic cells (Zhang et al., 2011). Opa1 depletion also leads to loss of dimerization of complex V and Opa1 and complex V together play a profound role in stabilization of cristae in the inner mitochondrial membrane (Paumard et al., 2002; Quintana-Cabrera et al., 2018). Hence we analyzed the function of complex IV and V in neuroblasts differentiation. Analysis of the inner membrane by removing subunits of complex IV (CoVa) and ATP synthase (ATPB) showed similar defects as Opa1 depletion. Both CoVa and ATPB depletion showed a decrease in the number of mature INP and GMCs (Figure D) confirming the specific role of the inner mitochondrial membrane in neuroblasts differentiation. However, forced outer membrane fusion could rescue mature INP numbers only in CoVa depletion and not complex V indicating the specific function of complex V in type II neuroblast differentiation. Mitochondrial inner membrane architecture is regulated by complex V and Opa1 (Ban et al., 2017; Cogliati et al., 2016; Olichon et al., 2003). Complex V dimerization is essential for cristae maturation. It has been shown that cristae maturation through complex V dimerization is required for germ cell differentiation in the

Drosophila ovary (Teixeira et al., 2015). Here we have demonstrated that downregulation of complex V also results in differentiation defect in type II neuroblast suggesting conserved function of complex V in stem cell differentiation. Apart from complex V, the role of Opa1 is also well established in the maintenance of cristae morphology. However, a detailed study of inner membrane architecture by electron microscopy is needed to confirm the involvement of cristae in neuroblast differentiation. Also, it is interesting to evaluate whether forced fusion in Drp1 and Opa1 double mutants leads to the reversal of cristae stabilization.

The interplay between the Notch signaling pathway and mitochondrial fusion is required during type II neuroblast differentiation

The Notch signaling pathway regulates the proliferation and differentiation of type II neuroblasts (Li et al., 2016). We showed a positive feedback loop between mitochondrial fusion and Notch signaling. Notch signaling in type II neuroblast maintains fused mitochondrial morphology. Further, mitochondrial fusion can rescue the differentiation defect in Notch loss of function mutants. Mitochondrial fragmentation caused by co-depletion of Opa1 and Marf reduces the Notch driven hyperproliferation of neuroblasts. It is interesting to test whether Notch driven tumor growth can be reduced by targeting mitochondrial fusion genes by pharmacological treatment. This will open new possible targets for cancer treatment as directly targeting Notch may lead to severe side effects in the patients.

In triple-negative breast cancer (TNBC) Notch signaling enhances mitochondrial fission via Drp1 (Chen et al., 2018) opposite to our findings. This suggests the regulation of mitochondrial morphology by Notch signaling is context-dependent and varies across different cell types. How Notch signaling and mitochondrial morphology regulate each other is still not clear. In *Drosophila* ovarian posterior follicle cells (PFCs), forced fusion induces an increase in mitochondrial membrane potential which further activates ERK (a downstream target of EGFR pathway) by phosphorylation. However increased levels of pERK do not translate into the activation of the EGFR pathway probably due to

cytoplasmic and possibly mitochondrial retention of pERK (Tomer et al., 2018). We found a cytoplasmic accumulation of Notch ICD in Opa1, complex IV and complex V mutants which might fail to enter into the nucleus to activate gene program essential for neuroblast proliferation. It would be interesting to see whether NICD is retained on mitochondria or any other subcellular compartments. Loss of Su(H) showed fragmented mitochondria and loss of differentiated cells in type II neuroblasts lineage similar to the downregulation of Notch. Since the action of both NICD and Su(H) is needed in the nucleus to activate downstream targets, it is possible that Notch regulates fused mitochondrial morphology through the nuclear program by enhancing expression genes such as Opa1, Marf and OxPhos in type II neuroblasts. A possible increase of mitochondrial fusion genes expression can be checked by analyzing mRNA level using RT-PCR in Notch overexpression mutants. Non canonical Notch pathway including mTOR and AKT is involved in the maintenance of self-renewal of type II neuroblast (Lee et al. 2013). It is interesting to see how canonical and non-canonical Notch pathways intersect with each other to ensure proper differentiation of type II neuroblasts.

In summary, we found that mitochondrial fusion and specifically inner membrane fusion and architecture regulatory proteins are involved in the neuroblast differentiation process and Notch signaling. Interestingly mitochondrial fission protein Drp1 has no specific role in neuroblast development. However, forced fusion by co-depletion of Drp1 rescues defect caused by Opa1 and CoVa depletion (Figure D). We also showed that the intact inner mitochondrial membrane is required for proper Notch activity during neuroblast differentiation. ATP synthase function is more critical in the differentiation process as forced outer membrane fusion did not rescue the defects caused by ATPB depletion (Figure D). As discussed previously, ATP synthase dimerization is needed for the formation and maturation of cristae. Since the complex is itself getting down-regulated, dimerization cannot occur in ATPB RNAi and hence probably we did not get rescue by force outer membrane fusion. At last, we propose ATP synthase dimerization is required for Notch-mediated type II neuroblast proliferation and differentiation. Future studies on how Notch signaling is regulated by inner membrane architecture and activity

will help decipher the mechanism by which mitochondrial structure interacts with signaling in differentiation.

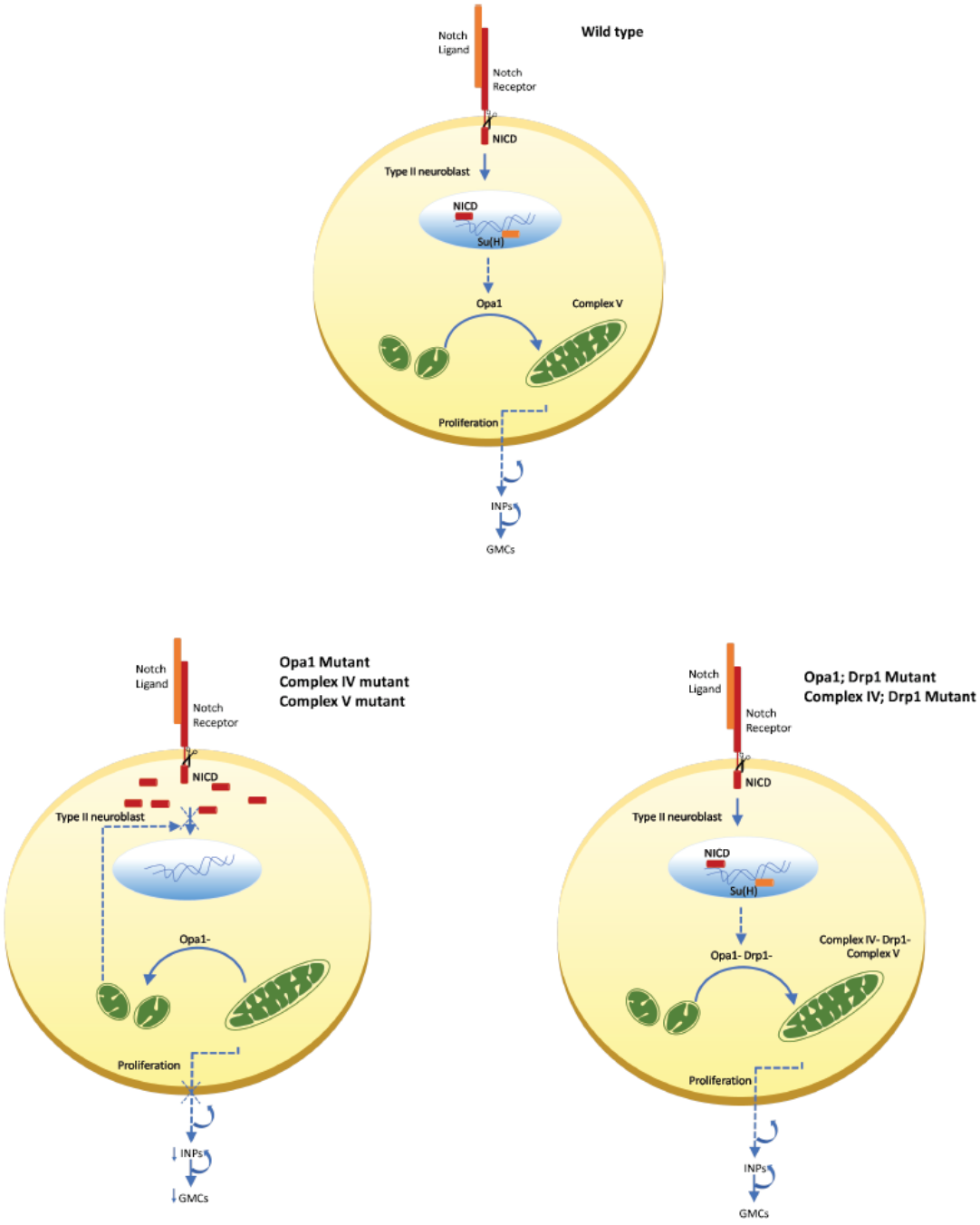

Figure D: Schematic summary for the regulation of neuroblasts type II differentiation by fused mitochondrial morphology

Mitochondria are maintained in a tubular morphology in type II neuroblasts by active Notch signaling. Mitochondrial fusion protein *opa1*, complex IV and complex V activity are essential for neuroblasts differentiation. Forced mitochondrial fusion leads to reversal of the type II neuroblasts differentiation defect *opa1* and complex IV mutants but not in complex V mutants. These data show that mitochondrial inner membrane morphology is essential for neuroblasts differentiation.

8 Appendix

8.1 Depletion of Opa1 and ATPB caused increased expression of Broad in type II neuroblasts.

Drosophila brain has been used as a reductionist model to study tumorigenesis and human brain development (Brand and Livesey, 2011; Hakes and Brand, 2019). Similar to neural precursor cells in the human brain, *Drosophila* neuroblasts also produce different kinds of neurons in a spatiotemporal manner (Doe, 2017; Homem and Knoblich, 2012). How the same neuroblast produces different types of neurons with time is still unclear. Studies from the last two decades have tried to address this question in detail. Embryonic neuroblasts express cascade of transcription factors in a temporal manner which can be inherited by GMCs (Homem and Knoblich, 2012; Isshiki et al., 2001). GMCs in the post-mitotic division are able to produce different types of neurons depending on the type of transcription factor they inherited from the neuroblast. This intrinsic cell timer ensures precise timing of the production of neurons with different identities in a precise spatiotemporal manner during brain development.

Neuroblasts sequentially express Hunchback, Sevenup, Krupel, Pdm1/Pdm2 (Pdm), Castor during embryonic developmental stages. Successful progression through cell division is essential for the expression of Sevenup and Krupel. A specific number of cell divisions are required for the transition from the expression of Hunchback to Krupel. The non-dividing neuroblasts fail to initiate the expression of Sevenup and Krupel and express the only Hunchback. However, expression of Pdm and Castor is cell cycle independent and able to express even in isolated and G2 arrested neuroblasts with time (Doe, 2017; Homem and Knoblich, 2012). At the end of embryonic stages neuroblast undergo quiescence and then re-enter into active cell division during larval stages (Tsuji et al., 2008). Castor expression persists during this transition and cascade of transcription factors resume their expression from Castor. In the larval stages, Castor expression is followed by the second wave of Sevenup expression. The transcription factor series in the larval stages is also paralleled by neuronal identity series.

Neuroblasts expressing both Sevenup and Castor produces neurons positive for early transcription factor Chinmo. Neurons produced in late larval stages express the Broad-core transcription factor (Homem and Knoblich, 2012). During the larval to pupal transition, neuroblasts undergo progressive cell size reduction and finally terminal differentiation (Homem et al., 2014). Hence very few neuroblasts retain at the pupal stage. The metabolism of larval neuroblast is dependent on aerobic glycolysis while mitochondrial OxPhos is required for size reduction and terminal differentiation (Homem et al., 2014). Recent literature suggests that mitochondrial OxPhos is not only required during larval to pupal transition but also essential for overall temporal patterning of neuroblasts (van den Ameele and Brand, 2019). We found that differentiated cells were reduced in Opa1, complex IV and complex V depleted type II neuroblast lineages. Temporal patterning of these lineages is possibly perturbed by change mitochondrial morphology. To test this, we immunostained Opa1 and complex V depleted brains with late neuronal transcription factor Broad. We found that nuclear Broad levels were upregulated in Opa1 and complex V depleted neuroblasts as compared to control (Figure A2 A). However, Broad positive cells were completely reduced in the downstream lineage of Opa1 and complex V depleted neuroblasts (Figure A2 B). It is possible that premature expression of late transcription factors might affect the differentiation profile of the neuroblasts. But how a change in mitochondrial morphology regulates expression of Broad is still not clear. Further experiments are needed to check the mitochondrial regulation of expression of temporal factors in neuroblasts. It will be interesting to see whether the loss of Notch signaling also gives rise to similar phenotypes as it also results in fragmented mitochondria.

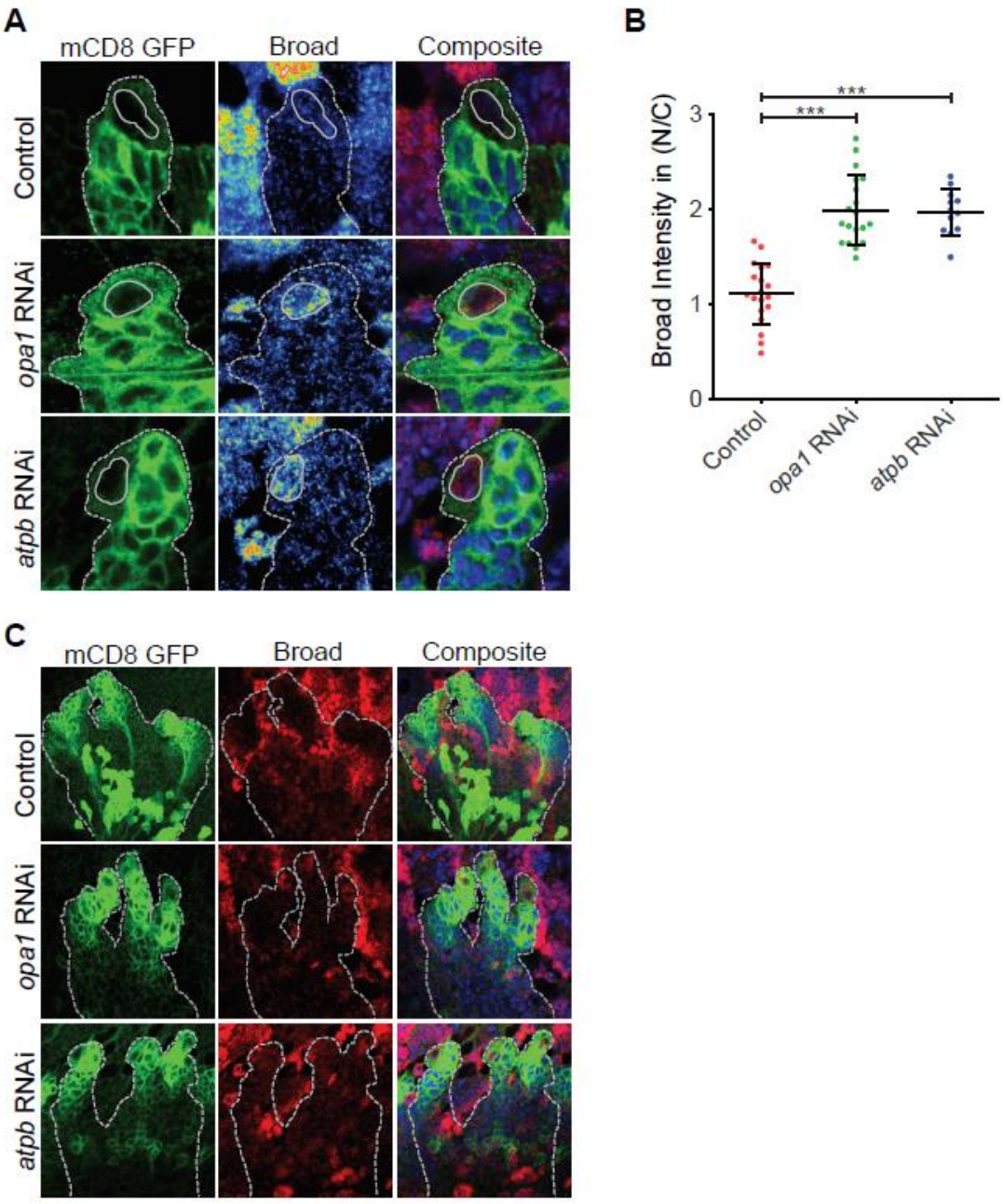

Figure A1: Depletion of Opa1 and ATPB caused increased expression of Broad in type II neuroblasts

A: Representative confocal images of type II neuroblasts stained with CD8-GFP (green) and Broad (rainbow color map) showing increased expression of Broad in *opa1* and *atpb* depleted neuroblasts.

B: Graph of nuclear to cytoplasmic ratios of Broad intensity from type II neuroblasts showing a two-fold increase in *opa1* and *atpb* RNAi. Control (19 Neuroblasts, 8 Brains), *opa1* RNAi (19,8), *atpb* RNAi (12,5). Student's t-test is performed for statistical analysis. ***- $p<0.001$.

C: Fluorescence confocal images of type II neuroblast lineages showing loss of Broad positive cells in

opa1 and *atpb* knockdown. Control (38 Type II neuroblasts lineages, 8 Brains), *opa1* RNAi (18, 5), *atpb* RNAi (20, 6).

8.2 PPR depletion does not affect neuroblast number and differentiation.

Pentatricopeptide Repeat (PPR) is a family of proteins involved in RNA splicing, RNA stabilization and translation (Manna, 2015). Its human homolog is LRPPRC which is a mitochondrial protein and mutation in the gene causes Leigh syndrome (Debray et al., 2011; Manna, 2015). LRPPRC is a key player in the stabilization of mtRNA by polyadenylation. It is also involved in the mtRNA translation process and mutation in LRPPRC leads to a decrease in mtRNA amount. This affects mitochondrial functions such as ETC activity and ATP production (Ruzzenente et al., 2012). In the *Drosophila* larval muscles, PPR localizes to the mitochondria. The depletion of PPR in *Drosophila* larvae causes an overall decrease in the levels of mRNA levels of OxPhos components (Jaiswal et al., 2015). We found that depleted levels of complex IV and complex V in *Drosophila* larval brain causes a reduction in neuroblast differentiation. Since PPR is responsible for OxPhos mRNA stabilization and translation, it is possible that the downregulation of PPR in neuroblasts could also result in the same phenotype as complex IV and V depletion. Hence we used PPR RNAi to deplete the levels of PPR in type I and type II neuroblasts. Further, we analyzed neuroblast number, differentiation profile and mitotic index. Interestingly, neuroblasts number and their differentiated progenies were unaffected in PPR RNAi (Figure A2 A-D & G-H). pH3 positive neuroblasts numbers were also not affected in PPR depletion (Figure A2 E-F). This data suggests that PPR function is dispensable for neuroblast development. Previously in our lab, mitochondrial clustering is observed upon depletion of PPR in *Drosophila* germ cells and follicle cells. (Bhavin Uttekar and Adikrishna K., unpublished data). However, a more detailed analysis by using a null mutant of PPR is required. It is also interesting to check whether PPR mutant causes any defect in mitochondrial architecture in neuroblasts.

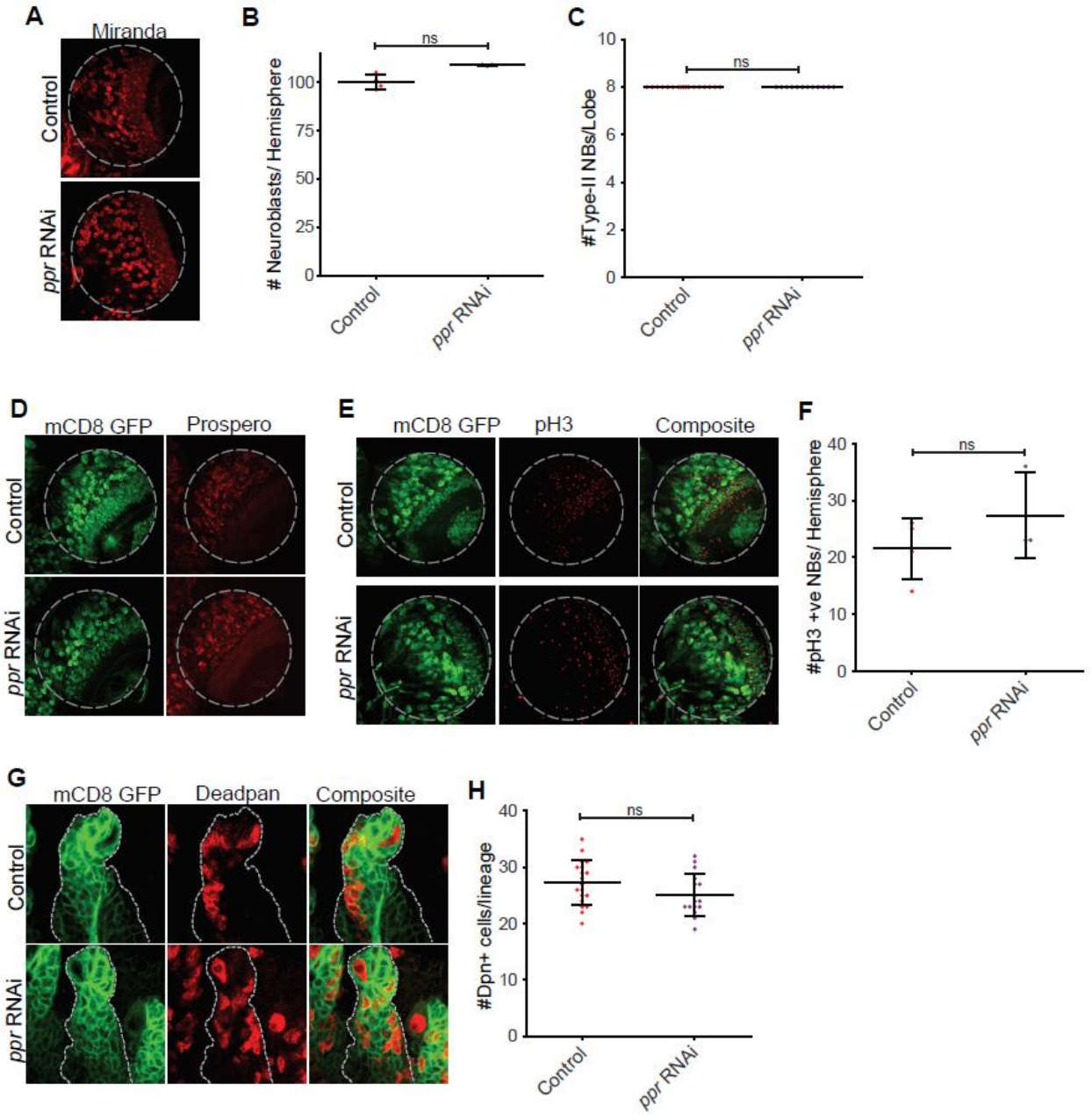

Figure A2: Depletion of PPR has no effect on neuroblast number and differentiation of type I and type II neuroblasts

A: Representative confocal images of larval brain hemisphere stained with Miranda (red) showing unchanged neuroblast numbers in *ppr* RNAi.

B-C: Analysis of type I (B) and type II neuroblasts (C) in control and *ppr* RNAi. Control (3 Brains), *ppr* RNAi (4 Brains).

D: Fluorescence confocal images of brain hemispheres showing CD8-GFP (green) and Pros (red) staining. Control (4 Brains), *ppr* RNAi (3 Brains).

E-F: Representative confocal images of larval brain hemispheres stained for GFP (green) and pH3 (red) staining (E) showing unchanged pH3 positive neuroblast numbers in *ppr* RNAi (F). Control (4 Brains), *ppr* RNAi (3 Brains).

G-H: Representative fluorescence images of type II neuroblast lineages stained with GFP (green) and Dpn (red) antibodies showing Dpn positive mature INPs are unaffected in *ppr* RNAi (G). Analysis of Dpn positive mature INPs (H). Control (19 Type II neuroblasts lineages, 4 Brains), *ppr* RNAi (16, 4).

Student's t-test is performed for statistical analysis. ns – Non significant

8.3 Co-depletion of cytochrome C and Opa1 partially rescues reduced mature INP number in type II neuroblast lineage.

Cytochrome C is a part of the ETC process where it shuttles electrons between complex III and complex IV. It is also a key player in the cell death process (Vempati et al., 2009). During apoptosis, it is released into the cytoplasm where it activates Apoptotic protease activating factor 1 (APAF1) which in turn activates different caspases. Activation of caspases irreversibly triggers DNA fragmentation, nuclear condensation, membrane blebbing and finally phagocytosis by neighboring cells (Shakeri et al., 2017). Approximately 85% of cytochrome C is stored in cristae (Cogliati et al., 2016). During the cristae remodeling, this stored cytochrome C gets released into the cytoplasm. We observed that depletion of Opa1 causes an increase in cytochrome C levels in *Drosophila* neuroblasts (Figure 4.3). But it did not cause cell death in neuroblast lineage as we observed no change in caspase 3 levels and TUNEL positive nuclei in these mutants. To check whether increased cytochrome C in Opa1 depletion caused the loss of mature INP, we co-depleted cytochrome C with Opa1 in type II neuroblasts. RNAi used against cytochrome C was able to deplete protein levels in the neuroblasts (Figure A3A). Further analysis of Deadpan positive mature INPs in co-depletion of cytochrome C and Opa1 showed the partial rescue in mature INP number in co-depletion. This data suggest that for Opa1 mediated differentiation defects in neuroblasts, cytochrome C is responsible to some extent. But how cytochrome C affects Opa1 mediated differentiation defects in type II neuroblast is still not clear. However, increased levels of cytochrome C in Opa1 RNAi clearly indicate defects in the inner mitochondrial membrane. It is interesting to check whether reduced cytochrome C in Opa1 depletion background ameliorate inner membrane architecture or not.

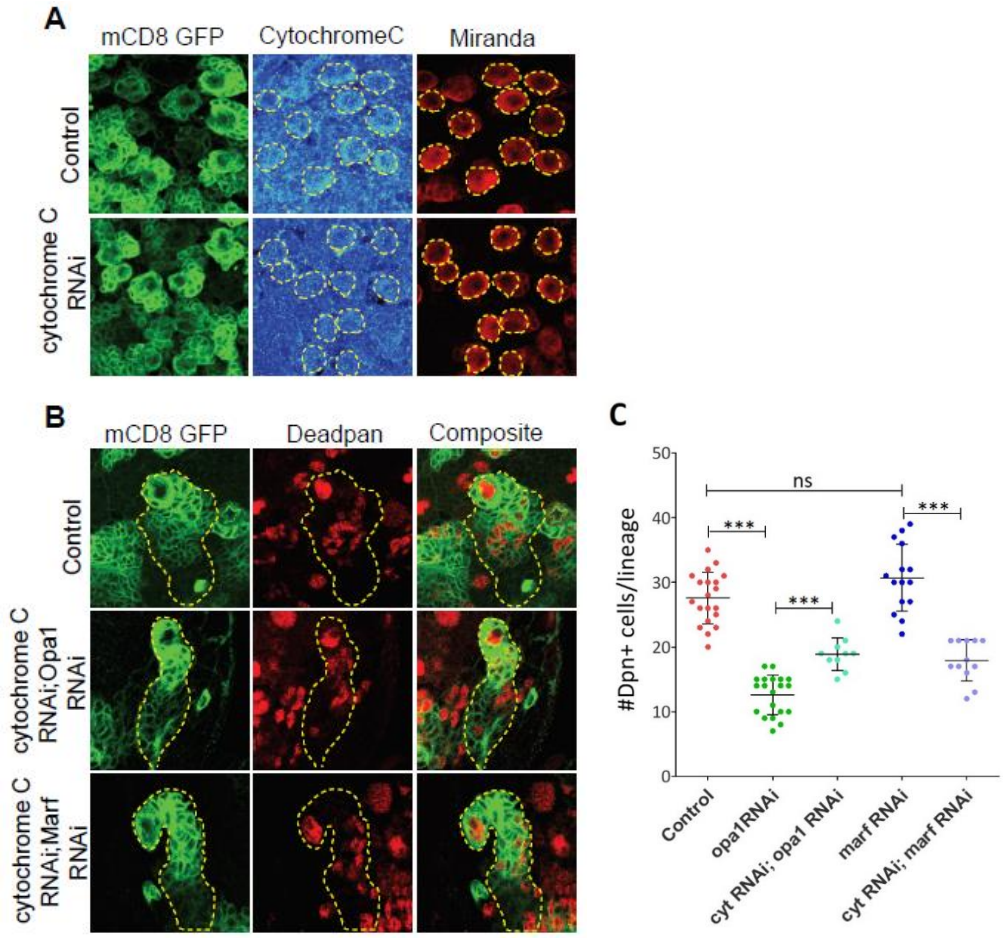

Figure A3: Co-depletion of cytochrome C and Opa1 partially rescues mature INP number in type II lineage.

A: Representative confocal images of neuroblasts immunostained with cytochrome C showing reduced levels in cytochrome C RNAi. Control (4 Brains), CytochromeC RNAi (3 Brains).

B: Confocal images of type I lineages stained with CD8-GFP (green) and Dpn (red) showing partial rescue in co-depletion of Opa1 and cytochrome C.

C: Analysis of Dpn positive mature INPs in Control (23 Lineages, 5 Brains), opa1 RNAi (20, 6), cytochrome C RNAi;opa1 RNAi (10, 3), marf RNAi (15, 8), cytochrome C RNAi;marf RNAi (12, 3). Student t-test. ns - non significant, *** >0.001

9 References

Akopova, O. V., Kolchinskaya, L. I., Nosar, V. I., Bouryi, V. A., Mankovska, I. N. and Sagach, V. F. (2012). Cytochrome c Is an Amplifier of Reactive Oxygen Species Release in Mitochondria. *Int. J. Physiol. Pathophysiol. Pharmacol.* **3**, 269–280.

Alexander, C., Votruba, M., Pesch, U. E., Thiselton, D. L., Mayer, S., Moore, A., Rodriguez, M., Kellner, U., Leo-Kottler, B., Auburger, G., et al. (2000). OPA1, encoding a dynamin-related GTPase, is mutated in autosomal dominant optic atrophy linked to chromosome 3q28. *Nat. Genet.* **26**, 211–215.

Amiri, H., Karlberg, O. and Andersson, S. G. E. (2003). Deep origin of plastid/parasite ATP/ADP translocases. *J. Mol. Evol.* **56**, 137–150.

Arama, E., Agapite, J. and Steller, H. (2003). Caspase Activity and a Specific Cytochrome C Are Required for Sperm Differentiation in Drosophila. *Developmental Cell* **4**, 687–697.

Archibald, J. (2014). *One Plus One Equals One: Symbiosis and the Evolution of Complex Life*. Oxford University Press.

Balaban, R. S. (1990). Regulation of oxidative phosphorylation in the mammalian cell. *Am. J. Physiol.* **258**, C377–89.

Ban, T., Ishihara, T., Kohno, H., Saita, S., Ichimura, A., Maenaka, K., Oka, T., Mihara, K. and Ishihara, N. (2017). Molecular basis of selective mitochondrial fusion by heterotypic action between OPA1 and cardiolipin. *Nat. Cell Biol.* **19**, 856.

Ban, T., Kohno, H., Ishihara, T. and Ishihara, N. (2018). Relationship between OPA1 and cardiolipin in mitochondrial inner-membrane fusion. *Biochim. Biophys. Acta Bioenerg.* **1859**, 951–957.

Bleazard, W., Michael McCaffery, J., King, E. J., Bale, S., Mozdy, A., Tieu, Q., Nunnari, J. and Shaw, J. M. (1999). The dynamin-related GTPase Dnm1 regulates mitochondrial fission in yeast. *Nat. Cell Biol.* **1**, 298.

Bossy-Wetzel, E. and Green, D. R. (1999). Caspases induce cytochrome c release from mitochondria by activating cytosolic factors. *J. Biol. Chem.* **274**, 17484–17490.

Brand, A. H. and Livesey, F. J. (2011). Neural stem cell biology in vertebrates and invertebrates: more alike than different? *Neuron* **70**, 719–729.

Brown, G. C. (1992). Control of respiration and ATP synthesis in mammalian mitochondria and cells. *Biochem. J* **284 (Pt 1)**, 1–13.

Büeler, H. (2010). Mitochondrial dynamics, cell death and the pathogenesis of Parkinson's disease. *Apoptosis* **15**, 1336–1353.

Cai, J., Yang, J. and Jones, D. (1998). Mitochondrial control of apoptosis: the role of cytochrome c. *Biochimica et Biophysica Acta (BBA) - Bioenergetics* **1366**, 139–149.

Chen, H. and Chan, D. C. (2017). Mitochondrial Dynamics in Regulating the Unique Phenotypes of Cancer and Stem Cells. *Cell Metab.* **26**, 39–48.

Chen, H., Detmer, S. A., Ewald, A. J., Griffin, E. E., Fraser, S. E. and Chan, D. C. (2003). Mitofusins Mfn1 and Mfn2 coordinately regulate mitochondrial fusion and are essential for embryonic development. *J. Cell Biol.* **160**, 189.

Chen, D., Gao, F., Li, B., Wang, H., Xu, Y., Zhu, C. and Wang, G. (2010). Parkin mono-ubiquitinates Bcl-2 and regulates autophagy. *J. Biol. Chem.* **285**, 38214–38223.

Chen, L., Zhang, J., Lyu, Z., Chen, Y., Ji, X., Cao, H., Jin, M., Zhu, J., Yang, J., Ling, R., et al. (2018). Positive feedback loop between mitochondrial fission and Notch signaling promotes survivin-mediated survival of TNBC cells. *Cell Death Dis.* **9**, 1050.

Chiong, M., Cartes-Saavedra, B., Norambuena-Soto, I., Mondaca-Ruff, D., Morales, P. E., García-Miguel, M. and Mellado, R. (2014). Mitochondrial metabolism and the control of vascular smooth muscle cell proliferation. *Front Cell Dev Biol* **2**, 72.

Cogliati, S., Frezza, C., Soriano, M. E., Varanita, T., Quintana-Cabrera, R., Corrado, M., Cipolat, S., Costa, V., Casarin, A., Gomes, L. C., et al. (2013). Mitochondrial cristae shape determines respiratory chain supercomplexes assembly and respiratory efficiency. *Cell* **155**, 160–171.

Cogliati, S., Enriquez, J. A. and Scorrano, L. (2016). Mitochondrial Cristae: Where Beauty Meets Functionality. *Trends Biochem. Sci.* **41**, 261–273.

Cummings, B. S. and Schnellmann, R. G. (2004). Measurement of cell death in mammalian cells. *Curr. Protoc. Pharmacol.* **Chapter 12**, Unit 12.8.

Davies, V. J., Hollins, A. J., Piechota, M. J., Yip, W., Davies, J. R., White, K. E., Nicols, P. P., Boulton, M. E. and Votruba, M. (2007). Opa1 deficiency in a mouse model of autosomal dominant optic atrophy impairs mitochondrial morphology, optic nerve structure and visual function. *Hum. Mol. Genet.* **16**, 1307–1318.

Debattisti, V., Pendin, D., Ziviani, E., Daga, A. and Scorrano, L. (2014). Reduction of endoplasmic reticulum stress attenuates the defects caused by Drosophila mitofusin depletion. *J. Cell Biol.* **204**, 303–312.

Debray, F.-G., Morin, C., Janvier, A., Villeneuve, J., Maranda, B., Laframboise, R., Lacroix, J., Decarie, J.-C., Robitaille, Y., Lambert, M., et al. (2011). LRPPRC mutations cause a phenotypically distinct form of Leigh syndrome with cytochrome c oxidase deficiency. *J. Med. Genet.* **48**, 183–189.

Delettre, C., Griffoin, J.-M., Kaplan, J., Dollfus, H., Lorenz, B., Faivre, L., Lenaers, G., Belenguer, P. and Hamel, C. P. (2001). Mutation spectrum and splicing variants in the OPA1 gene. *Hum. Genet.* **109**, 584–591.

Doe, C. Q. (2017). Temporal Patterning in the Drosophila CNS. *Annu. Rev. Cell Dev. Biol.* **33**, 219–240.

Duffy, J. B. (2002). GAL4 system in Drosophila: a fly geneticist's Swiss army knife. *Genesis* **34**, 1–15.

Egger, B., Chell, J. M. and Brand, A. H. (2008). Insights into neural stem cell biology from flies. *Philos. Trans. R. Soc. Lond. B Biol. Sci.* **363**, 39–56.

Ernster, L. (1977). Chemical and chemiosmotic aspects of electron transport-linked phosphorylation. *Annu. Rev. Biochem.* **46**, 981–995.

Falkenberg, M. and Larsson, N.-G. (2009). Structure casts light on mtDNA replication. *Cell* **139**, 231–233.

Feely, S. M. E., Laura, M., Siskind, C. E., Sottile, S., Davis, M., Gibbons, V. S., Reilly, M. M. and Shy, M. E. (2011). MFN2 mutations cause severe phenotypes in most patients with CMT2A. *Neurology* **76**, 1690–1696.

Fernández-Moreno, M. A., Farr, C. L., Kaguni, L. S. and Garesse, R. (2007). Drosophila melanogaster as a model system to study mitochondrial biology. *Methods Mol. Biol.* **372**, 33–49.

Ferree, A. and Shirihai, O. (2012). Mitochondrial dynamics: the intersection of form and function. *Adv. Exp. Med. Biol.* **748**, 13–40.

Fillingame, R. H. (1997). Coupling H+ transport and ATP synthesis in F1F0-ATP synthases: glimpses of interacting parts in a dynamic molecular machine. *J. Exp. Biol.* **200**, 217–224.

Flynn, J. M. and Melov, S. (2013). SOD2 in mitochondrial dysfunction and neurodegeneration. *Free Radic. Biol. Med.* **62**, 4–12.

Frezza, C. (2017). Mitochondrial metabolites: undercover signalling molecules. *Interface Focus* **7**, 20160100.

Frezza, C., Cipolat, S., Martins de Brito, O., Micaroni, M., Beznoussenko, G. V., Rudka, T., Bartoli, D., Polishuck, R. S., Danial, N. N., De Strooper, B., et al. (2006). OPA1 controls apoptotic cristae remodeling independently from mitochondrial fusion. *Cell* **126**, 177–189.

Fu, W., Liu, Y. and Yin, H. (2019). Mitochondrial Dynamics: Biogenesis, Fission, Fusion, and Mitophagy in the Regulation of Stem Cell Behaviors. *Stem Cells Int.* **2019**, 9757201.

Garrido, C., Galluzzi, L., Brunet, M., Puig, P. E., Didelot, C. and Kroemer, G. (2006). Mechanisms of cytochrome c release from mitochondria. *Cell Death Differ.* **13**, 1423–1433.

Gomes, L. C., Di Benedetto, G. and Scorrano, L. (2011). Essential amino acids and glutamine regulate induction of mitochondrial elongation during autophagy. *Cell Cycle* **10**, 2635–2639.

Gray, L. R., Tompkins, S. C. and Taylor, E. B. (2014). Regulation of pyruvate metabolism and human disease. *Cell. Mol. Life Sci.* **71**, 2577–2604.

Guo, R., Gu, J., Zong, S., Wu, M. and Yang, M. (2018). Structure and mechanism of mitochondrial electron transport chain. *Biomed. J.* **41**, 9–20.

Hacker, K. and Medler, K. F. (2008). Mitochondrial calcium buffering contributes to the maintenance of Basal calcium levels in mouse taste cells. *J. Neurophysiol.* **100**, 2177–2191.

Hakes, A. E. and Brand, A. H. (2019). Neural stem cell dynamics: the development of brain tumours. *Curr. Opin. Cell Biol.* **60**, 131–138.

Hardie, D. G., Ross, F. A. and Hawley, S. A. (2012). AMPK: a nutrient and energy sensor that maintains energy homeostasis. *Nat. Rev. Mol. Cell Biol.* **13**, 251–262.

Hatefi, Y. (1985). The mitochondrial electron transport and oxidative phosphorylation system. *Annu. Rev. Biochem.* **54**, 1015–1069.

Hermann, G. J., Thatcher, J. W., Mills, J. P., Hales, K. G., Fuller, M. T., Nunnari, J. and Shaw, J. M. (1998). Mitochondrial Fusion in Yeast Requires the Transmembrane GTPase Fzo1p. *J. Cell Biol.* **143**, 359–373.

Homem, C. C. F. and Knoblich, J. A. (2012). Drosophila neuroblasts: a model for stem cell biology. *Development* **139**, 4297–4310.

Homem, C. C. F., Steinmann, V., Burkard, T. R., Jais, A., Esterbauer, H. and Knoblich, J. A. (2014). Ecdysone and mediator change energy metabolism to terminate proliferation in Drosophila neural stem cells. *Cell* **158**, 874–888.

Hoque, A., Sivakumaran, P., Bond, S. T., Ling, N. X. Y., Kong, A. M., Scott, J. W., Bandara, N., Hernández, D., Liu, G.-S., Wong, R. C. B., et al. (2018). Mitochondrial fission protein Drp1 inhibition promotes cardiac mesodermal differentiation of human pluripotent stem cells. *Cell Death Discovery* **4**, 1–13.

Horecker, B. L. (1976). The biochemistry of sugars. *Int Z Vitam Ernahrungsforsch Beih* **15**, 1–21.

Isshiki, T., Pearson, B., Holbrook, S. and Doe, C. Q. (2001). Drosophila Neuroblasts Sequentially Express Transcription Factors which Specify the Temporal Identity of

Their Neuronal Progeny. *Cell* **106**, 511–521.

Jaiswal, M., Haelterman, N. A., Sandoval, H., Xiong, B., Donti, T., Kalsotra, A., Yamamoto, S., Cooper, T. A., Graham, B. H. and Bellen, H. J. (2015). Impaired Mitochondrial Energy Production Causes Light-Induced Photoreceptor Degeneration Independent of Oxidative Stress. *PLoS Biol.* **13**, e1002197.

Januschke, J. and Gonzalez, C. (2008). Drosophila asymmetric division, polarity and cancer. *Oncogene* **27**, 6994–7002.

Jiang, Y.-F., Lin, S.-S., Chen, J.-M., Tsai, H.-Z., Hsieh, T.-S. and Fu, C.-Y. (2017). Electron tomographic analysis reveals ultrastructural features of mitochondrial cristae architecture which reflect energetic state and aging. *Sci. Rep.* **7**, 1–11.

John, P. and Whatley, F. R. (1975). Paracoccus denitrificans and the evolutionary origin of the mitochondrion. *Nature* **254**, 495–498.

Jones, B. A. and Fangman, W. L. (1992). Mitochondrial DNA maintenance in yeast requires a protein containing a region related to the GTP-binding domain of dynamin. *Genes Dev.* **6**, 380–389.

Kang, C., Badr, M. A., Kyrychenko, V., Eskelinen, E.-L. and Shirokova, N. (2018). Deficit in PINK1/PARKIN-mediated mitochondrial autophagy at late stages of dystrophic cardiomyopathy. *Cardiovasc. Res.* **114**, 90–102.

Kasahara, A., Cipolat, S., Chen, Y., Dorn, G. W., 2nd and Scorrano, L. (2013). Mitochondrial fusion directs cardiomyocyte differentiation via calcineurin and Notch signaling. *Science* **342**, 734–737.

Khacho, M., Clark, A., Svoboda, D. S., Azzi, J., MacLaurin, J. G., Meghaizel, C., Sesaki, H., Lagace, D. C., Germain, M., Harper, M.-E., et al. (2016). Mitochondrial Dynamics Impacts Stem Cell Identity and Fate Decisions by Regulating a Nuclear Transcriptional Program. *Cell Stem Cell* **19**, 232–247.

Kianian, P. M. A. and Kianian, S. F. (2014). Mitochondrial dynamics and the cell cycle. *Front. Plant Sci.* **5**, 222.

Koshiba, T., Detmer, S. A., Kaiser, J. T., Chen, H., Michael McCaffery, J. and Chan, D. C. (2004). Structural Basis of Mitochondrial Tethering by Mitofusin Complexes. *Science* **305**, 858–862.

Kushnareva, Y., Seong, Y., Andreyev, A. Y., Kuwana, T., Kiosses, W. B., Votruba, M. and Newmeyer, D. D. (2016). Mitochondrial dysfunction in an Opa1(Q285STOP) mouse model of dominant optic atrophy results from Opa1 haploinsufficiency. *Cell Death Dis.* **7**, e2309.

Labrousse, A. M., Zappaterra, M. D., Rube1Alexander, D. A. and van der Bliek, M. (1999). C. elegans Dynamin-Related Protein DRP-1 Controls Severing of the

Mitochondrial Outer Membrane. *Mol. Cell* **4**, 815–826.

Lai, S.-L., Awasaki, T., Ito, K. and Lee, T. (2008). Clonal analysis of Drosophila antennal lobe neurons: diverse neuronal architectures in the lateral neuroblast lineage. *Development* **135**, 2883–2893.

Lane, N. and Martin, W. (2010). The energetics of genome complexity. *Nature* **467**, 929–934.

Lee, K.-S., Wu, Z., Song, Y., Mitra, S. S., Feroze, A. H., Cheshier, S. H. and Lu, B. (2013). Roles of PINK1, mTORC2, and mitochondria in preserving brain tumor-forming stem cells in a noncanonical Notch signaling pathway. *Genes Dev.* **27**, 2642–2647.

Lee, H., Smith, S. B. and Yoon, Y. (2017). The short variant of the mitochondrial dynamin OPA1 maintains mitochondrial energetics and cristae structure. *J. Biol. Chem.* **292**, 7115–7130.

Li, X., Xie, Y. and Zhu, S. (2016). Notch maintains Drosophila type II neuroblasts by suppressing expression of the Fez transcription factor Earmuff. *Development* **143**, 2511–2521.

Liesa, M. and Shirihai, O. S. (2013). Mitochondrial dynamics in the regulation of nutrient utilization and energy expenditure. *Cell Metab.* **17**, 491–506.

Lopez-Mejia, I. C. and Fajas, L. (2015). Cell cycle regulation of mitochondrial function. *Curr. Opin. Cell Biol.* **33**, 19–25.

Manna, S. (2015). An overview of pentatricopeptide repeat proteins and their applications. *Biochimie* **113**, 93–99.

Marchbank, N. J., Craig, J. E., Leek, J. P., Toohey, M., Churchill, A. J., Markham, A. F., Mackey, D. A., Toomes, C. and Inglehearn, C. F. (2002). Deletion of the OPA1 gene in a dominant optic atrophy family: evidence that haploinsufficiency is the cause of disease. *J. Med. Genet.* **39**, e47.

McLelland, G.-L., Goiran, T., Yi, W., Dorval, G., Chen, C. X., Lauinger, N. D., Krahn, A. I., Valimehr, S., Rakovic, A., Rouiller, I., et al. (2018). Mfn2 ubiquitination by PINK1/parkin gates the p97-dependent release of ER from mitochondria to drive mitophagy.

Mirzoyan, Z., Sollazzo, M., Allocca, M., Valenza, A. M., Grifoni, D. and Bellosta, P. (2019). : A Model Organism to Study Cancer. *Front. Genet.* **10**, 51.

Mitra, K., Wunder, C., Roysam, B., Lin, G. and Lippincott-Schwartz, J. (2009). A hyperfused mitochondrial state achieved at G1-S regulates cyclin E buildup and entry into S phase. *Proc. Natl. Acad. Sci. U. S. A.* **106**, 11960–11965.

Mitra, K., Rikhy, R., Lilly, M. and Lippincott-Schwartz, J. (2012). DRP1-dependent mitochondrial fission initiates follicle cell differentiation during Drosophila oogenesis. *J. Cell Biol.* **197**, 487–497.

Montgomery, C. M. and Leyden Webb, J. (1956). METABOLIC STUDIES ON HEART MITOCHONDRIA. *J. Biol. Chem.* **221**, 347–358.

Moore, B. A., Gonzalez Aviles, G. D., Larkins, C. E., Hillman, M. J. and Caspary, T. (2010). Mitochondrial retention of Opa1 is required for mouse embryogenesis. *Mamm. Genome* **21**, 350–360.

Muqit, M. M. K. and Feany, M. B. (2002). Modelling neurodegenerative diseases in Drosophila : a fruitful approach? *Nat. Rev. Neurosci.* **3**, 237–243.

Nunes-Nesi, {adriano, Araújo, W. L., Obata, T. and Fernie}, A. R. (2013). Regulation of the mitochondrial tricarboxylic acid cycle. *Curr. Opin. Plant Biol.* **16**, 335–343.

Nunnari, J. and Suomalainen, A. (2012). Mitochondria: in sickness and in health. *Cell* **148**, 1145–1159.

Olichon, A., Baricault, L., Gas, N., Guillou, E., Valette, A., Belenguer, P. and Lenaers, G. (2003). Loss of OPA1 perturbates the mitochondrial inner membrane structure and integrity, leading to cytochrome c release and apoptosis. *J. Biol. Chem.* **278**, 7743–7746.

O'Rourke, B. (2010). From bioblasts to mitochondria: ever expanding roles of mitochondria in cell physiology. *Front. Physiol.* **1**, 7.

Osellame, L. D., Blacker, T. S. and Duchen, M. R. (2012). Cellular and molecular mechanisms of mitochondrial function. *Best Pract. Res. Clin. Endocrinol. Metab.* **26**, 711–723.

Ott, M., Robertson, J. D., Gogvadze, V., Zhivotovsky, B. and Orrenius, S. (2002). Cytochrome c release from mitochondria proceeds by a two-step process. *Proc. Natl. Acad. Sci. U. S. A.* **99**, 1259–1263.

Patten, D. A., Wong, J., Khacho, M., Soubannier, V., Mailloux, R. J., Pilon-Larose, K., MacLaurin, J. G., Park, D. S., McBride, H. M., Trinkle-Mulcahy, L., et al. (2014). OPA1-dependent cristae modulation is essential for cellular adaptation to metabolic demand. *EMBO J.* **33**, 2676–2691.

Paumard, P., Vaillier, J., Coulary, B., Schaeffer, J., Soubannier, V., Mueller, D. M., Brèthes, D., di Rago, J. and Velours, J. (2002). The ATP synthase is involved in generating mitochondrial cristae morphology. *EMBO J.* **21**, 221–230.

Paupe, V. and Prudent, J. (2018). New insights into the role of mitochondrial calcium homeostasis in cell migration. *Biochem. Biophys. Res. Commun.* **500**, 75–86.

Pelloquin, L., Belenguer, P., Menon, Y. and Ducommun, B. (1998). Identification of a fission yeast dynamin-related protein involved in mitochondrial DNA maintenance. *Biochem. Biophys. Res. Commun.* **251**, 720–726.

Pesch, U. E. A., Fries, J. E., Bette, S., Kalbacher, H., Wissinger, B., Alexander, C. and Kohler, K. (2004). OPA1, the disease gene for autosomal dominant optic atrophy, is specifically expressed in ganglion cells and intrinsic neurons of the retina. *Invest. Ophthalmol. Vis. Sci.* **45**, 4217–4225.

Qi, Y., Yan, L., Yu, C., Guo, X., Zhou, X., Hu, X., Huang, X., Rao, Z., Lou, Z. and Hu, J. (2016). Structures of human mitofusin 1 provide insight into mitochondrial tethering. *J. Cell Biol.* **215**, 621–629.

Quintana-Cabrera, R., Quirin, C., Glytsou, C., Corrado, M., Urbani, A., Pellattiero, A., Calvo, E., Vázquez, J., Enríquez, J. A., Gerle, C., et al. (2018). The cristae modulator Optic atrophy 1 requires mitochondrial ATP synthase oligomers to safeguard mitochondrial function. *Nat. Commun.* **9**, 3399.

Rambold, A. S., Kostelecky, B., Elia, N. and Lippincott-Schwartz, J. (2011). Tubular network formation protects mitochondria from autophagosomal degradation during nutrient starvation. *Proc. Natl. Acad. Sci. U. S. A.* **108**, 10190–10195.

Ranieri, M., Brajkovic, S., Riboldi, G., Ronchi, D., Rizzo, F., Bresolin, N., Corti, S. and Comi, G. P. (2013). Mitochondrial fusion proteins and human diseases. *Neurol. Res. Int.* **2013**, 293893.

Rapaport, D., Brunner, M., Neupert, W. and Westermann, B. (1998). Fzo1p Is a Mitochondrial Outer Membrane Protein Essential for the Biogenesis of Functional Mitochondria in Saccharomyces cerevisiae. *J. Biol. Chem.* **273**, 20150–20155.

Redza-Dutordoir, M. and Averill-Bates, D. A. (2016). Activation of apoptosis signalling pathways by reactive oxygen species. *Biochim. Biophys. Acta* **1863**, 2977–2992.

Roger, A. J., Muñoz-Gómez, S. A. and Kamikawa, R. (2017). The Origin and Diversification of Mitochondria. *Curr. Biol.* **27**, R1177–R1192.

Rosen, D. R., Siddique, T., Patterson, D., Figlewicz, D. A., Sapp, P., Hentati, A., Donaldson, D., Goto, J., O'Regan, J. P. and Deng, H. X. (1993). Mutations in Cu/Zn superoxide dismutase gene are associated with familial amyotrophic lateral sclerosis. *Nature* **362**, 59–62.

Rout, A. K., Strub, M.-P., Piszczek, G. and Tjandra, N. (2014). Structure of Transmembrane Domain of Lysosome-associated Membrane Protein Type 2a (LAMP-2A) Reveals Key Features for Substrate Specificity in Chaperone-mediated Autophagy. *J. Biol. Chem.* **289**, 35111–35123.

Ruzzenente, B., Metodiev, M. D., Wredenberg, A., Bratic, A., Park, C. B., Cámara, Y., Milenkovic, D., Zickermann, V., Wibom, R., Hultenby, K., et al. (2012).

LRPPRC is necessary for polyadenylation and coordination of translation of mitochondrial mRNAs. *EMBO J.* **31**, 443–456.

Saleh, A., Srinivasula, S. M., Acharya, S., Fishel, R. and Alnemri, E. S. (1999). Cytochrome c and dATP-mediated oligomerization of Apaf-1 is a prerequisite for procaspase-9 activation. *J. Biol. Chem.* **274**, 17941–17945.

Sato, M. and Sato, K. (2013). Maternal inheritance of mitochondrial DNA by diverse mechanisms to eliminate paternal mitochondrial DNA. *Biochim. Biophys. Acta* **1833**, 1979–1984.

Schapira, A. H., Cooper, J. M., Dexter, D., Clark, J. B., Jenner, P. and Marsden, C. D. (1990). Mitochondrial complex I deficiency in Parkinson's disease. *J. Neurochem.* **54**, 823–827.

Schieber, M. and Chandel, N. S. (2014). ROS function in redox signaling and oxidative stress. *Curr. Biol.* **24**, R453–62.

Scott, R. C., Schuldiner, O. and Neufeld, T. P. (2004). Role and regulation of starvation-induced autophagy in the Drosophila fat body. *Dev. Cell* **7**, 167–178.

Sen, A., Damm, V. T. and Cox, R. T. (2013). Drosophila Clueless Is Highly Expressed in Larval Neuroblasts, Affects Mitochondrial Localization and Suppresses Mitochondrial Oxidative Damage. *PLoS One* **8**,.

Senior, A. E. (1988). ATP synthesis by oxidative phosphorylation. *Physiol. Rev.* **68**, 177–231.

Sesaki, H. and Jensen, R. E. (1999). Division versus Fusion: Dnm1p and Fzo1p Antagonistically Regulate Mitochondrial Shape. *J. Cell Biol.* **147**, 699–706.

Shakeri, R., Kheirollahi, A. and Davoodi, J. (2017). Apaf-1: Regulation and function in cell death. *Biochimie* **135**, 111–125.

Siegmund, S. E., Grassucci, R., Carter, S. D., Barca, E., Farino, Z. J., Juanola-Falgarona, M., Zhang, P., Tanji, K., Hirano, M., Schon, E. A., et al. (2018). Three-Dimensional Analysis of Mitochondrial Crista Ultrastructure in a Patient with Leigh Syndrome by In Situ Cryoelectron Tomography. *iScience* **6**, 83–91.

Smirnova, E., Griparic, L., Shurland, D. L. and van der Bliek, A. M. (2001). Dynamin-related protein Drp1 is required for mitochondrial division in mammalian cells. *Mol. Biol. Cell* **12**, 2245–2256.

Song, Z., Chen, H., Fiket, M., Alexander, C. and Chan, D. C. (2007). OPA1 processing controls mitochondrial fusion and is regulated by mRNA splicing, membrane potential, and Yme1L. *J. Cell Biol.* **178**, 749.

Spana, E. P., Kopczynski, C., Goodman, C. S. and Doe, C. Q. (1995). Asymmetric

localization of numb autonomously determines sibling neuron identity in the Drosophila CNS. *Development* **121**, 3489–3494.

Su, B., Wang, X., Zheng, L., Perry, G., Smith, M. A. and Zhu, X. (2010). Abnormal mitochondrial dynamics and neurodegenerative diseases. *Biochim. Biophys. Acta* **1802**, 135–142.

Sun, Y., Vashisht, A. A., Tchieu, J., Wohlschlegel, J. A. and Dreier, L. (2012). Voltage-dependent anion channels (VDACs) recruit Parkin to defective mitochondria to promote mitochondrial autophagy. *J. Biol. Chem.* **287**, 40652–40660.

Taguchi, N., Ishihara, N., Jofuku, A., Oka, T. and Mihara, K. (2007). Mitotic phosphorylation of dynamin-related GTPase Drp1 participates in mitochondrial fission. *J. Biol. Chem.* **282**, 11521–11529.

Teixeira, F. K., Sanchez, C. G., Hurd, T. R., Seifert, J. R. K., Czech, B., Preall, J. B., Hannon, G. J. and Lehmann, R. (2015). ATP synthase promotes germ cell differentiation independent of oxidative phosphorylation. *Nat. Cell Biol.* **17**, 689–696.

Thorsness, P. E. (1992). Structural dynamics of the mitochondrial compartment. *Mutat. Res.* **275**, 237–241.

Tilokani, L., Nagashima, S., Paupe, V. and Prudent, J. (2018). Mitochondrial dynamics: overview of molecular mechanisms. *Essays Biochem.* **62**, 341–360.

Tomer, D., Chippalkatti, R., Mitra, K. and Rikhy, R. (2018). ERK regulates mitochondrial membrane potential in fission deficient Drosophila follicle cells during differentiation. *Dev. Biol.* **434**, 48–62.

Trotta, A. P. and Chipuk, J. E. (2017). Mitochondrial dynamics as regulators of cancer biology. *Cell. Mol. Life Sci.* **74**, 1999–2017.

Tsuji, T., Hasegawa, E. and Isshiki, T. (2008). Neuroblast entry into quiescence is regulated intrinsically by the combined action of spatial Hox proteins and temporal identity factors. *Development* **135**, 3859–3869.

Vacca, R. A., Valenti, D., Bobba, A., Merafina, R. S., Passarella, S. and Marra, E. (2006). Cytochrome c Is Released in a Reactive Oxygen Species-Dependent Manner and Is Degraded via Caspase-Like Proteases in Tobacco Bright-Yellow 2 Cells en Route to Heat Shock-Induced Cell Death. *Plant Physiol.* **141**, 208.

Valapala, M., Hose, S., Gongora, C., Dong, L., Wawrousek, E. F., Samuel Zigler, J., Jr and Sinha, D. (2013). Impaired endolysosomal function disrupts Notch signalling in optic nerve astrocytes. *Nat. Commun.* **4**, 1629.

van den Ameele, J. and Brand, A. H. (2019). Neural stem cell temporal patterning and

brain tumour growth rely on oxidative phosphorylation. *Elife* **8**,.

van der Bliek, A. M. (2009). Fussy mitochondria fuse in response to stress. *EMBO J.* **28**, 1533–1534.

Vempati, U. D., Han, X. and Moraes, C. T. (2009). Lack of cytochrome c in mouse fibroblasts disrupts assembly/stability of respiratory complexes I and IV. *J. Biol. Chem.* **284**, 4383–4391.

Verma, S., Dixit, R. and Pandey, K. C. (2016). Cysteine Proteases: Modes of Activation and Future Prospects as Pharmacological Targets. *Front. Pharmacol.* **7**, 30433.

Wanet, A., Arnould, T., Najimi, M. and Renard, P. (2015). Connecting Mitochondria, Metabolism, and Stem Cell Fate. *Stem Cells Dev.* **24**, 1957–1971.

Wang, Z. A. and Kalderon, D. (2009). Cyclin E-dependent protein kinase activity regulates niche retention of Drosophila ovarian follicle stem cells. *Proc. Natl. Acad. Sci. U. S. A.* **106**, 21701–21706.

Wang, Z. and Wu, M. (2014). Phylogenomic reconstruction indicates mitochondrial ancestor was an energy parasite. *PLoS One* **9**, e110685.

Wang, Z. and Wu, M. (2015). An integrated phylogenomic approach toward pinpointing the origin of mitochondria. *Sci. Rep.* **5**, 7949.

Wang, C. and Youle, R. J. (2009). The role of mitochondria in apoptosis*. *Annu. Rev. Genet.* **43**, 95–118.

Wang, W., Fernandez-Sanz, C. and Sheu, S.-S. (2018). Regulation of mitochondrial bioenergetics by the non-canonical roles of mitochondrial dynamics proteins in the heart. *Biochim. Biophys. Acta Mol. Basis Dis.* **1864**, 1991–2001.

Wei, Y. H., Lu, C. Y., Lee, H. C., Pang, C. Y. and Ma, Y. S. (1998). Oxidative damage and mutation to mitochondrial DNA and age-dependent decline of mitochondrial respiratory function. *Ann. N. Y. Acad. Sci.* **854**, 155–170.

Westermann, B. (2012). Bioenergetic role of mitochondrial fusion and fission. *Biochim. Biophys. Acta* **1817**, 1833–1838.

Wodarz, A. and Huttner, W. B. (2003). Asymmetric cell division during neurogenesis in Drosophila and vertebrates. *Mech. Dev.* **120**, 1297–1309.

Xu, X., Duan, S., Yi, F., Ocampo, A., Liu, G.-H. and Izpisua Belmonte, J. C. (2013). Mitochondrial regulation in pluripotent stem cells. *Cell Metab.* **18**, 325–332.

Yamamoto, S., Charng, W.-L. and Bellen, H. J. (2010). Endocytosis and Intracellular Trafficking of Notch and Its Ligands. In *Notch Signaling*, pp. 165–200. Elsevier.

Yan, Y., Denef, N. and Schüpbach, T. (2009). The vacuolar proton pump, V-ATPase, is required for notch signaling and endosomal trafficking in Drosophila. *Dev. Cell* **17**, 387–402.

Yao, C.-H., Wang, R., Wang, Y., Kung, C.-P., Weber, J. D. and Patti, G. J. (2019). Mitochondrial fusion supports increased oxidative phosphorylation during cell proliferation. *Elife* **8**,.

Yoo, S.-M. and Jung, Y.-K. (2018). A Molecular Approach to Mitophagy and Mitochondrial Dynamics. *Mol. Cells* **41**, 18–26.

Yu, T., Robotham, J. L. and Yoon, Y. (2006). Increased production of reactive oxygen species in hyperglycemic conditions requires dynamic change of mitochondrial morphology. *Proc. Natl. Acad. Sci. U. S. A.* **103**, 2653–2658.

Zhang, Z., Wakabayashi, N., Wakabayashi, J., Tamura, Y., Song, W.-J., Sereda, S., Clerc, P., Polster, B. M., Aja, S. M., Pletnikov, M. V., et al. (2011). The dynamin-related GTPase Opa1 is required for glucose-stimulated ATP production in pancreatic beta cells. *Mol. Biol. Cell* **22**, 2235–2245.

Zhang, H., Menzies, K. J. and Auwerx, J. (2018). The role of mitochondria in stem cell fate and aging. *Development* **145**,.